

Gregor Kosec

# **Expression and characterization of cysteine peptidases metacaspases and autophagins from the parasite *Trypanosoma cruzi***

*Supervisor:* prof. Vito Turk, PhD.

*Co-supervisor:* prof. Juan José Cazzulo, PhD.

## **Doctoral Dissertation**

September 2006

**MEDNARODNA PODIPLOMSKA ŠOLA JOŽEFA STEFANA**  
JOŽEF STEFAN INTERNATIONAL POSTGRADUATE SCHOOL  
Ljubljana, Slovenia





# Index

<b>Abstract .....</b>	<b>V</b>
<b>Povzetek.....</b>	<b>VI</b>
<b>Abbreviations .....</b>	<b>VII</b>
<b>1 Introduction.....</b>	<b>1</b>
1.1 Peptidases .....	1
1.2 <i>Trypanosoma cruzi</i> and Chagas disease.....	1
1.2.1 Peptidases of <i>Trypanosoma cruzi</i> .....	3
1.2.1.1 Peptidases as virulence factors of <i>T. cruzi</i> .....	3
1.2.1.2 Cruzipain, the most abundant cysteine peptidase of <i>T. cruzi</i> .....	3
1.2.1.3 Cruzipain inhibitors as potential drugs for Chagas disease.....	3
1.2.2 Sequencing of the <i>Trypanosoma cruzi</i> genome.....	4
1.3 Cysteine peptidases.....	4
1.3.1 General characteristics of the clan CA .....	4
1.3.1.1 Emerging roles of cysteine cathepsins .....	5
1.3.2 C54 or the autophagin family .....	5
1.4 Autophagy.....	6
1.4.1 Protein turnover in the cell .....	6
1.4.2 Biological role of autophagy .....	7
1.4.3 Molecular mechanism of autophagy.....	7
1.5 Clan CD cysteine peptidases.....	9
1.5.1 Characteristics of caspases, paracaspases and metacaspases.....	10
1.5.1.1 Caspases.....	10
1.5.1.2 Paracaspases and metacaspases.....	11
1.5.1.3 Cysteine peptidases as signaling molecules – apoptosis.....	13
1.5.1.4 Biological function of the mammalian paracaspase.....	14
1.6 Programmed cell death in plants and unicellular organisms.....	15
1.6.1 Programmed cell death in plants .....	15
1.6.2 Programmed cell death in unicellular organisms.....	15
1.6.2.1 Overview.....	15
1.6.2.2 Programmed cell death in <i>Saccharomyces cerevisiae</i> .....	15
1.6.2.3 Programmed cell death in kinetoplastids .....	16
1.6.3 Theoretical considerations of programmed cell death in unicellular organisms .....	16
1.6.3.1 Possible origin of programmed cell death.....	16
1.6.3.2 Possible benefits of programmed cell death in kinetoplastids .....	17
1.7 Initial studies of metacaspase-3 in <i>Trypanosoma cruzi</i> .....	17
1.7.1 Metacaspase genes in the genome of <i>T. cruzi</i> .....	17
1.7.2 Strategies used to express recombinant metacaspase-3 from <i>T. cruzi</i> .....	19
<b>2 Aims and hypothesis.....</b>	<b>21</b>
<b>3 Materials and methods.....</b>	<b>23</b>
3.1 <i>ATG4</i> and <i>ATG8</i> genes sequence analysis .....	23
3.2 Pulse field gel electrophoresis (PFGE).....	23
3.3 Cloning and expression of recombinant proteins.....	23

3.3.1 Cloning and expression of the <i>TcMCA3</i> gene .....	23
3.3.2 Cloning and expression of <i>ATG4.1</i> , <i>ATG4.2</i> , <i>ATG8.1</i> and <i>ATG8.2</i> genes .....	24
3.4 Purification of recombinant proteins using metal chelating chromatography .....	25
3.4.1 Purification of metacaspase-3 in denaturing conditions for production of antibodies.....	25
3.4.2 Purification of metacaspase-3 in weakly disruptive conditions.....	25
3.4.3 Purification of autophagin-1 and -2 and of Atg8.1 and Atg8.2 proteins.....	25
3.5 Western blotting.....	25
3.5.1 Western blotting for detection of expression of metacaspase-3 in different <i>T. cruzi</i> developmental stages .....	25
3.5.2 Identification of recombinant proteins.....	25
3.6 Measurements of metacaspase-3 activity using combinatorial peptide libraries .....	25
3.7 Proteolytic activity of recombinant autophagins on recombinant Atg8.1 and Atg8.2 and fluorogenic synthetic substrate.....	26
3.7.1 Proteolytic activity of recombinant autophagins on recombinant Atg8.1 and Atg8.2.....	26
3.7.2 Proteolytic activity of recombinant autophagins on fluorescence quenched synthetic substrate Abz-TFGQ-EDDnp .....	26
3.8 Measuring of autophagin activity in cell free protein extracts of <i>T. cruzi</i> .....	27
3.9 Transformation of <i>atg4Δ</i> and <i>atg8Δ</i> yeasts with respective <i>T. cruzi</i> homologs .....	27
3.10 Parasite cultures and treatments.....	27
3.10.1 Induction of programmed cell death of <i>T. cruzi</i> epimastigotes.....	27
3.10.2 Starvation induction .....	28
3.10.3 Immunofluorescence studies.....	28
3.11 Assessment of binding of Atg8.1 and Atg8.2 to microtubules .....	28
<b>4 Results .....</b>	<b>29</b>
4.1 Chromosomal organization of <i>TcMCA3</i> genes .....	29
4.2 Expression of metacaspase-3 in different <i>T. cruzi</i> developmental stages .....	29
4.3 Recombinant expression of N-terminal truncated <i>TcMCA3</i> genes in <i>E. coli</i> .....	30
4.4 Metacaspase-3 changes its sub-cellular localization during epimastigote cell death.....	30
4.5 <i>ATG4</i> and <i>ATG8</i> homologs in <i>T. cruzi</i> genome .....	32
4.6 Expression and purification of recombinant autophagins and recombinant Atg8.1 and Atg8.2.....	35
4.7 Proteolytic activity of recombinant autophagins on recombinant Atg8.1 and Atg8.2 .....	37
4.8 Autophagin activity is expressed in all four <i>T. cruzi</i> developmental stages .....	41
4.9 <i>ATG4.1</i> , <i>ATG4.2</i> and <i>ATG8.1</i> reconstitute autophagy in autophagy deficient yeast knock-outs.....	41
4.10 Assessment of binding of Atg8.1 and Atg8.2 to microtubules <i>in vitro</i> .....	42
4.11 Atg8.1 and Atg8.2 are localized in small punctate pattern in <i>T. cruzi</i> epimastigotes and reveal larger structures in starvation conditions .....	43
<b>5 Discussion.....</b>	<b>45</b>
5.1 The metacaspase family.....	45
5.2 Autophagy and autophagins in <i>T. cruzi</i> .....	48
<b>6 Conclusions .....</b>	<b>53</b>
<b>7 Acknowledgements.....</b>	<b>55</b>
<b>8 References .....</b>	<b>57</b>
<b>Index of Figures .....</b>	<b>63</b>
<b>List of published articles .....</b>	<b>67</b>
<b>Razširjeni povzetek doktorske disertacije.....</b>	<b>69</b>

## Abstract

Cysteine peptidases have been demonstrated to be important virulence factors of protozoan parasites, including *Trypanosoma cruzi*. With genome sequence determination the existence of several novel families of cysteine peptidases can be envisioned in this parasite. We focused on two families, metacaspases from the clan CD and autophagins (or Atg4 proteases) from the clan CA. During our previous work on the metacaspase family in *T. cruzi* we identified two genes, metacaspase-3 and metacaspase-5. Metacaspase-3 gene was shown to be present in about 16 copies per haploid genome and now we prove that there are two tandem arrays of these copies located on two different chromosomes. We also show that metacaspase-3 is expressed in all mayor developmental stages of *T. cruzi*, a result supported by the fact, that almost all patients with chronic Chagas disease possess antibodies against the metacaspase-3. We were able to express N-terminally truncated form of the metacaspase-3 in soluble form. We used this protein to screen fluorescence quenched combinatorial libraries of synthetic substrates, however we were unable to detect proteolytic activity. Using polyclonal antibodies we detected that metacaspases are translocated from the cytosol to the nucleus during fresh human serum induced programmed cell death of epimastigotes and could mediate this process in *T. cruzi*.

We identified two genes belonging to the autophagin family in the genome of *T. cruzi*, *TcATG4.1* (autophagin-1) and *TcATG4.2* (autophagin-2). We also identified two genes homologous to ubiquitin-like *ATG8* genes, predicted substrates of autophagins, *TcATG8.1* and *TcATG8.2*. We expressed all four genes in *E. coli* and purified the proteins. Both TcAtg4.1 and TcAtg4.2 are active cysteine peptidases, although only TcAtg4.1 efficiently processes TcAtg8.1 and TcAtg8.2. Reconstitution experiments of knock out yeast strains showed that *TcATG4.1* and *TcATG4.2* could replace *S. cerevisiae ATG4* gene reconstituting autophagy whereas only *TcATG8.1* and not *TcATG8.2* could do so in *ScATG8* knockout strain. Further on, using polyclonal antibodies against TcAtg8.1 in immunofluorescence studies in *T. cruzi* we could observe the translocation of this protein to the autophagosomal membranes during prolonged starvation of epimastigotes. This suggests that *TcATG8.1* is functionally homologous to yeast *ATG8* gene and mammalian MAP1 LC3 mediating autophagosome growth and closure. Finally, autophagin activity is expressed in all developmental stages of *T. cruzi* suggesting a constitutive basal level of autophagy in this organism.

## Povzetek

Cisteinske peptidaze imajo vlogo virulenčnih dejavnikov pri mnogih praživalih, med drugim tudi pri parazitu *Trypanosoma cruzi*. Sekveniranje genoma tega organizma je nakazalo obstoj več novih družin cisteinskih peptidaz. Osredotočili smo se na dve družini: metakaspaze iz klana CD in avtofagine (oziroma Atg4 proteaze) iz klana CA. V svojem prejšnjem delu smo identificirali dva gene iz družine metakaspaz v *T. cruzi*: metakaspazo-3 in metakaspazo-5. Gen za metakaspazo-3 je prisoten v 16 kopijah na haploidni genom, zdaj pa smo ugotovili, da se dve tandemski ponovitvi teh kopij nahajata na različnih kromosomih. Ugotovili smo tudi, da se metakaspazo-3 izraža v vseh glavnih razvojnih stadijih *T. cruzi*, kar potrjuje dejstvo, da serumi skoraj vseh pacientov s kronično Chagasovo boleznijo vsebujejo protitelesa proti metakaspazi-3. V topni obliki nam je uspelo izraziti metakaspazo-3 s skrajšanim aminoterminalnim koncem. Ta protein smo uporabili za merjenje proteolitične aktivnosti s kombinatoričnimi knjižnicami fluorescenčnih sintetičnih substratov, vendar aktivnosti nismo zaznali. S poliklonskimi protitelesi smo ugotovili, da se metakaspazi premakneta iz citosola v jedro v procesu s svežim človeškim serumom inducirane programirane celične smrti epimastigotov in da morda aktivno sodelujeta pri tem procesu v *T. cruzi*.

V genomu *T. cruzi* smo identificirali dva gena iz družine avtofaginov, *TcATG4.1* (avtofagin-1) in *TcATG4.2* (avtofagin-2). Prav tako smo identificirali dva predvidena substrata avtofaginov, homologa ubikvitinu podobnega gena *ATG8*, *TcATG8.1* in *TcATG8.2*. Vse štiri gene smo izrazili v *E. coli* in proteine izolirali. Oba, *TcAtg4.1* in *TcAtg4.2* sta aktivni cisteinski peptidazi, čeprav samo *TcAtg4.1* učinkovito procesira *TcAtg8.1* in *TcAtg8.2*. Eksperimenti rekonstitucije pri kvasovkah so pokazali, da *TcATG4.1* in *TcATG4.2* lahko nadomestita gen *ATG4* iz *Saccharomyces cerevisiae* in vzpostavita avtofagijo. V sevu z izbitim genom *ScATG8* je to lahko storil le *TcATG8.1*, *TcATG8.2* pa ne. V nadaljevanju smo s poliklonskimi protitelesi proti *TcAtg8.1* v imunofluorescenčnih študijah v *T. cruzi* opazili, da se ta protein premakne v membrane avtofagosomov med podaljšanim stradanjem epimastigotov. Na podlagi teh rezultatov lahko sklepamo, da je *TcATG8.1* funkcijski homolog gena *ATG8* iz *S. cerevisiae* in sesalskega MAP1 LC3 in sodeluje pri tvorbi in rasti avtofagosomov. Pokazali smo tudi, da se aktivnost avtofaginov izraža v vseh razvojnih stadijih *T. cruzi*, kar nakazuje, da avtofagija na bazalni ravni v tem organizmu poteka ves čas.

## Abbreviations

Abz	=	<i>ortho</i> -aminobenzoic
API	=	aminopeptidase I
ATG	=	autophagy related gene
Atg (formerly Apg, Aut)	=	protein synthesized upon autophagy related gene
ATP	=	adenosine triphosphate
BHT	=	brain-heart-tryptose
BSA	=	bovine serum albumin
BSF	=	bloodstream form
C	=	carboxy-
CARD	=	caspase recruitment domain
Cvt	=	cytoplasm-to-vacuole
DAPI	=	4',6-diamidino-2-phenylindole
dCTP	=	deoxy-cytosine-triphosphate
DD	=	death domain
DED	=	death effector domain
DEVd-CHO	=	Asp-Glu-Val-Asp-aldehyde
DNA	=	deoxyribonucleic acid
DTE	=	dithioerithritol
DTT	=	dithithreitol
DUB	=	deubiquinating enzyme
E-64	=	<i>trans</i> -epoxysuccinyl-L-leucylamido-(4-guanidino)-butane
EDDnp-OH	=	N-(ethylendiamine)-2,4-dinitrophenyl amide
EDTA	=	ethylene-N,N-diamintetraacetic acid
ER	=	endoplasmic reticulum
FCS	=	fetal calf serum
FHS	=	fresh human serum
GABARAP	=	gamma aminobutyric acid receptor-associated protein
GATE 16	=	Golgi associated ATPase enhancer
Ig	=	immunoglobulin
IKK	=	I $\kappa$ B kinase
IPTG	=	<i>iso</i> -propyl- $\beta$ -D-thiogalactopyranoside
kb	=	10 <sup>3</sup> bases
LTR	=	long terminal repeat
MALT	=	mucosa-associated lymphoid tissue
MAP	=	microtubule-associated protein
MAP 1 LC3	=	microtubule associated protein 1 light chain 3
Mb	=	10 <sup>6</sup> bases
MHC	=	mayor histocompatibility complex
N	=	amino-
NF- $\kappa$ B	=	nuclear factor $\kappa$ B
NSF	=	N-ethylmaleimide-sensitive factor
NTA	=	nitrilotriacetic acid
OD <sub>600</sub>	=	optical density at 600 nm
ORF	=	open reading frame
PAGE	=	polyacrylamide gel electrophoresis
PAS	=	preautophagosomal structure
PBS	=	phosphate buffered saline
PCD	=	programmed cell death
PCR	=	polymerase chain reaction
PDB	=	protein database

PE	=	phosphatidylethanolamine
PEG	=	polyethylenglycol
PFGE	=	pulse field gel electrophoresis
PI3K	=	phosphatidylinositol 3' kinase
PKC	=	protein kinase C
PMSF	=	phenylmethylsulfonylfluoride
RNA	=	ribonucleic acid
ROS	=	reactive oxygen species
SDS	=	sodium dodecylsulphate
SNAP	=	soluble NSF attachment protein
SNARE	=	soluble SNAP receptor
SR-VAD-FMK	=	sulforhodamine derivative of Val-Ala-Asp fluoromethyl ketone
SUMO	=	Small ubiquitin-like modifier
TBS	=	tris buffered saline
TFA	=	trifluoroacetic acid
TNF	=	tumor necrosis factor
TOR	=	target of rapamycin
Ulp-1	=	Ubl specific protease 1
UV	=	ultra violet
VSG	=	variant surface glycoprotein
WGS	=	whole genome shotgun
WHO	=	World Health Organization
YNB	=	yeast nitrogen base
YVAD-ase activity	=	proteolytic cleavage after Tyr-Val-Ala-Asp sequence
zLFG-DAM	=	(carbobenzyloxy)-Leu-Phe-Gly-diazomethylketone

# 1 Introduction

## 1.1 Peptidases

Peptidase is the general name given to all enzymes that hydrolyze peptidic bonds in peptides and proteins. According to the position of the bond, they can be exopeptidases, if they hydrolyze either the N-terminal or the C-terminal residue, or endopeptidases, if they are able to hydrolyze internal peptidic bonds. Considering their reaction mechanism, Barrett (Barrett 2004) has divided peptidases into two main groups: those which use a protein nucleophile for catalysis (cysteine, serine and threonine peptidases) and those which use water as the nucleophile (aspartic and metallopeptidases).

## 1.2 *Trypanosoma cruzi* and Chagas disease

Trypanosomatids are among the first eukaryotic organisms that contain mitochondria. There is only one that has a specialized region, called the kinetoplast, which contains all the mitochondrial DNA, which in these organisms may account for up to 20 – 30 % of the total DNA, and was the first extra-nuclear DNA identified, almost a hundred years ago, using the Feulgen staining. Kinetoplastic DNA consists of a complex array of catenated circular molecules; most of them are very small (minicircles), and their function is encoding guide RNAs, necessary for a complex editing process which makes viable the mitochondrial mRNAs, encoded by a small number of longer circles (maxicircles), which thus represent the true mitochondrial DNA. This very peculiar structure gives the name to the Order Kinetoplastida, to which the family Trypanosomatidae belongs (De Souza 2002). Another structural peculiarity of trypanosomes is the presence of specialized peroxisomes, found so far exclusively in the Kinetoplastida, which are called glycosomes since they contain the first two-thirds of the glycolytic pathway. Kinetoplastida are the only eukaryotic cells in which glycolysis is not a completely cytosolic pathway, and this fact imposes a number of metabolic peculiarities and restrictions to them. Glucose is only incompletely oxidized even in aerobiosis, and fermentation products such as succinate and L-alanine are excreted into the medium (aerobic fermentation of glucose) (Cazzulo 1994).

In order to adapt to different environments *T. cruzi* has to differentiate into four different developmental stages. The parasite enters the mammalian host when the insect vector (for example *Triatoma infestans*) defecates in the vicinity of the bite and the natural infective stage, the metacyclic trypomastigote, carried in the wound by scratching, enter and infect nearby cells. Once inside the cell, trypomastigotes differentiate into amastigotes, a small form with a very short flagellum. The amastigotes then multiply inside the infected cell and, after an average of nine divisions, they differentiate into trypomastigotes, which are liberated into the bloodstream. This parasite stage is similar, but not identical, to the metacyclic trypomastigotes. Bloodstream trypomastigotes can infect new cells, perpetuating chagasic infection. When the insect vector bites an infected mammal, the trypomastigotes carried over with the blood meal differentiate into epimastigotes, which are a flagellated replicative form living in the insect gut. In the rectum, in the zone where the Malpighian tubules discharge the insect's urine, the epimastigotes bind to the intestinal epithelium through the flagellum, and differentiate to metacyclic trypomastigotes, which are able to start a new round of infection (De Souza 2002) (Figure 1; Figure 2).

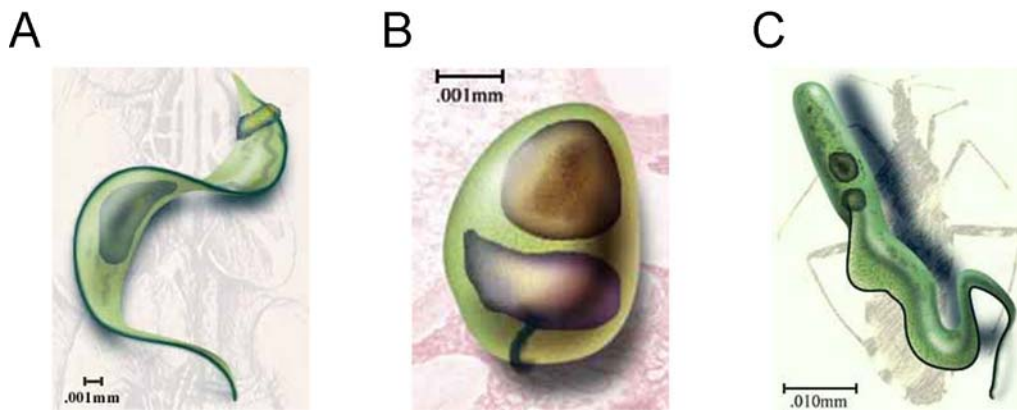


Figure 1 Typical morphology of *Trypanosoma cruzi* developmental stages. **A)** Trypomastigote, non-replicative form found in the bloodstream that is able to infect mammalian cells and measures about 12  $\mu\text{m}$  in length. Morphologically they are very similar to metacyclic trypomastigotes, but they have antigenic and metabolic differences. **B)** Amastigote, replicative and non-motile form present inside mammalian cells, that is only 5  $\mu\text{m}$  long. **C)** Epimastigote, the stage present in the insect vector gut, which is the form that can be readily grown in axenic culture, and is used for most biochemical studies for this reason. Drawings obtained from [www.uta.edu/chagas/html/biolTcru.html](http://www.uta.edu/chagas/html/biolTcru.html).

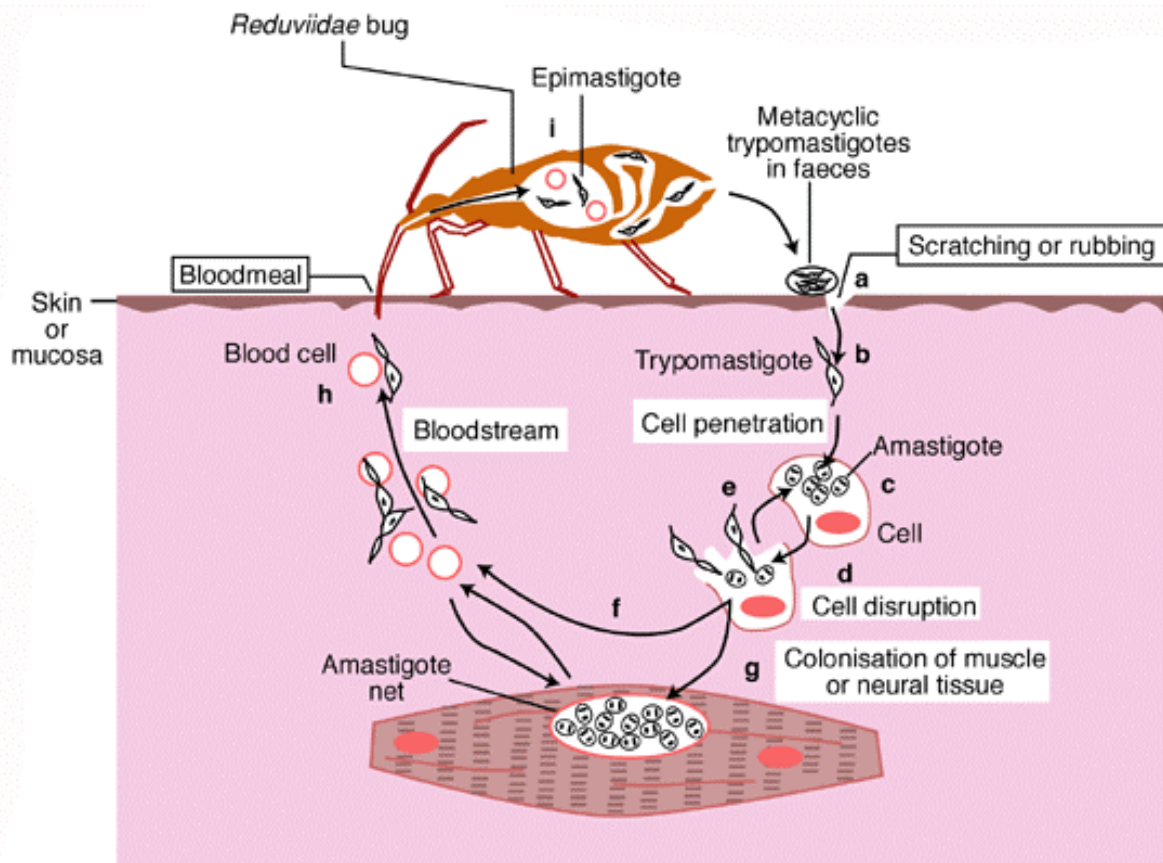


Figure 2 Schematic representation of the life cycle of the flagellate protozoan *Trypanosoma cruzi* (Macedo 2002).

Trypanosomatids are a group of flagellated parasitic protozoa that diverged from other eukaryotes about 1,8 billion years ago, this is before the appearance of red algae and fungi (Hedges 2002). They are the causative agents of endemic diseases prevalent mainly in developing countries, the most important being:

- *Leishmania* spp., which cause several forms of leishmaniasis ranging from small self-healing cutaneous leishmaniasis to possibly fatal visceral leishmaniasis
- African trypanosomes (*Trypanosoma brucei*, including several sub-species), which cause sleeping sickness in humans (*T. b. gambiense* and *T. b. rhodesiense*) and the cattle disease nagana (*T. b. brucei*).
- *Trypanosoma cruzi*, the causative agent of American trypanosomiasis or Chagas disease, affecting at least 18 million people in Latin America.

Humans are infected with *T. cruzi* when the infective stage of the parasite enters the body. A small sore often develops at the point of entrance. The acute form of the disease develops usually with fever, which in most cases may be mistaken with a prolonged flu. The lymph nodes may swell, and when the parasite entrance has been close to the eye a swelling, which closes the eye, occurs (sign of Romana, which has diagnostic value, but happens only in a small number of cases). This stage may be fatal in children, through meningoencephalitis or endomyocarditis, but in most cases the patient survives. The next phase is asymptomatic and may last for a number of years; it is the indeterminate period of the disease. However, the parasites invade and slowly affect most organs in the body; this eventually results in chronic symptoms, due to irreversible damage to the heart and intestines leading to heart enlargement and dysfunction, and/or gross enlargement of the esophagus or the colon (megaesophagus and megacolon). It is estimated that 27% of those infected develop heart problems which may cause sudden death, 6% develop abnormalities of the digestive system, and 3% show damage to the central and peripheral nervous systems (WHO 1997; Barrett et al. 2003).

## 1.2.1 Peptidases of *Trypanosoma cruzi*

### 1.2.1.1 Peptidases as virulence factors of *T. cruzi*

One of the important aspects of parasite entry into mammalian cells is *T. cruzi*-induced  $Ca^{2+}$  signaling. Trypomastigotes, the invasive stage of *T. cruzi*, elicit asynchronous and repetitive  $[Ca^{2+}]_i$ -transients in mammalian cells. Such changes in intracellular calcium levels regulate parasite invasion by promoting actin rearrangements and fusion of lysosomes and plasma membranes. Two peptidases seem to be involved in this process and both cleave precursors to yield active  $Ca^{2+}$  agonists (Burleigh and Woolsey 2002). One is a serine endopeptidase oligopeptidase B, which is postulated to cleave a parasite-derived agonist at an intracellular location (Burleigh et al. 1997). The other peptidase involved in invasion is cruzipain, which is partially secreted, apart from being abundant in lysosomes/reservosomes. At the site of secretion this peptidase cleaves host kininogen to short-lived kinins, which then promote  $[Ca^{2+}]_i$ -transients by acting on mammalian bradykinin receptors (Scharfstein et al. 2000). Apart from the two peptidases involved in  $Ca^{2+}$ -signalling, another peptidase, a prolyl oligopeptidase with collagen I degrading activity facilitates invasion into mammalian cells (Santana et al. 1997).

### 1.2.1.2 Cruzipain, the most abundant cysteine peptidase of *T. cruzi*

Several proteolytic activities have been demonstrated in epimastigotes and other developmental stages of *T. cruzi* (Cazzulo 2002). The most abundant cysteine peptidase, which accounts for up to several percent of total cell protein in epimastigotes, is cruzipain. Cruzipain belongs to clan CA and family C1 of papain like enzymes. Apart from the prodomain and catalytic domain it possesses an unusual C-terminal extension with several post-translational modifications, which is retained by the mature enzyme (Cazzulo et al. 1997). Cruzipain, especially its C-terminal domain is also an immunodominant antigen in human chronic Chagas disease (Martinez et al. 1991).

### 1.2.1.3 Cruzipain inhibitors as potential drugs for Chagas disease

The current therapy for Chagas disease is unsatisfactory because the two drugs that are used, nifurtimox and benznidazole, are significantly toxic, cure only about 60 % of acute patients and are little effective or completely ineffective in the chronic phase. The effect of irreversible diazomethane or fluoromethylketone inhibitors of cruzipain on growth and differentiation of the parasite was investigated in cell culture models of infection. The inhibitors effectively blocked the differentiation steps in the biological cycle of the parasite, and in some cases killed the trypanosomes (Meirelles et al. 1992; Harth et al. 1993; Franke de Cazzulo et al. 1994). Afterwards, a less toxic vinyl sulfone derivative was built into a pseudopeptide scaffold; experiments in mice showed that these cruzipain inhibitors rescued mice from a lethal acute infection and were also effective during the chronic phase. Treated parasites from cell cultures as well as those isolated from infected tissue showed interruption in the cell cycle due to inhibition of cruzipain processing at the Golgi complex (Engel et al. 1998). Although no effective drug has been developed yet based on a cruzipain inhibitor, a number of new classes of inhibitory compounds, both reversible and irreversible, are being developed, and cruzipain is considered as a validated target for chemotherapy.

### 1.2.2 Sequencing of the *Trypanosoma cruzi* genome

The taxon *T. cruzi* contains two defined groups, *T. cruzi* I and *T. cruzi* II and possibly others still not identified. *T. cruzi* I is mostly involved in the sylvatic transmission cycle and does not seem to infect humans, at least in the Southern Cone of Latin America. *T. cruzi* II, on the other hand, is associated with the domestic transmission cycle and infection of placental mammals, including humans. It consists of five subgroups: IIa, IIb, IIc, IId and IIe (Brisse et al. 2000). A member of the subgroup IIe, the CL Brener clone, was chosen for genome sequencing. *T. cruzi* is heterozygous at many loci with homologous chromosome pairs having different sizes (Pedroso et al. 2003; Sturm et al. 2003)

The genome was sequenced using the whole-genome-shotgun (WGS) technique, because the highly repetitive nature of the genome (> 50%) made the original “map as you go” approach unfeasible. Even so, the assembly of individual chromosome sequences is greatly impaired. The total size of the genome was estimated to be between 106,4 and 110,7 Mb. It contains about 12000 genes per haploid genome and many of them appear as dispersed tandems of repeated copies. Surface proteins (for example: trans-sialidase, mucin, gp63 surface metalloprotease) seem to be present in the highest number of copies. Interestingly, 20 out of about 12000 genes belong to cysteine peptidases (El-Sayed et al. 2005).

## 1.3 Cysteine peptidases

Peptidases in which the nucleophile that attacks the scissile peptide bond is the sulfhydryl group of a cysteine residue are termed cysteine peptidases. The catalytic mechanism is similar to that of the serine-type peptidases in that a nucleophile and a proton donor/general base are required. The proton donor in all cysteine peptidases in which it has been identified is a histidine residue, as in the majority of serine-type peptidases. In some families only the dyad of Cys and His seems to be essential for catalysis, whereas in others there is evidence that a third residue is required to orientate the imidazolium ring of the His (a role analogous to that of the essential aspartate in some serine peptidases) (Barrett 2004).

The proteolytic enzymes that depend upon a cysteine residue for activity have come from at least seven different evolutionary origins, each of which has produced a group of cysteine peptidases with distinctive structures and properties. Cysteine peptidases have been evolving for over three billion years. During such long period a single peptidase unit may have diversified first into a family of such units and then into a cluster of families that differ too much from one another to be considered homologous by the usual criteria. Despite their large differences in amino acid sequences, the families in such a cluster are ultimately related and this is shown in the conservation of their protein folds. This group of related families is called a ‘clan’ (Barrett and Rawlings 2001). The first clearly recognized cysteine peptidase was papain, and this forms the foundation of clan CA that contains about half of all cysteine peptidase families (Barrett 2004). Several additional clans have been identified since then and are organized in the MEROPS database: CD, CE, CF, CH and CL. There are several cysteine peptidases that have not yet been assigned to a clan or belong to clans whose members have different catalytic types (clans of mixed catalytic type) PA, PB or PC (Rawlings et al. 2006).

### 1.3.1 General characteristics of the clan CA

The crystal structure of papain (Figure 3) shows two structural domains that are separated by the active-site cleft. The N-terminal domain consists largely of a bundle of  $\alpha$ -helices, whereas the C-terminal domain contains a  $\beta$ -barrel. A long helix runs through the middle of the molecule, and the catalytic Cys is at its start. The sulfhydryl group of this Cys residue is involved in thioester intermediate formation on the reaction path of peptide bond hydrolysis. The second residue of the catalytic dyad is a His residue, whose imidazolium ring serves as electron donor or general base. Two other residues are important for catalysis in papain and its relatives. These are a Gln residue that helps in the formation of the ‘oxyanion hole’, an electrophilic center that stabilizes the tetrahedral intermediate, and an Asn residue (sometimes Asp), which is thought to orientate the imidazolium ring of the catalytic His. The order of these residues in the sequence is Gln, Cys, His, Asn/Asp (Barrett 2004).

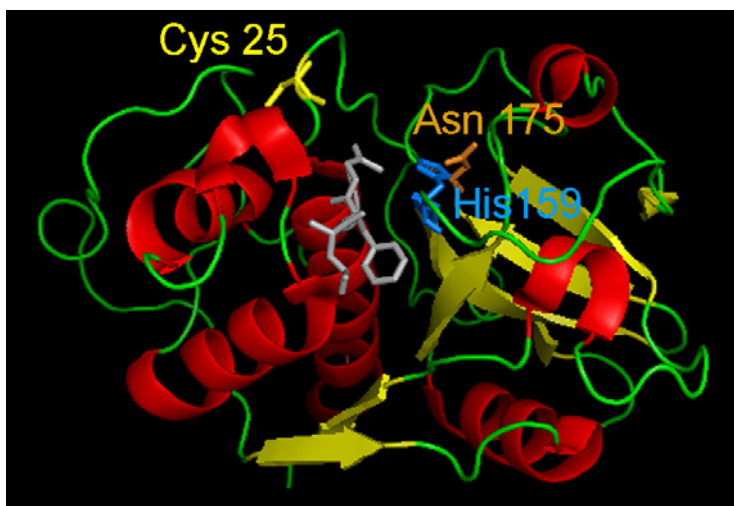


Figure 3 Crystal structure of papain in complex with zLFG-DAM. The image was prepared from the Protein Data Bank entry (1KHQ) (Janowski et al. 2004) with the PYMOL program. Chemical bonds of the catalytic residues are shown as sticks: Cys25 in yellow, His159 in blue and Asn175 in orange (numbering as in PDB entry). z-LFG-DAM is shown in gray.

Clan CA contains more than 20 families, C1 being evolutionarily oldest, most widely spread and its subfamily C1A the best studied. Members of the C1A subfamily are secretory pathway enzymes destined either to secretion or to the lysosomes. They contain a signal peptide and a propeptide at the N-terminus. The subfamily includes the plant enzymes papain, chymopapain and actinidain, mammalian lysosomal cathepsins B, H and L and also the most abundant protease of *Trypanosoma cruzi*, cruzipain (Cazzulo et al. 1997; Barrett 2004). These enzymes have rather short active-site cleft, comprising three well defined substrate binding subsites (S2, S1, and S1'). The S2 defines specificity for hydrophobic residues in case of the majority of enzymes, however, cathepsin B, cruzipain and several others show specificity towards basic residues (Turk and Guncar 2003; Barrett 2004). The compound E-64 and proteins of the cystatin family are general inhibitors of these enzymes and they can be of some use in identifying the enzymes.

### 1.3.1.1 Emerging roles of cysteine cathepsins

The cysteine peptidases first discovered – cysteine cathepsins - belong to the papain family. At first they were believed to non-selectively degrade proteins in lysosomes; recently however, they were found to be implicated in many important cellular processes. For example, Cathepsin K was shown to be crucial for normal bone remodeling and cathepsin S has a role in the processing of the MHC class II associated invariant chain, which is essential for the normal functioning of the immune system (Chapman et al. 1997; Turk et al. 2001). Apart from their function in the lysosomes, cathepsins also function outside this acidic compartment. They were recently proposed to have a signaling role in programmed cell death (Stoka et al. 2001) and even as transcriptional factor activators (Goulet et al. 2004).

### 1.3.2 C54 or the autophagin family

The first member of the C54 family, yeast Aut2/Apg4/Atg4 was discovered as a protein implicated in autophagy, a bulk cytosolic degradation pathway (Lang et al. 1998; Kirisako et al. 1999). This protease can process and deconjugate Atg8, another autophagy related protein with ubiquitin-like fold, by cleaving after a conserved Gly residue close to the C-terminal. The cleavage occurs independently of the downstream sequence. This property of ATG4 protease resembles those of deubiquinating enzymes (DUBs) and the related enzyme (Ulp-1 endopeptidase) that acts on SUMO-1/Smt3 conjugates (Wilkinson 1997; Li and Hochstrasser 1999). Later on, four human homologs were identified and were tentatively called autophagins (Marino et al. 2003).

Recently, the crystal structure of human Atg4B (autophagin-1) was deduced (Sugawara et al. 2005; Kumanomidou et al. 2006). Despite no obvious sequence homology with known proteases, the structure shows a classical papain-like fold confirming that the autophagin family (C54) belongs to the clan CA. In addition to the papain-fold region HsAtg4B has a small  $\alpha/\beta$ -fold domain, which is thought to be the binding site for Atg8 proteins. The active site cleft is masked by a loop (residues 259 – 262) implying a conformational change upon substrate binding (Figure 4). The catalytic triad is composed of Cys74, His280 and Asp278. The His residue appears at a non-canonical position with respect to the clan CA, nevertheless, the position of its side chain imidazolium ring is topologically equivalent. In addition, the evolutionary conserved Tyr54 is involved in the oxyanion hole formation, a task dependent on Gln residues in other families of the clan CA.

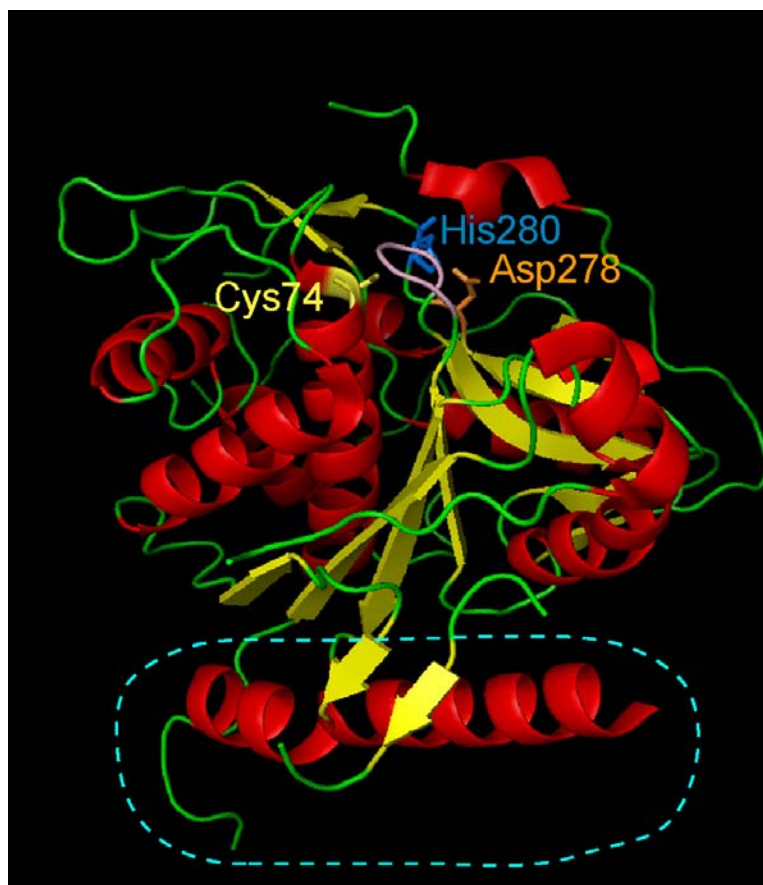


Figure 4 Crystal structure of HsAtg4B. The image was prepared from the Protein Data Bank entry (2CY7) (Sugawara et al. 2005) with the PYMOL program. Chemical bonds of the catalytic residues are shown as sticks: Cys74 in yellow, His280 in blue and Asp278 in orange (numbering as in PDB entry). The loop covering the active cleft (residues 259 – 262) is shown in pink and the  $\alpha/\beta$ -fold domain, specific for C54 family is surrounded with a cyan dashed line.

## 1.4 Autophagy

### 1.4.1 Protein turnover in the cell

A precisely regulated balance between protein synthesis and degradation is essential for the maintenance of cell homeostasis. Cells transduce environmental changes into anabolic or catabolic responses in order to adapt to adverse conditions, for example, during nutrient deprivation recycling of cellular components is necessary. The constitutive degradation of cytoplasmic proteins by the proteasome maintains the continuous protein turnover (Glickman and Ciechanover 2002). However, only short-lived cytoplasmic proteins can take part in this process, long-lived cytoplasmic proteins and organelles are recycled via another mechanism, using the degrading power of lysosomal hydrolases. This process is called autophagy and is morphologically conserved among yeasts, plants and animal cells (Marino and Lopez-Otin 2004).

Autophagy pathways are divided into three different types: macroautophagy, microautophagy and chaperone-mediated autophagy. Microautophagy denotes sequestering and subsequent degradation of the cytoplasm by invagination of the lysosomal membrane. Chaperone-mediated autophagy involves the selective delivery of cytoplasm proteins to the lysosome/vacuole after sequence motives of cytoplasmic proteins are recognized by lysosomal receptors. Macroautophagy is the most important lysosomal route for turnover of cytoplasmic components and organelles and is usually referred to as “autophagy” (Marino and Lopez-Otin 2004). In this process, portions of cytoplasm including organelles are first wrapped into double membrane vesicles called the autophagosomes, which later on fuse with lysosomes resulting in the degradation of their cargo (Figure 5).

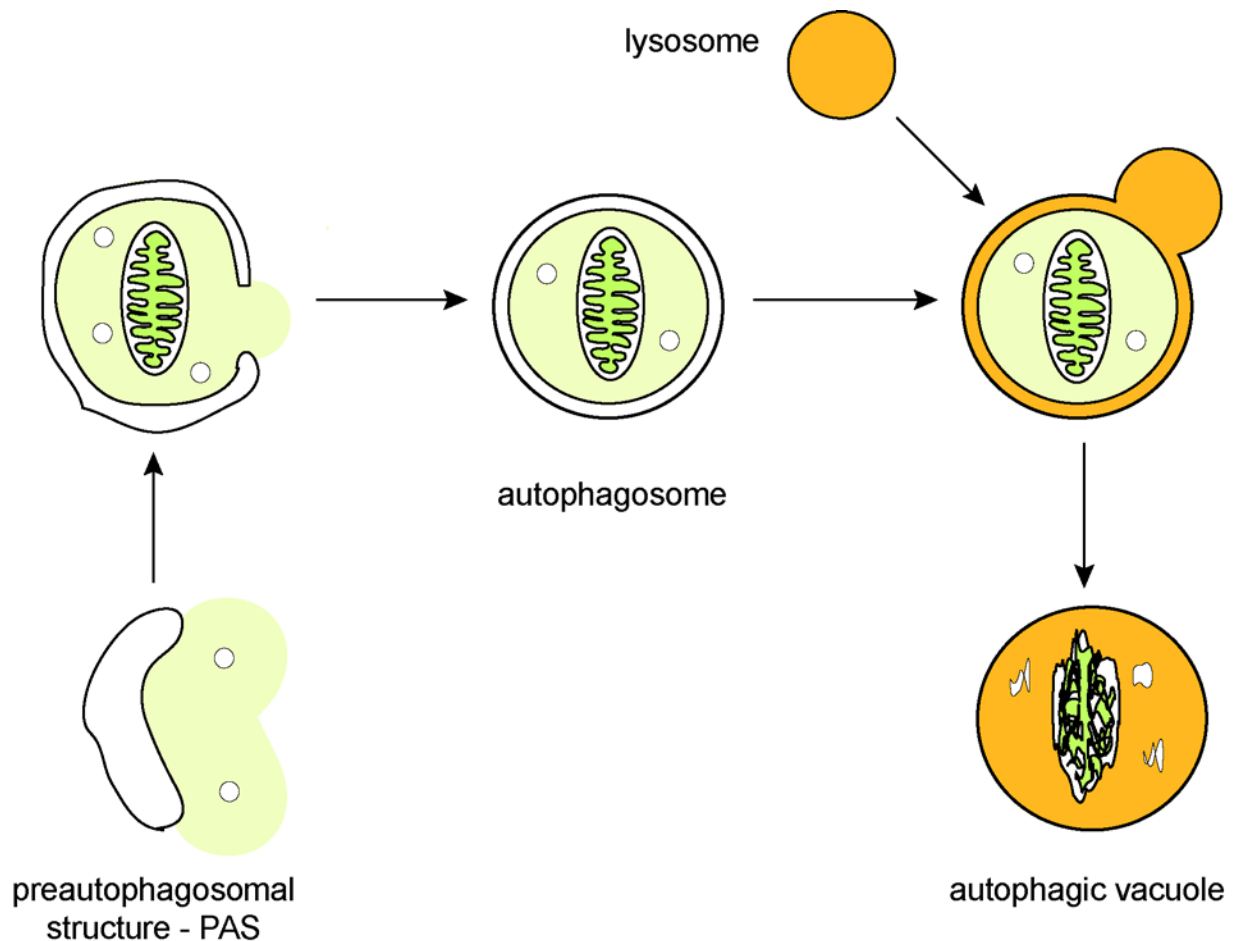


Figure 5 Crystal Scheme of macroautophagic pathway. A portion of cytoplasm is enclosed by the preautophagosomal structure to form an autophagosome. The outer membrane then fuses with lysosome to degrade inside materials. This pathway can also degrade organelles such as mitochondria and peroxisomes (Marino and Lopez-Otin 2004).

### 1.4.2 Biological role of autophagy

In a unicellular organism such as yeast the primary role of autophagy is a response to stress, usually resulting from nutrient deprivation. However, autophagy also has homeostatic and biosynthetic functions. When peroxisomes are no longer necessary, they are degraded through a specific type of autophagy called pexophagy (Kim and Klionsky 2000). In contrast, the cytoplasm-to-vacuole pathway (Cvt pathway) is a biosynthetic pathway used to deliver resident vacuolar hydrolases aminopeptidase I (API) and  $\alpha$ -mannosidase to the vacuole. The Cvt pathway uses most of the components needed for the degradative autophagy pathway (Scott et al. 1996; Klionsky 2005).

In other organisms autophagy may play diverse roles. It may promote a type of programmed cell death, distinct from apoptosis termed type II programmed cell death. It is also involved in a range of normal developmental processes, such as: sporulation in yeast, differentiation steps in *C. elegans*, *Drosophila melanogaster* and *Dictyostelium discoideum* and extension of lifespan as a consequence of caloric restriction (Levine and Klionsky 2004; Klionsky 2005). The pathway might also act as a part of innate immune response against cell invading bacteria and viruses, however, autophagy can also be subverted by pathogens to establish a replicative niche within the host cell (Dorn et al. 2002; Kirkegaard et al. 2004; Nakagawa et al. 2004). Autophagy has also been linked to several diseases: cancer (Yue et al. 2003), cardiomyopathy and neurodegenerative disorders such as Alzheimer's, Parkinson's and Huntington's disease and prion diseases (Yuan et al. 2003; Klionsky 2005).

### 1.4.3 Molecular mechanism of autophagy

Morphological changes typical of autophagy were first observed and characterized in mammalian cells. On the other hand, molecular components of autophagy were identified in yeast due to easy genetic manipulation. Subsequent studies revealed a striking conservation of the molecular machinery of autophagy throughout the eukaryotic kingdom (Reggiori and Klionsky 2002; Klionsky 2005). The nomenclature of genes and proteins involved was recently unified for all species. "ATG" followed by a number denotes a gene involved in autophagy and the corresponding protein is termed "Atg" followed by the same number. 27 genes have been identified so far

which are involved predominantly in autophagy. (Klionsky et al. 2003).

Autophagy can be divided into several discrete steps (Klionsky 2005):

- induction
- cargo selection and packaging
- nucleation of vesicle formation
- vesicle expansion and completion
- retrieval
- targeting, docking and fusion of the autophagosome with the lysosome/vacuole
- breakdown of the intraluminal vesicle

One of the most important regulatory components for the induction of autophagy is the protein kinase TOR (target of rapamycin) (Noda and Ohsumi 1998). TOR causes hyperphosphorylation of Atg13 which causes reduced interaction of this protein with Atg1 and subsequent reduction of autophagy. If TOR is inhibited by starvation or treatment by rapamycin, Atg13 is dephosphorylated, which allows induction of autophagy. TOR also affects several transcription and translation factors related to autophagy (Klionsky 2005). In addition, autophagy is regulated by class III phosphatidylinositol 3-kinase (PI3K). Autophagy is readily inhibited by 3-methyladenine, wortmannin and LY294002 all potent inhibitors of PI3K (Marino and Lopez-Otin 2004).

Autophagy is generally considered to be a non-specific process where portions of cytoplasm are randomly incorporated into the autophagosomes. However, several exceptions can be found to this rule, yeast Cvt-pathway and pexophagy being the most prominent ones. Atg11 and Atg19 are believed to be responsible for selective packaging to the Cvt-vesicles (Klionsky 2005).

Vesicle nucleation is a step little understood in autophagy. The source of the autophagosomal membrane is still not clear, however, endoplasmic reticulum and de novo formation in the cytosol seem to be possible hypotheses (Figure 5) (Reggiori et al. 2004). Many Atg proteins transiently localize to the preautophagosomal structure (PAS) in yeast but the proteins that play a role in the nucleation have not been clearly identified. Nevertheless, PI3K seems to function primarily in the PAS (Kametaka et al. 1998; Klionsky 2005).

Vesicle expansion and completion is regulated by two sets of components that involve ubiquitin-like proteins (Ohsumi 2001). Atg8 is a ubiquitin-like protein that is synthesized with a short C-terminal peptide which is cleaved soon after translation by Atg4 protease or the autophagin (see above). This exposes a Gly residue that is then covalently attached to phosphatidylethanolamine (PE) and the Atg8 comes from soluble to membrane-associated form (Kirisako et al. 1999). Atg8 is the only known vesicle associated protein that is thought to play a structural role and is involved in vesicle enlargement. It has been widely used as autophagosomal marker in electron and fluorescent microscopy observations of autophagy (Kabeya et al. 2000). The absence of Atg8 in yeast prevents Cvt-vesicle formation in normal growth conditions, however, in starvation conditions aberrantly small autophagosomes are formed. Atg12 is another ubiquitin like protein. It is covalently attached to Atg5 (Kametaka et al. 1996). A third protein Atg16 multimerizes and links the Atg12-Atg5 conjugate to form a tetrameric complex (Mizushima et al. 1999). The function of this protein complex is not known but it might act as a transient coat (Figure 6) (Klionsky 2005).

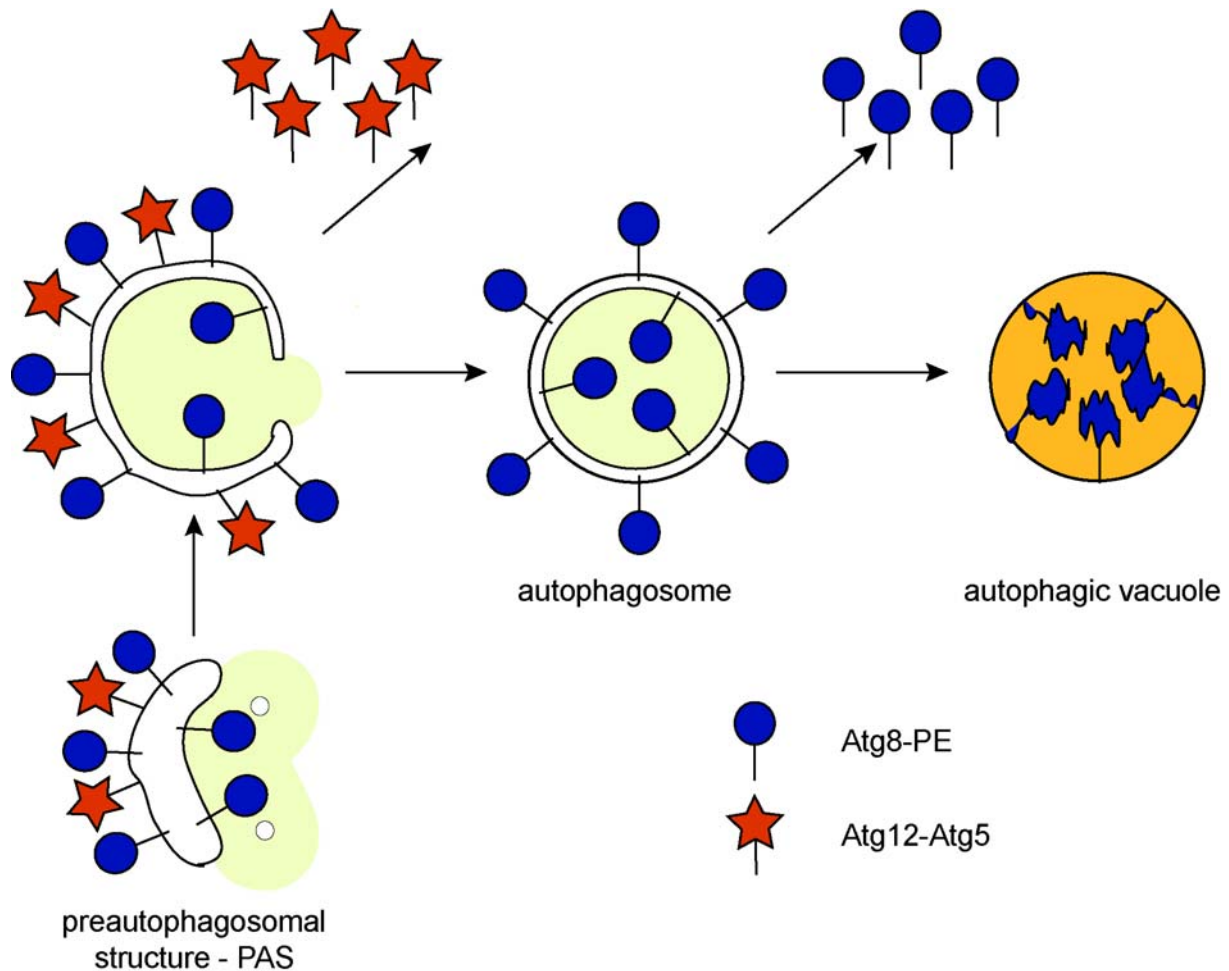


Figure 6 The role of two ubiquitin like proteins Atg8 and Atg12 in vesicle expansion and completion. Atg8 is cleaved at the C-terminal by Atg4 (autophagin) to expose a Gly residue, which is then conjugated to phosphatidylethanolamine (PE). Atg8-PE is inserted into both faces of the preautophagosomal structure and remains inserted in inner and outer autophagosome membrane. Atg8 from the outer membrane is released back to the cytosol in a deconjugation reaction mediated by Atg4 (autophagin) peptidase. Atg12 is conjugated to Atg5 and together with Atg16 the complex is believed to form a transient coat during vesicle expansion.

Interestingly, several Atg8 homologs are found in mammalian cells. The most abundant is microtubule associated protein 1 light chain 3 (MAP 1 LC3) that first drew attention for its microtubule binding properties (Mann and Hammarback 1994). Later on, its important role in autophagy was elucidated (Kabeya et al. 2000). GATE 16 (Golgi associated ATPase enhancer) is believed to play a role in intra-Golgi transport and post mitotic Golgi reassembly (Sagiv et al. 2000). GABARAP (gamma aminobutyric acid receptor-associated protein) localizes to intracellular membranes including Golgi apparatus and post-synaptic cisternae and has been proposed to be involved in intracellular membrane trafficking (Kneussel 2002). In addition, a more recent study suggests that all three proteins are localized to autophagosomal membranes (Kabeya et al. 2004).

Most of the Atg proteins are soluble and can cycle off from the vesicle after completion. Atg8 is an exception to this rule as it is anchored to the membrane by its PE moiety. However, Atg4 (autophagin) apart from the peptidase activity is also able to deconjugate Atg8 from this lipid (Figure 6). It is not known when exactly this occurs, nevertheless, Atg8 could also be involved in the process of autophagosome fusion with the lysosome/vacuole, which is generally believed to be mediated by the SNARE, SNAP, NSF and GDI families of proteins (Klionsky 2005).

The hydrolases involved in the last stage of autophagy, the degradation of the inner vesicle and its contents are probably poorly conserved among the species. Resident lysosomal/vacuolar peptidases, lipases, nucleases, glycosidases etc. are of course essential for this process.

## 1.5 Clan CD cysteine peptidases

The first crystal structures of caspases showed that their active site Cys and His residue are positioned at the ends

of strands, embedded in a unique  $\alpha/\beta$ -fold that does not resemble the folds in previously known clan CA peptidases (Walker et al. 1994; Wilson et al. 1994) (Figure 7). Later on, catalytic Cys and His residues were found in a similar context in several other peptidases: human legumains or hemoglobinas, gingipains from *Porphyromonas gingivalis*, clostripains from *Clostridium* sp. (Chen et al. 1998) and more recently in separases, eukaryote-specific sister chromatid-separating proteases (Uhlmann et al. 2000). All these proteases and several others therefore comprise the clan CD (Barrett 2004).

The peptidases in clan CD are all endopeptidases with restricted specificity dominated by selectivity for the P1 residue of the substrate. Thus, in the caspase family cleavage occurs exclusively after Asp, in legumains after Asn, in clostripains and separases after Arg, and in gingipains after Arg or Lys depending on the peptidase. This P1-dominated type of specificity is quite unlike the clan CA (Barrett 2004). Therefore, in contrast to most enzymes in clan CA, none of these peptidases are inhibited by E-64 because this compound lacks a suitable amino acid residue at the P1 site (Mottram et al. 2003). However, recently developed compounds aza-peptide epoxides were shown to be potent and specific inhibitors of clan CD peptidases. The aza-Asn derivatives are effective legumain inhibitors, while the aza-Asp epoxides were specific for caspases. The inhibitors are little or no inhibitory to other proteases such as chymotrypsin, papain, or cathepsin B (Asgian et al. 2002).

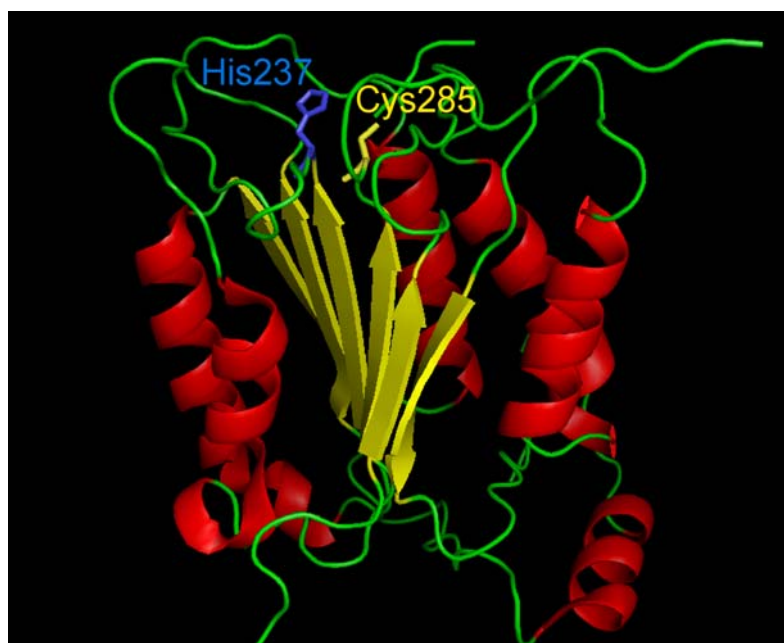


Figure 7 Crystal structure of caspase-1 representing the conserved structural core of the clan CD cysteine peptidases. The image was prepared from the Protein Data Bank entry (1ICE) (Wilson et al. 1994) with the PYMOL program. Chemical bonds of the catalytic residues are shown as sticks: Cys285 in yellow and His237 in blue (numbering as in PDB entry).

Peptidase families of the clan CD have very diverse phyletic distributions. Legumains and separases are known to be highly conserved in all eukaryotes but so far have not been detected in prokaryotes (Aravind and Koonin 2002). Caspases are restricted in their distribution to animal lineage, paracaspases, their distantly related group, are found in *Dichtyostelium* and metacaspases, the most distant group of the superfamily are present in plants, fungi and early branching eukaryotes but not in animals (Uren et al. 2000; Aravind et al. 2001). In contrast, clostripains and gingipains are limited to few bacterial lineages with no close homologs found elsewhere (Aravind and Koonin 2002).

## 1.5.1 Characteristics of caspases, paracaspases and metacaspases

### 1.5.1.1 Caspases

As expected, caspases show a His – Cys order of catalytic residues, characteristic of the clan CD. They are synthesized as a single-chain precursor, and activated by cleavage after several aspartyl bonds. The mature endopeptidase is a heterodimer of a heavy chain of about 20 kDa (p20 subunit) and a light chain of about 10 kDa (p10 subunit) (Yamin et al. 1996; Barrett 2004). In single-chain precursors the subunits are connected with a short peptide. In addition, N-terminal prodomains are present, some containing CARD (caspase recruitment domain) or DED (death effector domain) interaction modules (Figure 8) (Grutter 2000).

To date, 14 mammalian caspase sequences have been reported, of which eleven are of human and three of

murine origin. According to the length of the prodomain initiator and executioner caspases can be identified. Initiator caspases have long proregions (more than 90 amino acid residues) with CARD and DED domains and they are activated in apoptosis by clustering and high local concentration of zymogens, which show limited catalytic activity. Active initiator caspases can then activate executioner caspases by proteolytic cleavage after conserved Asp-residues (Grutter 2000).

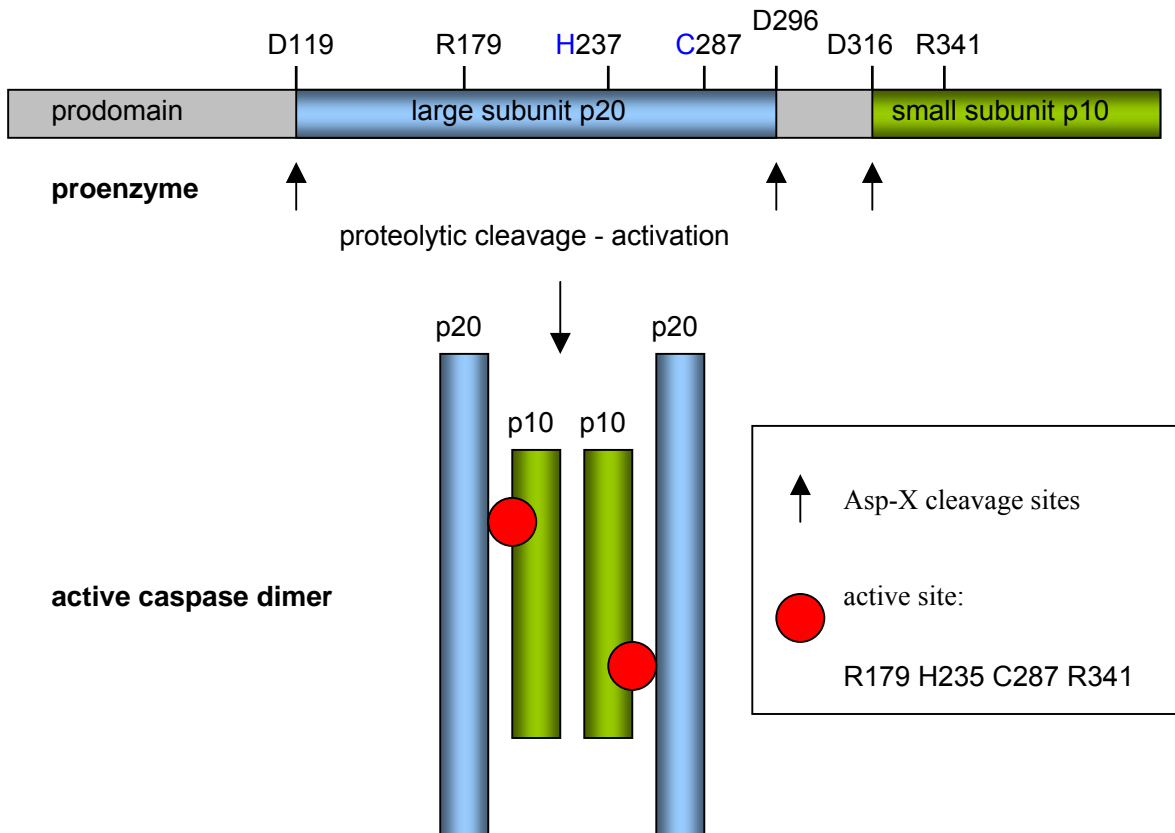


Figure 8 Schematic representation of the proteolytic activation of caspases. Caspases are synthesized as single-chain precursors. Activation proceeds by cleavage of the N-terminal peptide at Asp119 and at the conserved sites Asp296 and Asp316 (all caspase-1 numbering convention), leading to the formation of a large p20 subunit and a small p10 subunit. The activity- and specificity-determining residues Arg179, His237, Cys285 and Arg341 are brought into the characteristic structural arrangement for catalysis. Cys285 is the catalytic nucleophile and His237 represents the general base (Grutter 2000).

The caspase fold consists of a large p20 subunit and a small p10 subunit. Each p20/p10 heterodimer comprises six  $\beta$  strands, five parallel and one antiparallel, that form a twisted  $\beta$ -sheet structure with two  $\alpha$  helices on one side and three  $\alpha$  helices on the other, running approximately parallel to the  $\beta$  strands. The active site cavity is located at the C-terminal end of the parallel  $\beta$  strands within each p20/p10 heterodimer. Two heterodimers associate and are related by a twofold axis perpendicular to the plane. The entire quaternary arrangement can be described as an (p20/p10)<sub>2</sub> tetramer composed of two symmetry related p20/p10 heterodimers as the folding unit. Recognition of the substrate occurs predominantly in a cleft formed by the loop regions of the p20 and p10 $\beta$  subunits. The cleft recognizes a tetrapeptide located N-terminal to the canonical cleavage site Asp-X (Figure 7; Figure 8) (Grutter 2000).

### 1.5.1.2 Paracaspases and metacaspases

Paracaspase and metacaspase genes were identified as distant caspase homologs by screening genomes of different organisms with the PSI-BLAST program. At first, paracaspases were found in the human genome, in *Caenorhabditis elegans* and in the slime mold *Dichtyostelium discoideum* (Aravind et al. 1999). Further on, more distantly related sequences were found in yeast, plants and protozoa and were termed metacaspases. Interestingly, the latter do not seem to be present in the genomes of metazoans (animals). All these sequences conserve the His-Cys catalytic dyad of the clan CD (Figure 9; Figure 10) (Uren et al. 2000).

A spectrum of conserved domains is also present in paracaspases and metacaspases outside their caspase-

related portions (Figure 9). Similarly to traditional caspases that contain CARD and DED homotypic interaction modules, paracaspases of humans, zebrafish and *C. elegans* contain a death domain (DD) followed by one or two immunoglobulin (Ig) domains. Equivalently to CARD and DED, the DD is a homotypic interaction module. Metacaspases from yeast and some from plants contain a Pro-rich region at their N terminus (Figure 5A). The plant metacaspases can be divided into two subclasses based on the sequence similarity within their caspase-like domain and their overall domain structure. Type I plant metacaspases contain a prodomain that consists of a Pro-rich region and a Zn finger motif typical of plant proteins that function in the hypersensitive response pathway. Type II plant metacaspases possess no obvious prodomain but have a conserved insertion of approximately 180 amino acids between the regions corresponding to caspase p20 and p10 subunits (Uren et al. 2000).

Initial experimental analysis of human paracaspase revealed that it does not appear to function as a classical caspase. It does not induce apoptosis when expressed in mammalian cells, it does not undergo autoprocessing and it does not seem to cleave typical synthetic substrates of caspases (Uren et al. 2000). Further on, a more detailed biochemical study of the caspase-like catalytic domain of the paracaspase failed to detect any amidolytic activity using combinatorial peptide library approach. However, paracaspase did bind a Leu-based acyloxymethyl ketone probe that covalently labels cysteine peptidases. Therefore paracaspase seems to show specificity for hydrophobic residues at P1 site. Nevertheless, the probe did not bind to the predicted catalytic Cys residue based on sequence comparisons with other clan CD cysteine peptidases, but to a Cys residue juxtaposed to the catalytic site of caspases (Snipas et al. 2004). Further experiments will have to be done to see whether paracaspase is a peptidase and to determine its specificity.

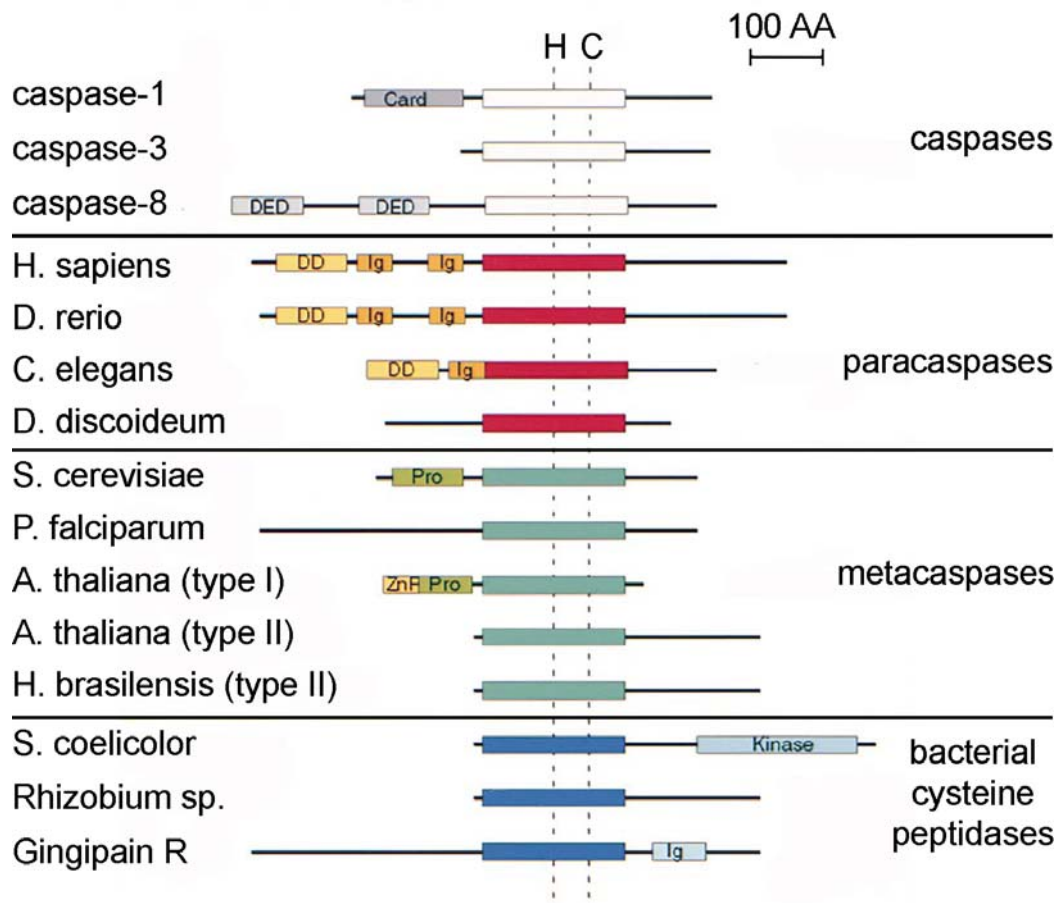


Figure 9 Domain structure of caspases, paracaspases and metacaspases. Traditional caspases contain a C-terminal caspase domain (empty box) and in some cases a prodomain with CARD or DED oligomerization motifs. Paracaspases, metacaspases, and a number of bacterial cysteine proteases also contain a predicted caspase-like proteolytic domain. Metazoan paracaspase prodomains encode a death domain (“DD”) and either one or two Ig domains. Metacaspases fall into two classes, type I and type II, based on overall structure and the level of sequence similarity. Type I metacaspases from fungi and plants have prodomains with a proline-rich repeat motif (“Pro”). Plant type I metacaspases also have a zinc finger motif (“Zn”) similar to those of the plant hypersensitive response protein lsd-1. Type II metacaspases (in plants) have no prodomain but an insertion of approximately 200 amino acids directly C-terminal to their p20-like subunit. pk3, a protein from *Streptomyces coelicolor*, contains a caspase-like domain and a protein kinase domain. *Rhizobium* sp. plasmid also encodes a caspase-like protein. Gingipain R has a caspase-like catalytic domain (empty box) followed by an Ig-like domain. All sequences are represented as their unprocessed zymogen forms (Uren et al. 2000).

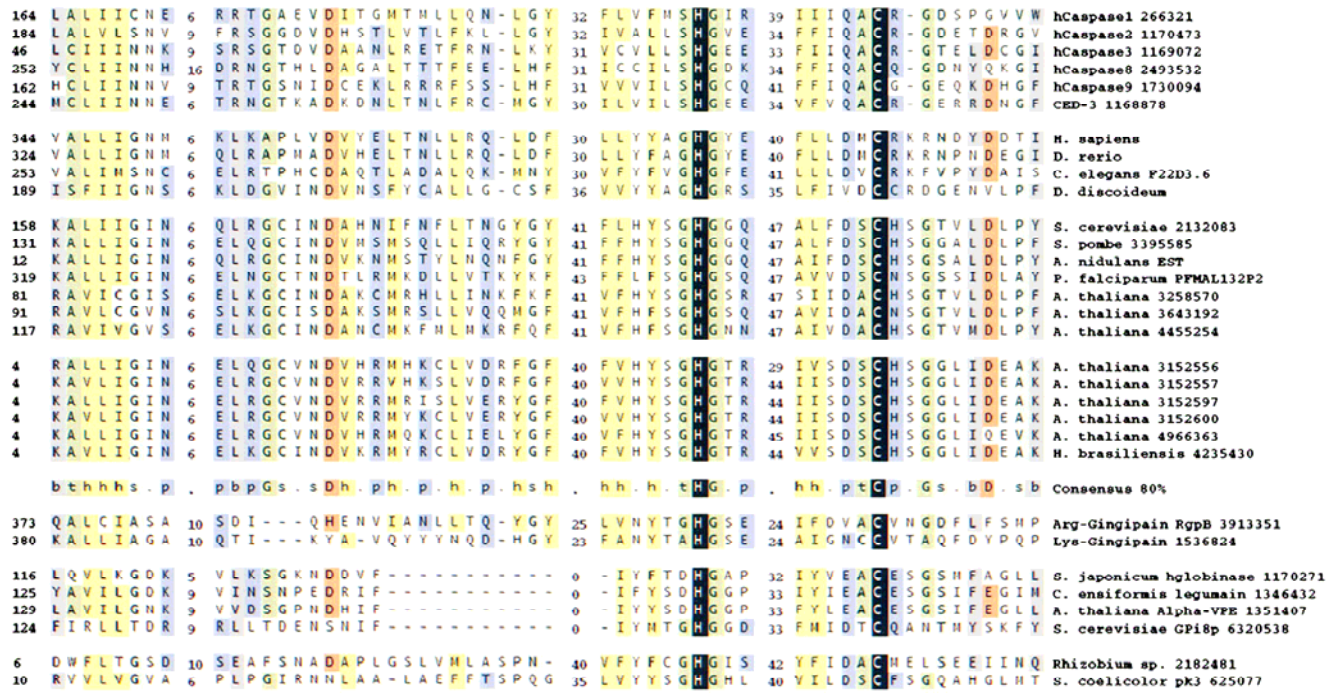


Figure 10. Alignment of the p20 subunits of caspases, paracaspases, and metacaspases. From top to bottom the sequences are grouped as caspases, paracaspases, type I metacaspases, type II metacaspases, gingipains, miscellaneous eukaryotic cysteine peptidases, and miscellaneous bacterial cysteine peptidases. The 80% consensus is compiled from the caspase, paracaspase, and metacaspase sequences. Residues matching the 80% consensus are shaded as follows: hydrophobic (h, yellow); polar (p, blue); charged (c, red); tiny (t, dark green); small (s, light green); big (b, gray). The Cys-His catalytic diad is shaded black (Uren et al. 2000).

Plant type II metacaspases have been recently characterized biochemically. *Arabidopsis thaliana* metacaspase-4 and metacaspase-9 were expressed in *E. coli* and they showed catalytic cysteine-dependent autocatalytic processing to p20-like and p10-like subunits (Figure 4). Interestingly, they were shown to be specific for Arg/Lys residues at P1 position. Atmca4 seems to be active at neutral pH whereas Atmca9 is active at pH 5,0 to 5,5 (Vercaemmen et al. 2004). Type I metacaspases still lack biochemical characterization; however, a study in *Saccharomyces cerevisiae* indicates that they could have similar specificity as the mammalian caspases (Madeo et al. 2002).

### 1.5.1.3 Cysteine peptidases as signaling molecules – apoptosis

In contrast to clan CA peptidases, where signaling roles are just starting to be envisioned, caspases are well known to be involved in inflammation and programmed cell death signalization. Programmed cell death is essential for development and homeostasis of multicellular organisms. Eukaryotic cells that die in this way exhibit surprisingly conserved morphological features, which depend on the common program termed apoptosis (Leist and Jaattela 2001). The characteristics that differentiate apoptosis from other, more primitive forms of programmed death are:

- condensed chromatin of regular shapes
- transfer of phosphatidylserine to outer membrane layer
- cytoplasm shrinkage
- zeiosis (dynamic membrane blebbing)
- degradation of genomic DNA

Cells, processed in this way – also termed apoptotic bodies – are then removed by phagocytosis. In this way, their contents are not spilled and inflammatory response is avoided.

The highly regulated apoptotic process involves an intricate cascade of events. Currently, two major pathways, in which apical caspases are involved, are described. One relies on a cell surface stimulus and is known as the extrinsic pathway. The death signal is transmitted through the binding of an extracellular death ligand, such as

tumor necrosis factor (TNF), to its receptor. For both the ligands and the receptors, a number of different homologous proteins are known that fulfil different functions in cells that need to die during development, following viral infections or during development of the immune system. The death receptors transmit signals to the interior of the cells, where the apical peptidases of the extrinsic pathway, caspase-8 and caspase-10, are recruited (Ashkenazi and Dixit 1998). The intrinsic pathway occurs as a consequence of cellular stress and is mediated by cytochrome c in the mitochondrion. In this case, caspase-9 is activated (Green and Reed 1998). Both pathways lead to the activation of downstream executioner caspases, which, in turn—by limited proteolysis— inactivate or activate their specific cellular protein targets (Figure 11). The effects of these cleavage events are the modification of the function of the target proteins, which results in disassembly of the cell and marking of the dying cell for disposal. Human caspase-1 and mouse caspase-11 function mainly as cytokine processors (Figure 7) (Green 1998; Grutter 2000).

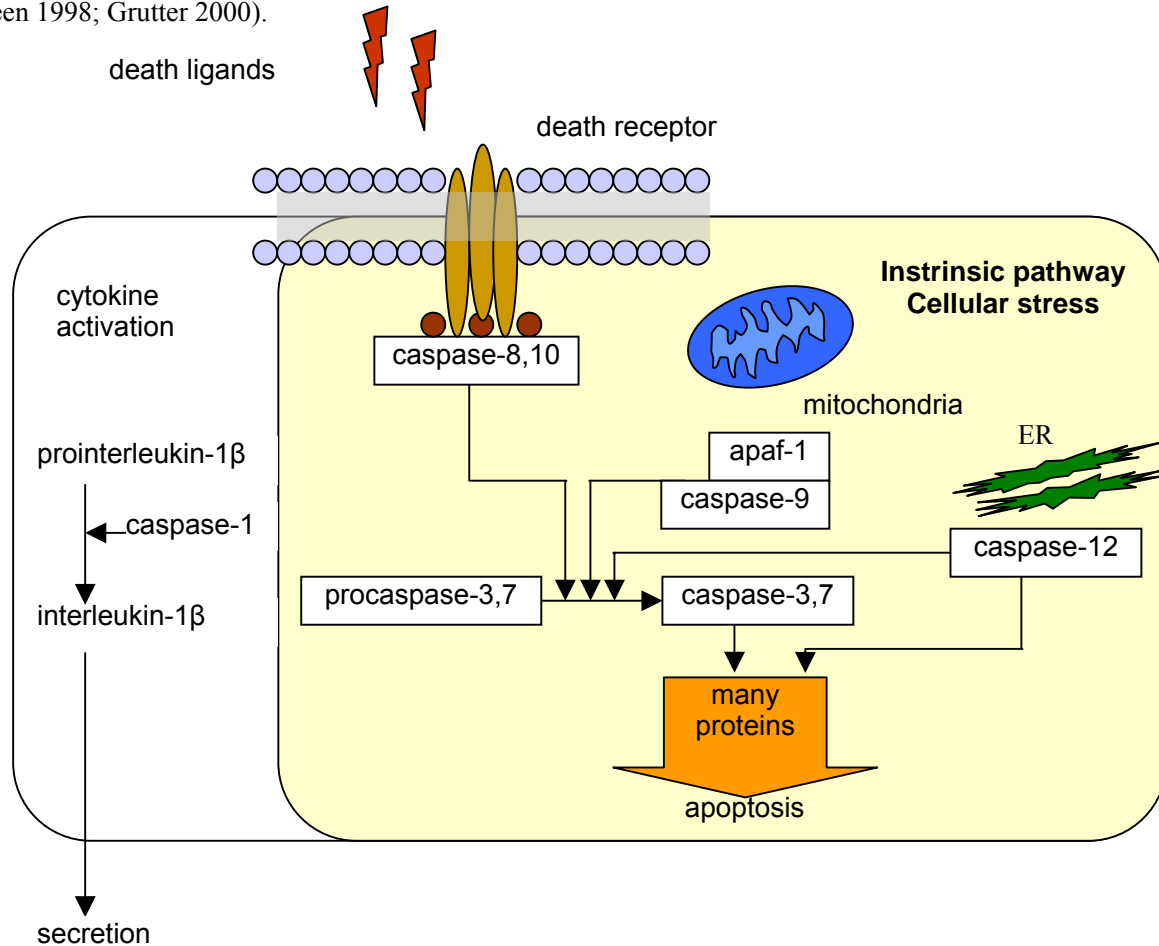


Figure 11 Schematic representation of the known apoptotic pathways in which caspases are involved. The cytokine pathway leading to inflammation is activated by caspase-1 (Grutter 2000).

#### 1.5.1.4 Biological function of the mammalian paracaspase

Although its biochemical characteristics are still largely unknown, mammalian paracaspase was found to take part in an important signaling pathway. The human paracaspase (also termed MALT1) prodomain was found to bind Bcl10, a protein involved in the t(1;14)(p22;q32) translocation of mucosa-associated lymphoid tissue (MALT) lymphoma. Another MALT lymphoma translocation t(11;18)(q21;q21), fuses the IAP-2 gene to the paracaspase. Both fusions were found to be potent activators of NF- $\kappa$ B. (Uren et al. 2000).

Further on, it was found out that paracaspase and Bcl10 are essential for the activation of I $\kappa$ B kinase (IKK) and NF- $\kappa$ B response to T cell receptor (TCR) stimulation (Ruefli-Brasse et al. 2003). IKK phosphorylates I $\kappa$ B, the inhibitor which retains NF- $\kappa$ B in the cytoplasm. This phosphorylation causes NF- $\kappa$ B to detach from the inhibitor and translocate to the nucleus. In a detailed study, the following model of IKK activation was proposed. Engagement of TCR with MHC/antigen complex together with costimulation of CD28 initiates a tyrosine phosphorylation cascade that leads to the activation of PKC $\theta$  and subsequent recruitment of the CARD domain-containing adaptor protein BCL10 to the immunological synapse. The lipid raft environment in the immunological synapse promotes the oligomerization of BCL10, which in turn binds to the Ig domains of the paracaspase and

promotes paracaspase oligomerization. Oligomerized paracaspase binds to the IRAK family protein TRAF6 through its C-terminal TRAF6 binding sites and induces the oligomerization of TRAF6. The ubiquitin ligase activity of TRAF6 is activated to mediate K63 polyubiquitination of itself and other substrates. Ubiquitinated TRAF6 then activates TAK1 kinase, which then phosphorylates IKK $\beta$  in the activation loop, thereby activating IKK (Sun et al. 2004).

Interestingly, genetic ablation studies show that paracaspase from *Diclyostelium discoideum* is probably not involved in vacuolar developmental death process of this organism, therefore, its role in this unicellular remains obscure (Roisin-Bouffay et al. 2004).

## 1.6 Programmed cell death in plants and unicellular organisms

### 1.6.1 Programmed cell death in plants

In comparison with the detailed studies of apoptosis in animals, programmed cell death in multicellular plants has long remained neglected. The best studied form of PCD in plants is the ‘hypersensitivity response’ that plays an important role in plant defenses against infectious pathogens and shares some phenotypic features of apoptosis (Levine et al. 1996). The ‘hypersensitivity response’ is a process of self-destruction that occurs in the infected cells and in the neighboring cells in response to the presence of the microorganism, and is genetically regulated. Cysteine peptidase activity has been associated with plant cell death and cystatin, an inhibitor of clan CA peptidases prevented death (Solomon et al. 1999). Interestingly, although no direct caspase homologs can be detected in plant genomes, caspase specific inhibitors were also shown to inhibit plant cell death (del Pozo and Lam 1998) and VEID-ase was shown to be a principal caspase-like activity involved in plant cell death (Bozhkov et al. 2004). Now that metacaspases have been identified in plant genomes it will be interesting to observe their role in the process (Ameisen 2002).

### 1.6.2 Programmed cell death in unicellular organisms

#### 1.6.2.1 Overview

To date, ten species of unicellular organisms have been described to undergo some form of regulated cell death. Their phyletic divergence is believed to range from around two to one billion years ago. These species include (reviewed in (Al-Olayan et al. 2002; Ameisen 2002):

- the kinetoplastid parasites *Trypanosoma cruzi*, *Trypanosoma brucei rhodesiense*, *Trypanosoma brucei brucei*, *Leishmania amazonensis*, *Leishmania donovani* and *Leishmania major* that are believed to be amongst earliest diverging eukaryotes
- the apicomplexan parasite *Plasmodium sp*
- the free living slime mold *Diclyostelium discoideum*, a single celled organism whose cells can transiently form a multicellular aggregated body
- the free living ciliate *Tetrahymena thermophila*
- the free living dinoflagellate *Peridinium gatunense*
- the yeast *Saccharomyces cerevisiae*

Several morphological features, resembling animal apoptosis were observed in death processes of these organisms. Some of them are: maintenance of plasma membrane integrity, phosphatidylserine exposure, loss of mitochondrial membrane potential, nuclear chromatin condensation and DNA-fragmentation (ladder). The stimuli usually used for the induction of death are different antimicrobial drugs, nutrient deprivation, oxidative stress, heat shock, etc. General molecular mechanisms of these processes remain poorly understood; however, some features are becoming to be elucidated in individual organisms.

#### 1.6.2.2 Programmed cell death in *Saccharomyces cerevisiae*

Morphological features of apoptosis were seen in yeast subjected to oxidative stress, in knock-out strain for *CDC48* ATPase gene or yeasts overexpressing a mammalian apoptosis inducer Bax (Latterich et al. 1995; Ligr et al. 1998; Madeo et al. 2002). In all cases accumulation of active oxygen species (ROS) was observed implying that ROS are responsible for expression of the apoptotic phenotype.

Interestingly, yeast metacaspase, also termed yeast caspase 1, seems to take part in PCD execution. Moreover, yeast metacaspase shows a similar processing pattern to mammalian caspases and cleaves synthetic substrates with Asp residue at P1 site (Madeo et al. 2002). However, these results have been questioned recently, since some

metacaspases probably cleave after Arg or Lys residues. Moreover, another study claimed that caspase specific fluorescent probes bind unspecifically to dead yeast cells, irrespective of whether they express the metacaspase or not (Vercammen et al. 2004; Wysocki and Kron 2004). Therefore, whether yeasts undergo programmed cell death and whether caspase-like activity is involved, remains an open question.

### 1.6.2.3 Programmed cell death in kinetoplastids

Programmed cell death can be induced by a variety of stimuli in *Leishmania* sp. These include stationary phase cultures, nitric oxide, staurosporine, antileishmanial drugs and even low concentrations of detergents. Several features of animal apoptosis are observed, the most prominent being a nuclear apoptotic phenotype with condensation of chromatin and DNA-degradation, loss of mitochondrial membrane potential, cytochrome c release, phosphatidylserine exposure and cysteine peptidase activation. (Arnoult et al. 2002; Zangger et al. 2002). Some molecular features were also elucidated. For example, purified mammalian Bax protein is able to provoke cytochrome c release from purified mitochondria of *Leishmania*. Two nucleases, whose activity does not depend on  $Ca^{2+}$  or  $Mg^{2+}$ , were found responsible for the observed nuclear changes and, moreover, extracts of *Leishmania* undergoing PCD were able to induce an apoptotic phenotype in isolated mammalian nuclei. Cysteine peptidase activities were augmented and lysosomal papain-like peptidases identified as a possible cause. A model was proposed in which due to leakage through the very fragile lysosomal membrane, nucleases, peptidases and other hydrolytic enzymes are released first into the cytosol and then into the nucleus, which eventually causes the observed apoptotic-like phenotype (Zangger et al. 2002). Interestingly, several studies in mammalian cells observed a related mechanism of lysosomal leakage coupled to apoptosis (Cirman et al. 2004), however, much more complex and better regulated caspase dependent mechanisms seem to have prevailed in multicellular organisms. *T. brucei* shows similar morphological characteristics in response to prostaglandin D<sub>2</sub> addition to *in vitro* cultures of the bloodstream form of the parasite (Figarella et al. 2005).

Axenic cultures of *Trypanosoma cruzi* epimastigotes can be grown *in vitro* in suitable media. Epimastigotes proliferate and progressively differentiate into non-dividing metacyclic trypomastigotes (Camargo 1964). It has been found that this process is associated with death of epimastigotes, which denotes the stationary phase of the culture. Light microscopy reveals that dead epimastigotes have a spheroid-like shape and have lost motility. Under an electron microscope, these cells show morphological changes typical of apoptosis: membrane blebbing (pitting), margination and condensation of nuclear chromatin, DNA-fragmentation (Ameisen 1995). It was also shown that this process can be greatly accelerated by exposing epimastigotes to unheated human serum as a source of complement and, in addition, due to the synchronous induction, DNA is cleaved to oligonucleosomal fragments showing a ladder in agarose electrophoresis gels. In contrast, metacyclic trypomastigotes are insensitive to complement exposure. Epimastigotes can be stimulated to “apoptotic” death also by the antibiotic G418 (geneticin); however, exposure to saponin causes a much more rapid “necrotic” type of death (Ameisen 1995). Further on, caspase-like activity was implicated in the process and death was shown to be inhibited by nitric oxide or polyamines (Piacenza et al. 2001).

## 1.6.3 Theoretical considerations of programmed cell death in unicellular organisms

### 1.6.3.1 Possible origin of programmed cell death

Programmed cell death was originally thought to be limited to multicellular organisms. The first reason for this is that cells of a multicellular organism are condemned to live together in a body and their genes can be transmitted to the next generation only if the whole body shows a successful phenotype. Therefore an ‘altruistic’ cell suicide seems justified if it benefits the survival of the body as a whole. The idea that programmed cell death emerged with multicellularity was further supported by a complementary view that such a program would be counterselected in unicellular organisms. Namely, as in unicellulars the cell is the only vehicle of its genes to the next generation, ‘selfishness’ rather than ‘altruism’ programs were postulated to be the only ones that could be selected. According to this view, if a mutation randomly appeared that would enable regulated form of death, such a mutant would be rapidly counterselected (Ameisen 2002).

However, several unicellular organisms with broad phyletic distribution show forms of regulated death and morphological similarities to apoptosis were observed (see above). In such a context it must be considered that the frontiers between unicellular and multicellular organisms are not as clear as usually believed. In fact, the slime mold *Dictyostelium discoideum* can build multicellular bodies and in this organism - on transition from unicellularity to multicellularity - regulated death can be seen as social control of cell fates in a colony of genetically equal individuals. We cannot affirm, however, that such programmed form of death was present at the beginning of the evolution of unicellular eukaryotes. Many of them, e. g. kinetoplastid protozoa are obligate parasites of multicellular organisms, therefore, programmed cell death could have evolved only after the beginning of the parasite-host relationship. (Ameisen 2002).

Nevertheless, a theory of the emergence of cell death has been postulated. It is based on addiction modules encoded on some bacterial plasmids that enable the propagation of the plasmid to future generations. Such a module consists of two genes, a toxin that is stable and long-lived and an antidote that is unstable and short-lived (Gerdes et al. 1986). If a daughter cell fails to inherit such plasmid, the long-lived toxin can exert its effect in the absence of the short-lived antidote. Such an ‘addiction module’ could then be transferred to the chromosome and, if coupled to appropriate signaling cascade, be used as a primitive death effector providing an evolutionary advantage to a colony of such bacteria. A parallel can be drawn to unicellular eukaryotes in the sense of incorporation of the mitochondrial endosymbiont. It is believed that eukaryotic cell ancestors captured bacteria of  $\alpha$ -proteobacterial origin that possessed oxidative phosphorylation systems. However, as present day intracellular bacteria, the ancient pre-mitochondrial bacteria might have invaded the pre-eukaryotic cell and employed an ‘addiction module’ coupled protein effectors to persist inside the eukaryotic cell. Later on, the genes were transferred from the mitochondrial to the nuclear genome and ‘addiction modules’ could have been selected to be suitable programmed death effectors where this feature resulted beneficial to the colony of newly formed symbiotic organisms. This is further supported by the central role of mitochondria in apoptosis of all eukaryotic cells. (Ameisen 2002).

### 1.6.3.2 Possible benefits of programmed cell death in kinetoplastids

As mentioned above kinetoplastids are of ancient evolutionary origin; however, they have subsequently evolved into obligate parasites of vertebrate and invertebrate hosts. Several additional benefits might have been attributed to *Leishmania* and the trypanosomes by a cell death program during this transition (Ameisen 2002). As infections are usually clonal, this would be complementary to the genetic equality of individuals in a colony.

One aspect is that the population of parasites in the insect vector gut must be strictly regulated in order to enable successful transition to the new mammalian host. In fact, the insect vector doesn’t seem to be affected at all by the parasitic infection so it seems that, similarly to stationary phase of in vitro cultures, death of superfluous parasites is taking place. (Welburn and Maudlin 1999). In the parasite – mammal interaction, PCD could be useful in situations where macrophage deactivation (in response to phosphatidylserine exposure in the outer membrane layer) and avoidance of inflammatory reaction are conditions for parasite survival (DosReis and Barcinski 2001). It was also pointed out that the intake of apoptotic T cells favours growth of intracellular forms of *Trypanosoma cruzi* in the infected macrophages (Freire-de-Lima et al. 2000). Further more, PCD of epimastigote stage of *Trypanosoma cruzi* can prevent an early inflammatory response in case epimastigotes accidentally enter mammalian bloodstream (Zeledon et al. 1984).

## 1.7 Initial studies of metacaspase-3 in *Trypanosoma cruzi*

### 1.7.1 Metacaspase genes in the genome of *T. cruzi*

In our previous studies we identified two metacaspase genes in *T. cruzi*, *TcMCA3* and *TcMCA5*, homologous to *TbMCA3* and *TbMCA5* from *T. brucei*. Using statistical methods *TcMCA3* was calculated to be present in approx. 16 copies per haploid genome. All copies have equal length (1074 bp), share 92 – 95% identity and predict an intact His – Cys catalytic diad. Some copies show a mutation of a conserved Gly residue for a Cys in position adjacent to the catalytic His. These copies could represent inactive proteases, otherwise widely spread among the clan CD (Kosec 2004).

We performed a Southern blot of *T. cruzi* genomic DNA, digested with various restriction endonucleases (Figure 12A). Radioactive *TcMCA3* probe was used for hybridization. *TcMCA3* copies are organized in tandem repeats, so that the 5'-end of the next gene always follows the 3'-end of the former one. The length of the repeats is 4,4 kbp, 1,1 kbp belonging to the ORF and 3,3 kbp to the intergenic region. Figure 12B shows the genome sequence data deduced for the *TcMCA3* tandem. Short sequences homologous to *T. brucei* TRS non-LTR retrotransposon and 3'-end of cysteinyl-tRNA synthetase gene are present in the uniform intergenic region (Kosec 2004; Kosec et al. 2006).

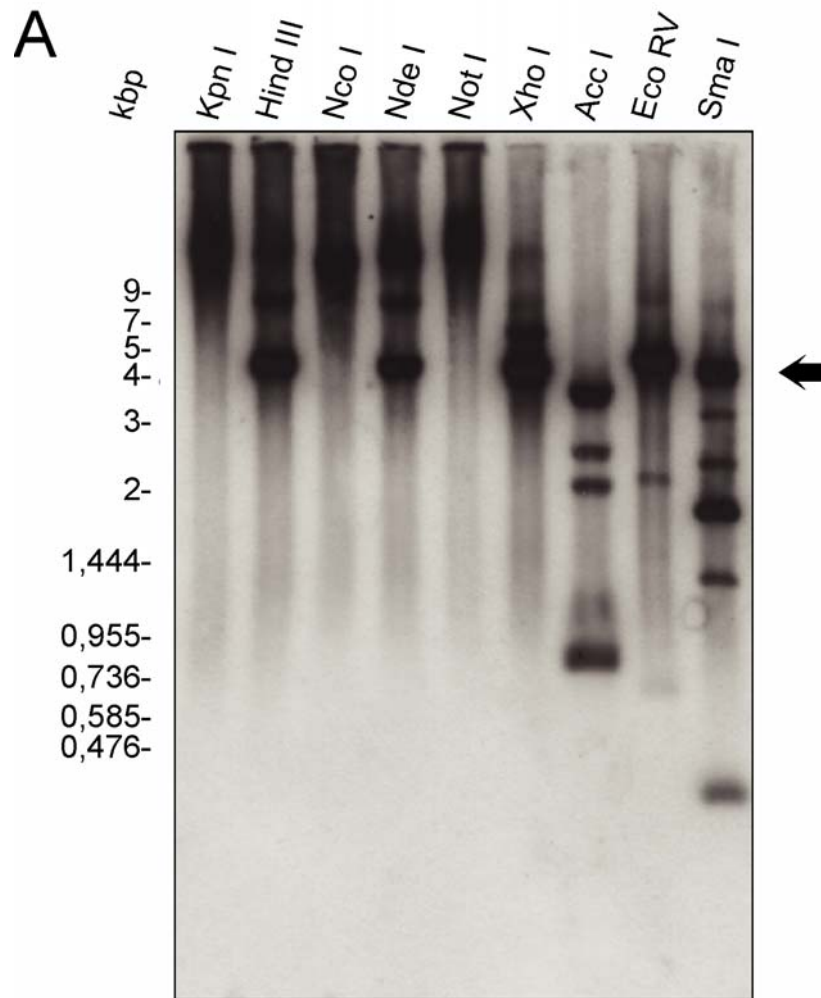


Figure 12A Genomic organization of *TcMCA3* copies. Southern blot of *T. cruzi* genomic DNA, digested with several low frequency restriction enzymes and hybridized with radioactive *TcMCA3* specific probe is shown. A major band of 4.4 kbp corresponding to the uniform repetitive region is indicated with an arrow. A ladder of 1 kbp and pUC19 digested with *Sau3A* I and *Taq* I were used as molecular weight markers.

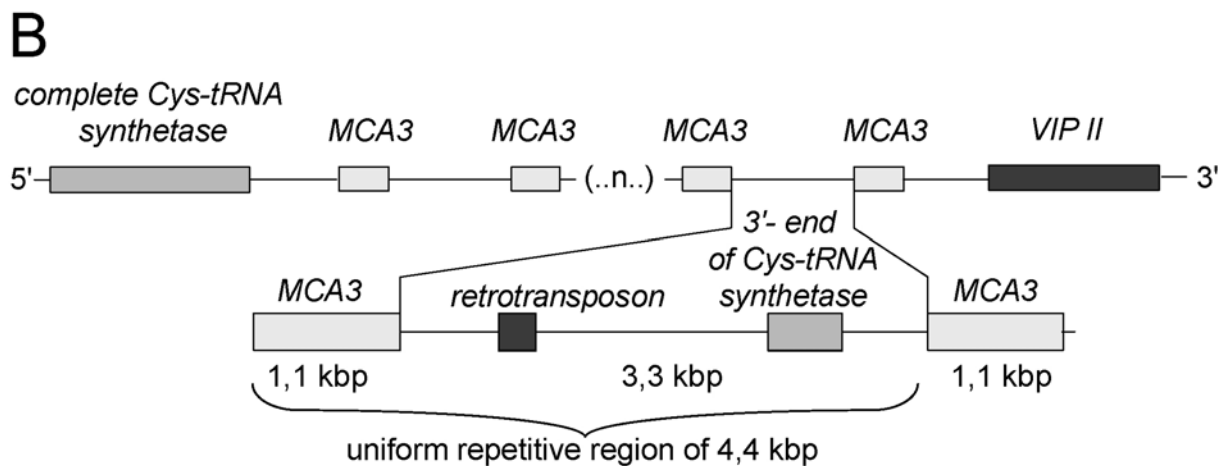


Figure 12B Genomic organization of *TcMCA3* copies. Genome sequence data deduced for one *TcMCA3* tandem (Kosec et al. 2006).

We found antibodies against metacaspase-3 in 15 out of 16 chronic Chagasic patients sera, which proves that the protein is expressed in one of the mammalian host stages of *T. cruzi*.

### **1.7.2 Strategies used to express recombinant metacaspase-3 from *T. cruzi***

We tried to express recombinant metacaspase-3 in bacterial, yeast (*Pichia pastoris*) and insect cells - baculovirus expression systems. Using pET-28 vector *Escherichia coli* cells produced the protein exclusively in the form of inclusion bodies, which were used to produce polyclonal antibodies. In order to obtain a soluble product we used pET-32 vector, which adds an N-terminal thioredoxin fusion to the expressed protein. Unfortunately no soluble fusion protein was produced. Using pET-43 vector with an N-terminal NusA fusion we obtained a soluble protein, however, we later realized that the fusion protein was not expressed with a stable two-domain structure. Using yeast system, no expression of metacaspase-3 could be detected, neither for intracellular or medium-targeted expression. In the baculovirus system we expressed recombinant metacaspase-3 in the cytoplasm of Sf-9 and Sf-21 cells. After cell lysis the recombinant protein was partially purified by Ni-chelating chromatography, however small amounts of the expressed protein prevented us from performing biochemical analysis.



## 2 Aims and hypothesis

Cysteine peptidases have an important role in signalization of essential cellular processes, such as apoptosis and autophagy mediated starvation response and differentiation. Peptidases are also believed to be important virulence factors of numerous microorganisms, among them the early divergent eukaryote *Trypanosoma cruzi*. We screened genome sequence databases of this parasite for the presence of cysteine peptidase homologs and found about 20 genes coding for cysteine peptidases. We decided to focus on the metacaspase and the autophagin (*ATG4*) family as we believed that characterizing these proteases would open us new insights into programmed cell death and autophagy in *T. cruzi*. Moreover, investigating signaling pathways of these processes in a simple organism like *T. cruzi* could give us so far unsuspected suggestions to clarify them in the cells of more complex organisms like mammals.

Further on, we suspected that both processes, the programmed cell death and differentiation of *T. cruzi* might play an important role in the parasite-host relationship during natural infections. A more detailed knowledge of them might enable the development of new strategies for future treatment of Chagas disease, an illness affecting millions of people, still without suitable chemotherapy.

The hypothesis of our work is that genes homologous to two families of cysteine peptidases, the metacaspases and the autophagins, are expressed in *T. cruzi*, yielding functional peptidases and that these peptidases are involved in programmed cell death and autophagy respectively. Further, we expected that the recombinant expression of *ATG8* gene homologs would be necessary in order to demonstrate the proteolytic activity of the autophagins and to show the implication of ATG8 conjugation system in autophagy of *T. cruzi*.



### 3 Materials and methods

#### 3.1 *ATG4* and *ATG8* genes sequence analysis

*T. cruzi* *ATG4* and *ATG8* homologs were identified using the BLAST engine in the CL-Brenner clone Genome Project database (El-Sayed et al. 2005) website [www.genedb.org](http://www.genedb.org). Amino acid sequences of C54 family peptidase domains in *ATG4*-like genes were used for alignment with ClustalW program and its Score values were taken as percentage of identity between two sequences. Similarly for *ATG8* genes analysis we used amino acid sequences from N-terminal Met to the conserved Gly residue at P1 site of autophagin cleavage.

#### 3.2 Pulse field gel electrophoresis (PFGE)

Agarose blocks containing *T. cruzi* epimastigotes were prepared and lysed as described (Henriksson et al. 1990). Amounts of DNA corresponding to  $40 \times 10^6$  epimastigotes were used in each well and the separation was carried out in a 1,2% agarose gel. PFGE was performed in a CHEF-DR<sup>®</sup> III Pulse Field Electrophoresis System apparatus (BioRad). The running conditions were as follows: block 1: run time: 24 h, 60 s-120 s with time ramp, included angle:120°, voltage: 4 V/cm; block 2: run time: 24 h, 120 s-350 s with time ramp, included angle:120°, voltage: 4 V/cm. In parallel, chromosomes of *S. cerevisiae* yeast strain YNN 295 (Biorad) were run as molecular weight markers. DNA was transferred to nylon filters after nicking in 0.25 M HCl for 15 min and UV cross-linked. PCR-amplified fragments of the complete *TcMCA3* open reading frame (ORF) were labeled with [ $\alpha$ -<sup>32</sup>P] dCTP by standard procedures (Sambrook 1989) using pGEM T Easy vector with *TcMCA3* (see “Cloning and expression of the *TcMCA3* gene”) as template. Filters were hybridized with the different probes for 12 h at 60 °C in 0.5 M NaH<sub>2</sub>PO<sub>4</sub>, 1 mM EDTA, 1% BSA, 7% SDS, pH 7.4. The membranes were thoroughly washed at 60°C with 0.2 x SSC (1 x SSC is 0.15 M NaCl plus 15 mM sodium citrate), 0.1% SDS and subjected to autoradiography (Kodak Biomax XAR).

#### 3.3 Cloning and expression of recombinant proteins

##### 3.3.1 Cloning and expression of the *TcMCA3* gene

*TcMCA3* gene was obtained by performing PCR on genomic DNA from *T. cruzi* epimastigotes. Primers were designed according to the sequence data obtained from the *T. cruzi* Genome Project database search (El-Sayed et al. 2005), (Kosec et al. 2006). The complete open reading frame of the gene was used to produce the radioactively labeled probe in PFGE experiment and to express insoluble protein for antibody production. Restriction site for the *Nco I* enzyme was inserted at the 5'-end and *Hind III* at the 3'-end. The primers used were as follows: sense primer 5'-TTTCCATGGGCTTTGATTTTGGCTGTC-3' and reverse primer 5'-TTTAAGCTTAAGACATGTGGCGACGGGTGG-3'.

On the other hand, for expression of soluble protein we designed two internal primers in order to express N-terminal truncated forms of the gene (Figure 13). Constructs were designed in a way to express the ORF from the second and third internal Met residues. In this case the primers were as follows: for the second Met sense primer 5'-TTCCAATGGAAATCGGACTGAACC-3' and the third Met sense primer 5'-TTTCCATGGAACGCCACCGAGGG-3'; reverse primer was the same in both cases 5'-TTTAACGTTACATGTGGCGACGGCTGG-3'. In both cases the PCR products were isolated from agarose gel, purified by Qiaquick columns (Qiagen) and cloned into pGEM-T Easy vector (Promega). In order to express the sequences inserts were liberated with respective restriction enzymes (New England Biolabs) and cloned into pET-28 expression vector (Novagene). Constructs, that add (His)<sub>6</sub> tag to the C-termini of native proteins were used for transformation *E. coli* BL21 (DE3) pLysS cells.

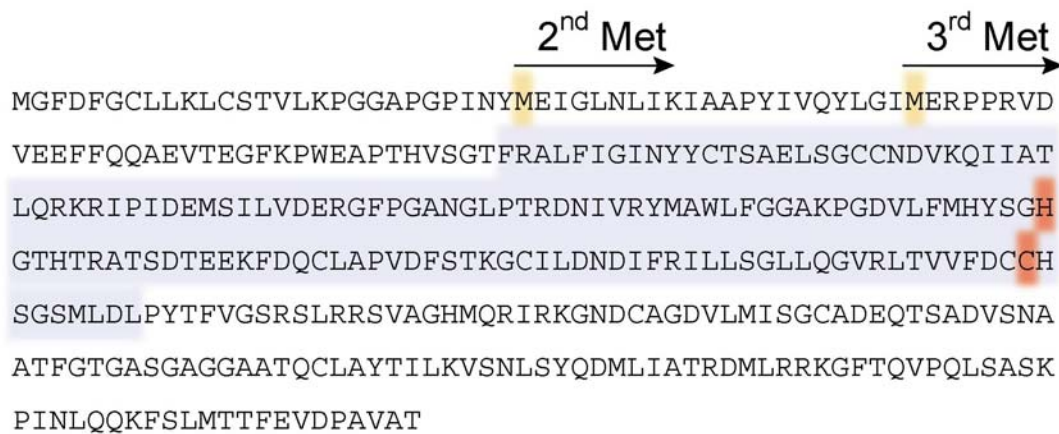


Figure 13 In order to express a soluble metacaspase-3 two N-terminal truncated sequences were obtained starting from the proteins second and third Met residue (marked in yellow). In both cases the putative p20-like subunit (marked in cyan) remains intact together with the His and Cys residues of the catalytic site (marked in red).

In order to produce insoluble protein in form of inclusion bodies protein expression was induced by 1 mM IPTG for 3 h at 37 °C. Cultures were centrifuged and resuspended in lysis buffer (50 mM Tris-Cl, 0,5 M NaCl, 0,1 % Triton X-100, pH =7,6). Suspensions were incubated on ice until their viscosity was greatly increased. Afterwards several 30 s sonification pulses were applied to fragment genomic DNA, always taking care that the temperature of the sample remained low. Samples were centrifuged at 20000 × g for 20 min at 4 °C to separate soluble and insoluble fraction. In order to purify inclusion bodies (Middelberg 2002) the insoluble fraction was first resuspended in wash buffer (Tris-Cl 100 mM, 100 mM NaCl, pH 7,6) and then twice more in wash buffer containing sodium deoxycholate (2mg/mL) and wash buffer containing Triton X-100 (0,5 %). Finally, inclusion bodies were washed three times with distilled water.

When producing soluble protein, protein expression was induced with 0,5 mM IPTG for 7 h at 18 °C. Cells were resuspended in lysis buffer (Tris-Cl 50 mM, NaCl 500 mM, urea 2,2 M). After lysis DNA was fragmented by sonification and the suspension was centrifuged at 20000 × g.

### 3.3.2 Cloning and expression of *ATG4.1*, *ATG4.2*, *ATG8.1* and *ATG8.2* genes

*ATG4.1*, *ATG4.2*, *ATG8.1* and *ATG8.2* genes were obtained by performing PCR on genomic DNA from *T. cruzi* epimastigotes. Primers were designed according to the sequence data obtained from the *T. cruzi* Genome Project database search. For *ATG4.1* and *ATG4.2* cloning sites for *Nde I* and *Bam HI* were added and for *ATG8.1* and *ATG8.2* we used cloning sites for *Nco I* and *Bam HI*. The sequences of the primers were as follows: for *ATG4.1* sense primer 5'-AACATATGCAAGGTACAATGACG-3' and reverse primer 5'-AAGGATCCTCAAGAAGAAAAAGTGTCTC-3'; for *ATG4.2* sense primer 5'-AACATATGGAGTGGTTGAAAATTG-3 and reverse primer 5'-AAGGATCCTACTCCGCCACGTCC-3'; for *ATG8.1* sense primer 5'-AACCATGGCGCAAAGAAATTG-3' and reverse primer 5'-AAGGATCCCACCAAGAACCAAAAAGTTG-3'; for *ATG8.2* sense primer 5'-AACCATGGCACGCAAATATCGCTACCA-3' and reverse primer 5'-AAGGATCCGAATTCCGCCGCACAGCCG-3'. The PCR products were isolated from agarose gel, purified by Qiaquick columns (Qiagen) and cloned into pGEM-T Easy vector (Promega). Sequencing of the products was performed by Macrogen. Inserts were liberated with respective restriction enzymes (New England Biolabs) and cloned into pET-28 protein expression vector (Novagene). Constructs, that add 20 aminoacid residues including a (His)<sub>6</sub> tag to the C-termini of native proteins were used to transform *E. coli* BL21 (DE3) pLysS cells. Expression was induced by 0,5 mM IPTG for 8 h at 18 °C for *ATG4.1* and *ATG4.2* and for 4,5 h at 28 °C for *ATG8.1* and *ATG8.2*. Soluble extracts were obtained as described for the *TcMCA3* gene. Cells were pelleted, frozen, lysed, sonicated and centrifuged to remove debris. Supernatants were applied directly to fast flow Ni-NTA (Amersham Biosciences) and proteins were eluted at 150 mM imidazole. Eluates containing recombinant proteins were pooled and desalted to TBS (Tris-Cl 50 mM, NaCl 150 mM, pH7,6) using PD-10 columns (Amersham Biosciences).

### 3.4 Purification of recombinant proteins using metal chelating chromatography

#### 3.4.1 Purification of metacaspase-3 in denaturing conditions for production of antibodies

Purified inclusion bodies of *TcMCA3* expressing bacteria were dissolved in 8M Urea, Tris-Cl 50 mM, pH 7,6. The solution was applied onto Ni-NTA (Invitrogen) affinity chromatography resin under denaturing conditions. The column was washed and proteins eluted in Tris-Cl 50 mM, urea 6M, imidazole 150 mM. Eluates containing metacaspase-3 were pooled and dialysed against PBS (10 mM Na<sub>2</sub>HPO<sub>4</sub>, 150 mM NaCl, pH 7,2). In order to produce antibodies the protein was injected into two mice using standard protocols.

#### 3.4.2 Purification of metacaspase-3 in weakly disruptive conditions

A soluble extract of metacaspase-3 producing bacteria was applied to Ni-NTA affinity chromatography column (Amersham Biosciences) with a moderate concentration of urea (2,2 M) for enhanced binding. Washing steps were performed without urea as well as elution that was performed in Tris-Cl 50 mM, NaCl 500 mM, imidazole 150 mM. Fractions containing metacaspase-3 were pooled and desalted against PBS.

#### 3.4.3 Purification of autophagin-1 and -2 and of Atg8.1 and Atg8.2 proteins

Soluble bacterial extracts in Tris-Cl 50 mM, NaCl 500 mM were applied directly to fast flow Ni-NTA (Amersham Biosciences). Columns were washed with at least 20 column volumes of washing buffer (Tris-Cl 50 mM, NaCl 500 mM, imidazole 30 mM) and proteins were eluted at 150 mM imidazole. Eluates containing recombinant proteins were pooled and desalted to TBS (Tris-Cl 50 mM, NaCl 150 mM, pH7,6) using PD-10 columns (Amersham Biosciences).

### 3.5 Western blotting

#### 3.5.1 Western blotting for detection of expression of metacaspase-3 in different *T. cruzi* developmental stages

The different forms of the parasite's life cycle were resuspended in PBS containing protease inhibitors and cells were broken by three rounds of freezing at -20 °C and thawing. After centrifugation at 26,900 × g for 15 min at 4 °C, the cell-free extract was retained and the pellet was discarded. Samples of each extract, corresponding to 180 µg of proteins, were cracked in Laemmli sample buffer, run on 12,5 % polyacrylamide gel and transferred to a nitrocellulose membrane. Anti-metacaspase-3 antiserum (see above) in dilution of 1/500 was used as primary antibody and horseradish conjugated goat anti mouse antibody as secondary antibody. Chemiluminescence was used for blot development (SuperSignal West Pico Chemiluminescent Substrate, Pierce).

#### 3.5.2 Identification of recombinant proteins

When identifying recombinant protein bands in different fractions less sensitive and more practical methods were applied for western blot development. One of them consisted of a secondary antibody conjugated with alkaline phosphatase and development with 5-bromo-4-chloro-3-indolyl phosphate p-toluidinium salt and nitro blue tetrazolium chloride. The other used horseradish peroxidase conjugated secondary antibody and development with diaminobenzidine and H<sub>2</sub>O<sub>2</sub>.

### 3.6 Measurements of metacaspase-3 activity using combinatorial peptide libraries

Eluates from the Ni-NTA column containing metacaspase-3 and control eluates resulting from the same purification protocol but originating in bacteria transformed with empty pET-28 vector were pooled and desalted to PBS using PD-10 columns (Amersham Biosciences). They were used as samples to screen fluorescence quenched combinatorial peptide libraries of general structure Abz-XXZXXQ-EDDnp-OH where Abz is *ortho*-aminobenzoic acid, Z represents R, D, Q, F, L, G or P, X represents randomly incorporated residues and EDDnp-OH is N-(ethylendiamine)-2,4-dinitrophenyl amide (Melo et al. 2001) (We are grateful to dr. Luiz Juliano, Sao Paulo, Brazil for letting us use his libraries). We tested each of these substrates and additionally several other peptides (Abz-FRQ-EDDnp, Abz-GKXRXX-(Dnp)-OH, Abz-KRRSSQ-EDDnp and Abz-KLLSSKQ-EDDnp) in different combinations of conditions (Buffer, ionic strength, reducing agent, detergent) (Table 1)

N°	buffer	pH	ionic strength	reducing agent	detergent	additional
1	Tris, 50 mM	7,0	NaCl, 0,15 M	DTE , 2,5 mM		
2	Tris, 50 mM	8,0	NaCl, 0,15 M	DTE , 2,5 mM		
3	sodium acetate, 100 mM	5,5		DTE , 2,5 mM	Brij 35, 0,0125 %	CaCl <sub>2</sub> , 25 mM
4	Tris, 100 mM	8,0	sulphate, 1 M	DTE , 2,5 mM	Brij 35, 0,0125 %	
5	Tris, 100 mM	8,0	citrate, 1M	DTE , 2,5 mM	Brij 35, 0,0125 %	
6	Tris, 100 mM	8,0	sulphate, 1 M	DTE , 2,5 mM	Brij 35, 0,0125 %	urea, 0,5 M
7	sodium phosphate, 100 mM	7,5	NaCl, 0,3 M	DTE , 2,5 mM	Brij 35, 0,0125 %	
8	sodium acetate, 100 mM	5,5		DTE , 2,5 mM	Brij 35, 0,0125 %	

Table 1 Combinations of conditions for measurement of metacaspase-3 activity with combinatorial peptide libraries.

In addition, prolonged periods of autoactivation and activation by cruzipain were also tried.

Assay conditions were as follows. The sample was preincubated in buffer containing DTE for 5 minutes and mixed with other reaction components in a spectrofluorometer cuvette. Hydrolysis of internally quenched fluorogenic peptides was followed by fluorescence measurements at  $\lambda_{\text{ex}} = 320$  nm and  $\lambda_{\text{em}} = 420$  nm (excitation and emission wavelengths for Abz) in a Hitachi F-2000 spectrofluorometer. Final concentrations of substrates of substrates were about 10 mM and the amount of added metacaspase about 1  $\mu\text{g}$ .

### 3.7 Proteolytic activity of recombinant autophagins on recombinant Atg8.1 and Atg8.2 and fluorogenic synthetic substrate

#### 3.7.1 Proteolytic activity of recombinant autophagins on recombinant Atg8.1 and Atg8.2

For cleavage assay of recombinant TcAtg8 by recombinant TcAtg4, 17,2  $\mu\text{g}$  of purified TcAtg8.1 or TcAtg8.2 were incubated with different amounts (750 ng – 7,5  $\mu\text{g}$ ) of purified autophagin-1 and in 100  $\mu\text{L}$  TBS containing 1 mM EDTA and 1 mM DTT at room temperature for 35 min. Due to slow reaction rates 2 and 0,2  $\mu\text{g}$  of autophagin-2 were used and the time of reaction was prolonged to 18 hours. To stop the reaction, Laemmli sample buffer was added to the mixture and the mixture was boiled for 5 min. Proteins present in 20  $\mu\text{L}$  of each reaction were separated on 17,5 % SDS-PAGE and analyzed by Coomassie Brilliant Blue staining.

In order to assay the effects of protease inhibitors, equivalent reactions were carried out in the presence of 2 mM iodoacetamide, 2,5 mM N-ethylmaleimide, 100  $\mu\text{M}$  E-64, 39 ng/ $\mu\text{L}$  cystatin C, 2,5 mM EDTA, 2 mM o-phenantroline, 2 mM PMSF or 0,33 mM pepstatin.

To determine the exact cleavage sites of TcAtg8.1 and TcAtg8.2, similar reaction solutions were applied to a C8 reverse phase Aquapore RP-300 Brownlee<sup>TM</sup> HPLC column (Applied Biosystems) on Hewlett Packard 1100 series system. The column was equilibrated with 0.1 % trifluoroacetic acid (TFA) and peptides were eluted using a gradient 0-90% acetonitrile with 0.1% TFA solution. The fraction corresponding to the peak that only appears after treatment with autophagin was dried in speedvac and N-terminal sequencing was performed by Edman degradation on Procise Protein Sequencing System 492 (Applied Biosystems) following manufacturer's instructions.

#### 3.7.2 Proteolytic activity of recombinant autophagins on fluorescence quenched synthetic substrate Abz-TFGQ-EDDnp

A fluorescence quenched peptide substrate was synthesized according to the consensus ATG8 cleavage site (kind gift from dr. Luiz Juliano) with the structure of Abz-TFGQ-EDDnp where Abz is *ortho*-aminobenzoic acid fluorescent group and EDDnp is N-(ethylendiamine)-2,4-dinitrophenyl amide, a quenching group (Melo et al. 2001).

Activity assays were performed in 96 well plates in Safire spectrofluorometer (Tecan). The reaction buffer was TBS with 2 mM DTT, 1 mM EDTA and 1 mM PMSF, substrate concentration 10  $\mu\text{g}/\text{mL}$  and 2  $\mu\text{g}$  of either autophagin was added. Fluorescence was measured over 30 min at  $\lambda_{\text{ex}} = 320$  nm and  $\lambda_{\text{em}} = 420$  nm (excitation and emission wavelengths for Abz).

### 3.8 Measuring of autophagin activity in cell free protein extracts of *T. cruzi*

17,2 µg of recombinant Atg8.1 or Atg8.2 were incubated in TBS containing 1 mM DTT, 2 mM PMSF, 2 mM EDTA, 2 mM *o*-phenantroline and 10 µM E-64. 100 µg of proteins from cell free extracts of the four *T. cruzi* developmental stages were added and the reactions were incubated for 18 hours at RT. In parallel equivalent reactions 3 mM iodoacetamide was included as an inhibitor. The extracts were prepared by resuspending the parasites in TBS containing 1mM DTT, 100 µM E-64, 2 mM PMSF and 2,5 mM EDTA. Cells were broken by three rounds of freezing at -20 °C and thawing and the extract obtained by centrifugation at 26900 x g. One third of the reaction mixture was cracked in Laemmli sample buffer, applied to a 17,5 % SDS-PAGE gel and transferred to a nitrocellulose membrane (Amersham Biosciences). To detect the cleavage fragments, antisera raised against recombinant TcAtg8.1 or TcAtg8.2 were used as primary antibodies and goat anti-rabbit alkaline phosphatase conjugated was used as secondary antibody. The blots were developed using 5-bromo-4-chloro-3-indolyl phosphate p-toluidinium salt and nitro blue tetrazolium chloride.

### 3.9 Transformation of *atg4Δ* and *atg8Δ* yeasts with respective *T. cruzi* homologs

PCR was performed previously isolated clones in order to insert new restriction enzyme sites for cloning *ATG4.1*, *ATG4.2*, *ATG8.1* and *ATG8.2*. *Bam* *HI* site was used on the 5'- end and *Not* *I* on the 3'-end of all genes. The sequences of the primers were as follows: for *ATG4.1* sense primer 5'-TTAGGATCCATGCAAGGTACAATGACG-3' and reverse primer 5'-AATGCGGCCGCTCAAGAAAAAGTGTC-3'; for *ATG4.2* sense primer 5'-TTAGGATCCATGGAGTGGTTGAAAATTG-3' and reverse primer 5'-AATGCGGCCGCTACTCCGCCACGTCC-3'; for *ATG8.1* sense primer 5'-TTAGGATCCATGGCGCCAAAGAAA-3' and reverse primer 5'-AATGCGGCCGCTACCAAGAACCAAAAAGTTG-3'; for *ATG8.2* sense primer 5'-TTAGGATCCATGGCACGCAAATATC-3' and reverse primer 5'-AATGCGGCCGCTCAATTCCGCCGCACAGC-3'. The PCR products were isolated from agarose gel, purified by Qiaquick columns (Qiagen) and cloned into pGEM-T Easy vector (Promega). Sequencing of the products was performed by Macrogen. Inserts were liberated with respective restriction enzymes (New England Biolabs) and cloned into pCM190 vector. This vector exhibits tetO<sub>7</sub>-promoter-driven transcription hence gene expression can be regulated by the presence of tetracycline or derivatives in growth medium (Gari et al. 1997). *atg4Δ* and *atg8Δ* WCG strain *S. cerevisiae* (kind gift from dr. Michael. Thumm) were transformed. Either *TcATG4.1*-pCM190 or *TcATG4.2*-pCM190 were transformed into *atg4Δ* strain and *TcATG8.1*-pCM190 or *TcATG8.2*-pCM190 were transformed into *atg8Δ* strain. Transformations were performed using the lithium acetate method (Ausubel 1998). Overnight cultures of yeast knockout strains in YPD media were diluted to OD<sub>600</sub> = 0,1 and further grown to OD<sub>600</sub> = 0,5. They were centrifuged and washed first with water and then with 0,1 M lithium acetate and finally resuspended in lithium acetate. Yeasts were then mixed with transformation mixture (33 % PEG 3350, 0,1 M LiOAc, 0,25 µg/µL salmon sperm denatured DNA, 1 µg plasmid for transformation per 360 µL) and vortexed. Later on, they were incubated at 30 °C for 30 min, at 42 °C for 20 min, washed twice with water and plated on YNB-agar plates containing aminoacids and lacking uracil for positive clone selection.

Transformant cultures were grown in YNB media with 0,5 % ammonium sulphate without uracil (Ausubel 1998) to approx. OD = 1 and were subsequently split into two parts. One of them was centrifuged, resuspended in 1 % potassium acetate and grown for additional 7 hours to induce starvation response. Fresh growth medium was added to another part as control. Wild type control WCG strain yeasts were grown in YPD medium.

Cultures were centrifuged, SDS-PAGE cracking buffer and glass beads were added to the pelleted cells and the mixture was vortexed vigorously to break cell walls. Yeast proteins were run in 10 % gels and transferred to nitrocellulose membrane. Immunodetection was performed with anti-(pro)aminopeptidase I primary antibodies (gift from I. V. Sandoval and M. J. Mazon) and horseradish peroxidase conjugated anti-rabbit secondary antibodies. Chemiluminescence was used for blot development (Amersham Biosciences).

### 3.10 Parasite cultures and treatments

The different forms of the parasite's life cycle (epimastigote, metacyclic trypomastigote, cell-derived trypomastigote, and amastigote) of the *T. cruzi* CL Brener cloned stock (Zingales et al. 1997) were obtained as previously described (Franke de Cazzulo et al. 1994).

#### 3.10.1 Induction of programmed cell death of *T. cruzi* epimastigotes

For apoptosis induction epimastigotes of *T. cruzi* were cultured to a density of 50 x 10<sup>6</sup>/ml (mid-exponential

phase) and incubated for 4 h at 28 °C in the presence or absence of 10% fresh human serum. Parasites were counted in a Neubauer chamber under the light microscope at the indicated times. Spheroid shaped epimastigotes that had lost motility were counted as dead, as described by Ameisen et al (Ameisen 1995).

### 3.10.2 Starvation induction

Epimastigotes of the CL Brenner clone were grown in brain-heart-tryptose (BHT) medium with 10 % FCS to a density of  $50 \times 10^6$ /mL. For induction of starvation they were washed twice with PBS and then resuspended in PBS at equal density. They were incubated for 20 h at 28 °C with gentle shaking. Control epimastigotes were grown in the same media as before.

### 3.10.3 Immunofluorescence studies

Parasites were fixed for 30 min with 4 % paraformaldehyde in PBS and then layered onto poly (L-lysine) precoated slides. Coverslips were saturated in blocking buffer (3 % goat serum, 2 % bovine serum albumin, 0,1 % saponin in PBS) for 30 min and incubated for 2 h with anti-TcATG8.1 and anti-TcATG8.2 antibodies diluted 1/375 in blocking buffer. Coverslips were washed three times and incubated with AlexaFluor 488- or AlexaFluor 546-conjugated goat anti-rabbit immunoglobulins (Molecular Probes) for 1 h. After extensive washing with PBS coverslips were mounted using FluorSave<sup>TM</sup> reagent (Calbiochem) with DAPI. Preparations were analyzed using a fluorescence microscope (Nikon Eclipse E600) and image capture was performed by using a Spot RT Slider Model No. 2.3.1 digital camera (Diagnostic Instruments).

## 3.11 Assessment of binding of Atg8.1 and Atg8.2 to microtubules

Similarly to previously described procedure (Ketelaar et al. 2004) 250 ng of lyophilized purified bovine tubulin (Cytoskeleton) were dissolved in ice cold G-PEM buffer (80 mM PIPES pH =6,9; 1 mM MgCl<sub>2</sub>, 1 mM EGTA, 1 mM GTP). The solution was incubated at 37 °C for 30 min to obtain microtubules. Five fold molar excess of either Atg8.1 or Atg8.2 was added and the solutions were incubated for another 30 min at 37 °C. Afterwards proteins were cross linked by the addition of glutaraldehyde to a final concentration of 0,5 % and solutions were transferred to poly (L-lysine) coated cover slides. Cover slides were thoroughly washed with PBS blocked with PBS and 1 % BSA, incubated with primary rabbit derived anti-Atg8.1 or antiAtg8.2 antibody (dilution 1/500) and anti-tubulin mouse monoclonal IgM antibody (Biovendor). After washing in PBS AlexaFluor-488 conjugated goat anti rabbit immunoglobulins (Molecular Probes) and AlexaFluor-546 conjugated goat anti mouse IgM immunoglobulins (Molecular probes) were used as secondary antibodies. Cover slides were washed again in PBS and mounted using SlowFade<sup>®</sup> Gold antifade reagent (Molecular Probes) and observed with Olympus IX 71 fluorescence microscope.

## 4 Results

### 4.1 Chromosomal organization of *TcMCA3* genes

In our previous work (Kosec et al. 2006) we demonstrated that *TcMCA3* genes are present as tandemly repeated copies. However, it was suspected that more than one tandem of genes might be present. To confirm this hypothesis we performed PFGE of whole *T. cruzi* chromosomes and using a radioactively labeled probe in a southern blot experiment we confirmed that there are at least two tandems of genes present. *TcMCA3* genes localized on two chromosomes of apparent sizes of 0,98 Mbp and 0,54 Mbp (Figure 14 A).

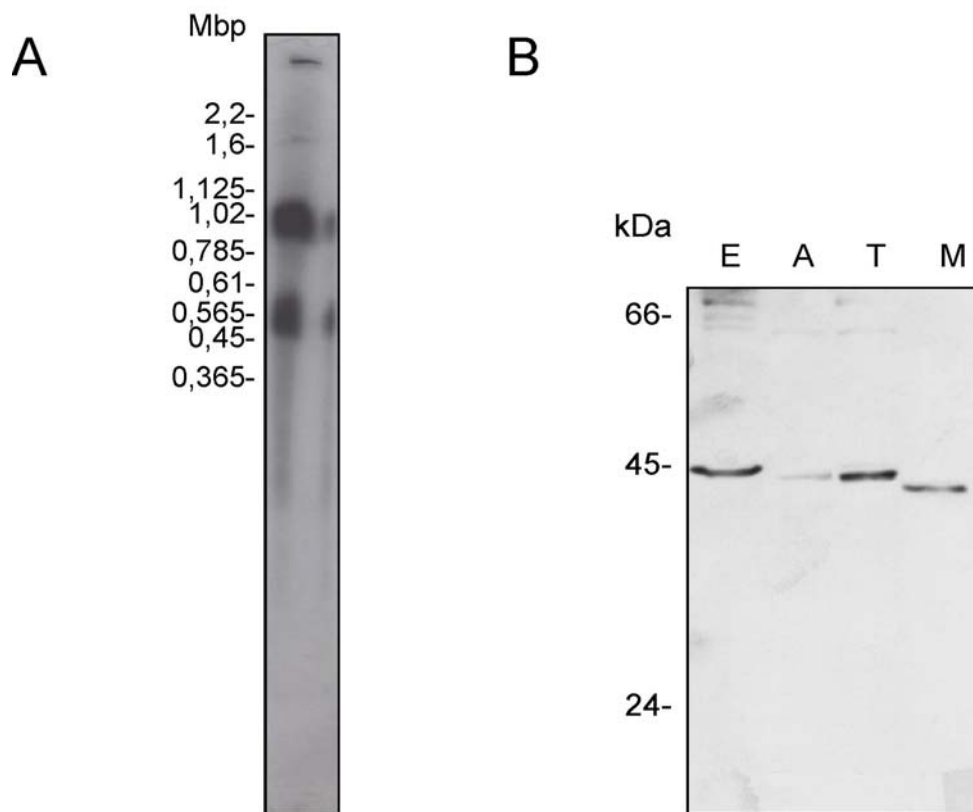


Figure 14 **A)** PFGE – Southern blot of *T. cruzi* chromosomes developed with radioactively labeled *TcMCA3* probe. Two strong bands are visible at 0,98 and 0,54 Mbp. *S. cerevisiae* chromosomes were run as molecular weight markers. **B)** Differential expression of metacaspase-3 in *T. cruzi* developmental stages. Western blots of soluble extracts of epimastigotes (E), amastigotes (A), cell derived trypomastigotes (T) and metacyclic trypomastigotes (M) probed with anti-metacaspase-3 antibody.

### 4.2 Expression of metacaspase-3 in different *T. cruzi* developmental stages

In order to analyze the expression of metacaspases in all developmental stages of *T. cruzi*, we obtained polyclonal antibodies against metacaspase-3 (See Methods). Cell free extracts of epimastigotes, amastigotes, cell derived trypomastigotes and metacyclic trypomastigotes were subjected to Western blot analysis. Antibodies raised against metacaspase-3 recognized a band with an apparent molecular mass of 44 kDa in epimastigotes, amastigotes and cell derived trypomastigotes and a slightly faster migrating band in metacyclic trypomastigotes (Figure 14 B). We could not observe any faster migrating bands corresponding to a possible cleavage between

p20-like and p10-like domains similar to what is seen in caspase family members.

### 4.3 Recombinant expression of N-terminal truncated *TcMCA3* genes in *E. coli*

As a new strategy for obtaining soluble recombinant metacaspase-3 in sufficient amounts, N-terminal truncated genes (see Methods) were expressed in *E. coli* BL21 (DE3) cells. Soluble and insoluble fractions were analyzed for the presence of the recombinant proteins using polyclonal anti-metacaspase-3 antibodies. We could observe that the shorter protein, starting from the third Met residue is found to some extent in the soluble fraction. On the other hand, the vast majority of the longer protein, starting from the second Met residue is expressed in insoluble form as inclusion bodies, similarly to the full-length protein evaluated in previous experiments (Kosec 2004) (Figure 15 A).

Both constructs added (His)<sub>6</sub> tag to the carboxyterminus of the recombinant metacaspase-3 to facilitate their purification. Extract of bacteria expressing the shorter 3<sup>rd</sup> Met construct was applied to Ni-NTA column and eluates checked for the presence of recombinant metacaspase (Figure 15 B). Eluate fractions were greatly enriched in metacaspase-3 (about 20 % of total protein).

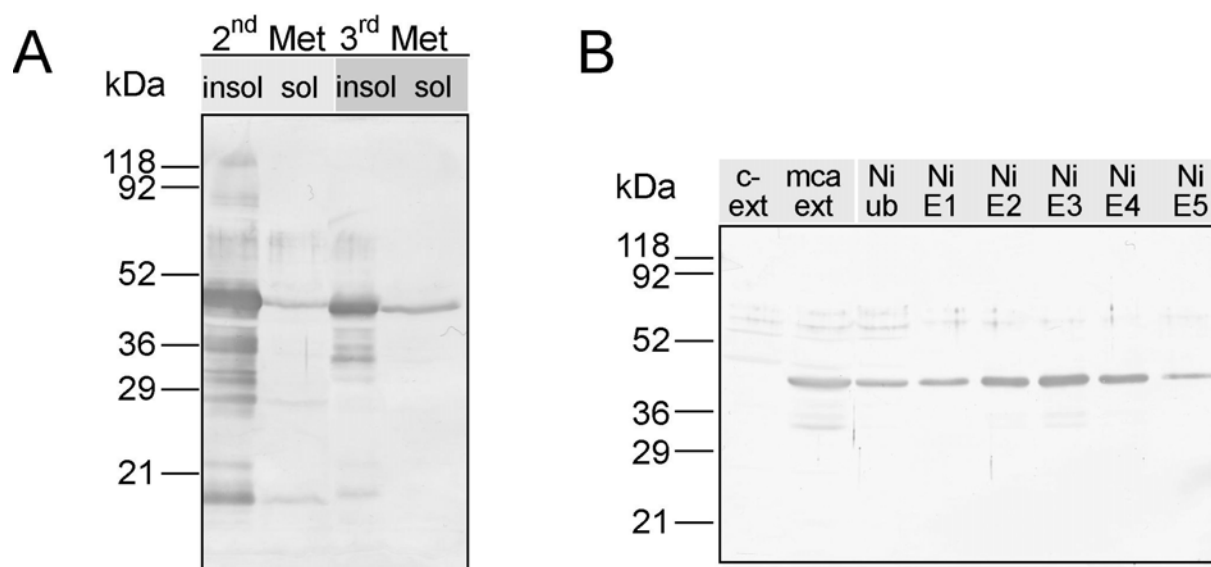


Figure 15 Expression of recombinant metacaspase-3 in *E. coli* BL21 (DE3) cells observed in a western blot with anti-metacaspase-3 antibodies and developed with diaminobenzidine method. **A)** Two N-terminal truncated forms of metacaspase-3 were expressed. When translations started at the second Met residue, a vast majority of the protein was found in the insoluble fraction of bacterial cells (first lane), showing several degradation bands. Only very little was present in the soluble fraction (second lane). However, when 3<sup>rd</sup> Met construct was expressed a greater proportion of metacaspase-3 was expressed as a soluble protein (third & fourth lanes). **B)** Cell free protein extract of bacteria expressing metacaspase-3<sup>Met</sup> was applied to Ni-NTA chromatograph column. The first lane shows an extract of bacteria transformed with empty pET28 vector as negative control and in the second lane (extract of metacaspase-3 producing bacteria) a strong band corresponding to soluble metacaspase-3 can be observed. This band diminishes in intensity in the third lane (Ni-NTA unbound fraction) and is intensified in next lanes corresponding to subsequent eluates of Ni-NTA column (Ni E1 to Ni E5).

### 4.4 Metacaspase-3 changes its sub-cellular localization during epimastigote cell death

When cultures containing both epimastigotes and metacyclic trypomastigotes of *T. cruzi* are exposed to FHS, epimastigotes respond undergoing rapid and massive cell death with morphological changes typical of apoptosis whereas the preadapted metacyclic trypomastigotes remain unaffected (Ameisen 1995). Under the light microscope, dead epimastigotes appear as spheroid shaped cells that have lost motility, whereas live epimastigotes keep their normal morphology and most of them are motile (Figure 16 A). As shown in Figure 16 B, after 30 min of exposure to 10% FHS, 67% of the epimastigotes were spheroidal, while after one hour of treatment 85% of the epimastigotes were dead and by 3 hours almost all epimastigotes (98,4%) were spheroid shaped and non-motile. In contrast, metacyclic trypomastigotes demonstrated no change in shape and motility during this treatment.

We explored the possible participation of metacaspase-3 in the serum-induced cell death by performing an indirect immunofluorescence technique using anti-TcMca3 antibodies (Figure. 16 C). Both antibodies revealed reactive material distributed in the whole cell body of untreated epimastigotes. Surprisingly, after FHS treatment, a notorious change in the pattern of fluorescence was observed, metacaspase-3 being now mainly located in the nucleus of dying parasites and co-localizing with DAPI staining.

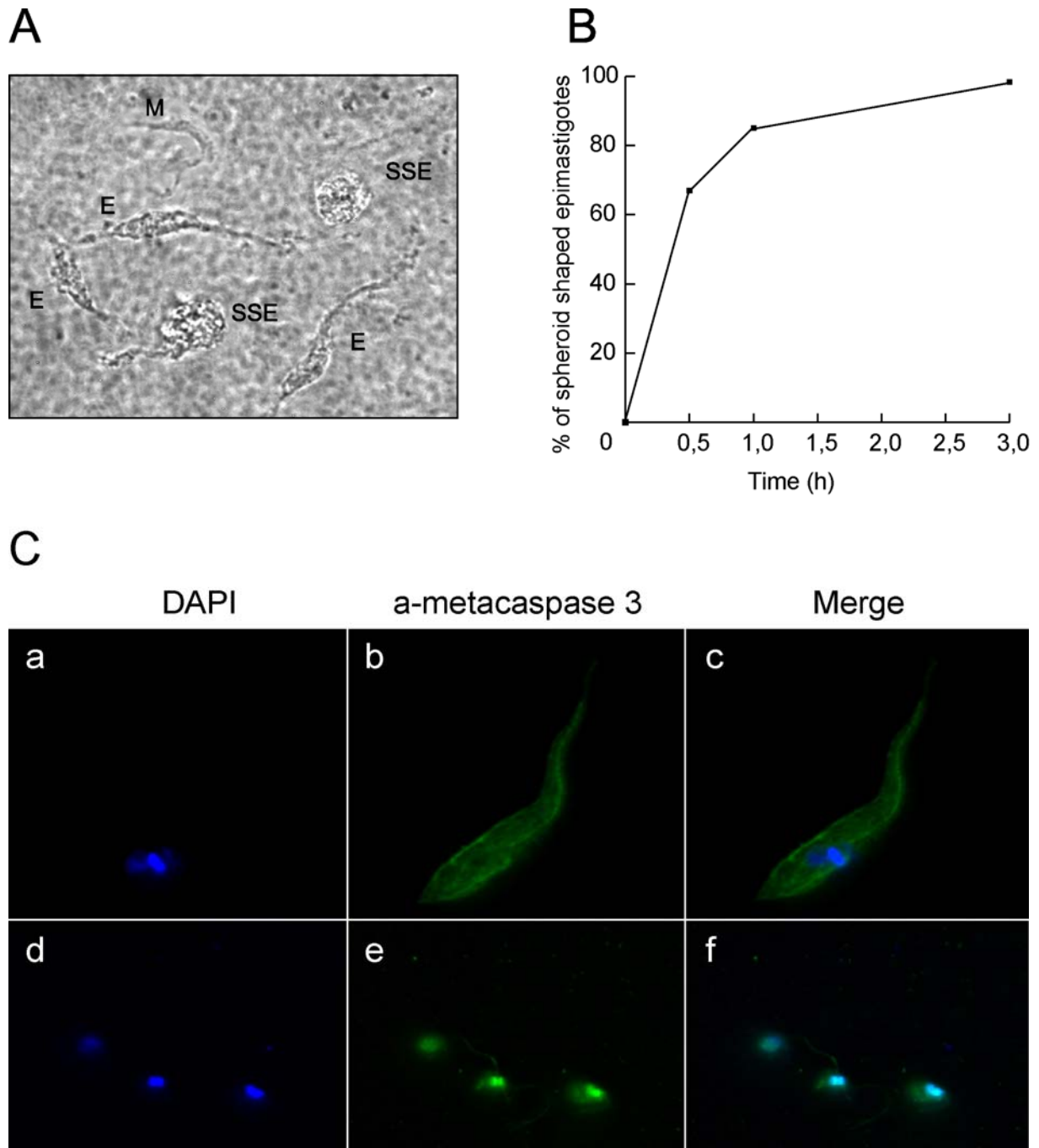


Figure 16 **A**) Light microscopy analysis of FHS treated epimastigotes. Normal epimastigotes (E), metacyclic trypomastigotes (M) and spheroid shaped epimastigotes (SSE) are depicted in the figure. **B**) Parasites were exposed to 10 % FHS and at different times after the treatment the numbers of dead (spheroid shaped, non-motile) epimastigotes were assessed under the light microscope. **C**) Localization of DAPI staining (a and d) and anti-metacaspase-3 antibody signal (b and e) during FHS-induced PCD of *T. cruzi* epimastigotes (d – f) and control epimastigotes (a – c). (c and f) Merge images of a + b and d + e respectively.

#### **4.5 *ATG4* and *ATG8* homologs in *T. cruzi* genome**

We have searched the recently completed genome of *T. cruzi* (El-Sayed et al. 2005) for sequences related to the yeast Atg4 and Atg8 proteins. In the case of *ATG4*, BLAST analysis identified two candidates showing 20% and 30% identity with yeast *ATG4*, which we termed as *TcATG4.1* and *TcATG4.2*, respectively. Both candidates code for active site Cys, His and Asp residues and are 21% identical to each other when comparing the region corresponding to the conserved C54 family domain. The absence in autophagins of a recognizable signal peptide is also remarkable. This indicates that these proteins are cytoplasmic enzymes and therefore distinct from members of the large papain family of secreted or reservosomal cysteine peptidases. Interestingly, for each *TcATG4* clear orthology candidates are evident in *T. brucei* (Tb927.6.1690 and Tb11.01.7970) and *L. major* (LmjF32.3890 and LmjF30.0270) genomes (Figure 17, Table 2).

TcATG4.2	RNGFFLLTYRMNFSPLPHSS-----VTSDKGGWGLV	31
TcATG4.1	TEALLYFSYRNRIIVPLMNGA-----TTDLFWGMI	30
ScATG4	VQSRVNFTYRTRFVPIARAPDGPSPSLNLLVVRTNP	60
TbATG4.2	ENSFYLFYRRYFDPLPYST-----LTSDKGGWGLA	31
TbATG4.1	ACKLLYFSYRCQFEPLRNGS-----TTDIGWGCTI	30
LmATG4.2	TDTFLIFTYRDGFPAIPAVTR-----LIETDQGGWGLL	33
LmATG4.1	TKKLLYFSYRNCFPPLPSGS-----TTDTHWGGLV	30
HsATG4b	VASRLWFTYRKNFPAIGGTG-----PTSDTGGWGL	31
	::** : .:	:* **
TcATG4.2	RSSQMLLAHALWRYS-----ANDCRLDHFDRMDTEDSTP	79
TcATG4.1	RTGQMMLAHAFMRYFNGGGPHIGS-ERLQELRARTQTLF	89
ScATG4	RTGQSLLGNALQILHLGRDFRVNG-NESLERESKFVNWF	119
TbATG4.2	RATQMLLACSLRRHS-----AQDCKLQYFADLDDEQ	79
TbATG4.1	RAGQMMLAHALMRYKNGGGASFED-SIVPSLKQATQHL	89
LmATG4.2	RTSQMLLAHFLVWHGR-----PADRKLSLFFDHS-AE	80
LmATG4.1	RTTQMLVGTCLLRYHCKGAYVLP-ADNAELKERISRL	89
HsATG4b	RCGQMIFAQALVCRHLGRDWRWTQRKRQPDYSYFV	91
	* * :. . :	: .:*
TcATG4.2	DVFRPEYWTSPSQCEAIR-----CCVNAVDRKLIP-	110
TcATG4.1	VNCG-EWFGPTPIAKTLS-----ALMASYLAAGGEGP	120
ScATG4	DKRPGEWFGPAATARSIQ-----SLIYGFPECGIDDC	151
TbATG4.2	ESLRPVYWAPSPQCEAIS-----GCVKRATERGILSS	111
TbATG4.1	APCG-SWFGPTHVAVVMG-----ALMEDYLRNGGQGP	120
LmATG4.2	RVFKAEYWSPSQCEAIK-----RTVQGAVKTEQLQT	112
LmATG4.1	VKYA-SMLSPTEAGMAIA-----AALIAFRAQGGDVP	120
HsATG4b	KSIG-QWYGPNTVAQVLKKLAVFDTWSSSLAVHIAMD	150
	* :	
TcATG4.2	PIRVVCSQGCLLAREICSNLEFG--TVLILAPMRCGAS	168
TcATG4.1	VVLAFPERQ--IFLEEVKELLRQSTHVLLIPVMLG--	176
ScATG4	IVSVS--SGDIYENEVEKVFNAENPNSRILFLLGVK	208
TbATG4.2	PLSVVITVAGAVPAEEVVSCHLKE-SR-NVLILAPLRC	170
TbATG4.1	DVLVLRDRQ--VMEDEVKILLKSKHVLLIPVMLG--	176
LmATG4.2	RVMVVTSTNGCIYADEVQHTFKQGADVVLVLASVRV	172
LmATG4.1	FTFCCESRH--IDEPAVMAKLLLEGQHVVLIIPVVLG	176
HsATG4b	PADSDRHCNGFPAGAEVTNRPSRPLVLLIPLRLG--	208
	: : : : :	
TcATG4.2	GVVGGVPQRSYYILGTSGQR-LLYLDPHCMTQEALVSS	227
TcATG4.1	GILGGKRSRSLFLFGHQDDD-VFFLDPHCVQPAFTSSG	229
ScATG4	GIAGGRPSSSLYFFGYQGNE-FLHFDPHIPQPAVEDSF	261
TbATG4.2	GMVGGVPNRYGYYIIGTGAQELLLYLDPHCKTQDALL	230
TbATG4.1	GAVGGKEGSAFFFMGYQGGN-LIVLDPHYAQSAFTCS	229
LmATG4.2	GVVGGVPGRSYYFFAHNQTTQ-LFYLDPHQRTAAALL	231
LmATG4.1	GIAGGFKQASLYMFGHQGRS-VFFMDPHYVQNAYTSS	229
HsATG4b	GVVGGKPNSAHYFIGYVGGEE-LIYLDPHITTPAVEP	267
	* ** . : : . : : : : : : :	
TcATG4.2	VDTSCFLGFLVDSFAEWLEL	247
TcATG4.1	YDTSMTLGFYISSLDSLALF	249
ScATG4	MDPSMLIGILIKGEKDWQQW	281
TbATG4.2	VDTSFFLGFVDSQSRWESL	250
TbATG4.1	CSTSVLLGFYIHSPDSFSQF	249
LmATG4.2	VDTSLFLAFVTTREDEWAAL	251
LmATG4.1	FDPCMVLGFYLHTPEDYRVF	249

Figure 17 Alignment of C54 family peptidase domain amino acid sequences of *ATG4*-like genes from trypanosomatid organisms, yeast and humans. (Tc = *Trypanosoma cruzi*, Tb = *Trypanosoma brucei*, Lm = *Leishmania major*, Sc = *Saccharomyces cerevisiae*, Hs = *Homo sapiens*). Active site C, D and H residues are marked in red and, additionally, Y residue that participates in the oxyanion hole formation (Sugawara et al. 2005) is marked in yellow.

	<i>Tc</i> <i>ATG4.2</i>	<i>Tc</i> <i>ATG4.1</i>	<i>Sc</i> <i>ATG4</i>	<i>Tb</i> <i>ATG4.2</i>	<i>Tb</i> <i>ATG4.1</i>	<i>Lm</i> <i>ATG4.2</i>	<i>Lm</i> <i>ATG4.1</i>	<i>Hs</i> <i>ATG4.b</i>
<i>TcATG4.2</i>		21	21	56	20	41	19	23
<i>TcATG4.1</i>	21		30	25	53	22	39	28
<i>ScATG4</i>	21	30		21	28	21	25	29
<i>TbATG4.2</i>	56	25	21		25	37	19	24
<i>TbATG4.1</i>	20	53	28	25		20	34	32
<i>LmATG4.2</i>	41	22	21	37	20		22	21
<i>LmATG4.1</i>	19	39	25	19	34	22		19
<i>HsATG4.b</i>	23	28	29	24	32	21	19	

Table 2. Percentage of identity among C54 peptidase family amino acid sequences of *ATG4*-like genes.

A similar situation was found for *ATG8* where two candidates, which we named as *TcATG8.1* and *TcATG8.2*, were found in the *T. cruzi* genome. In addition to an overall similarity in amino acid sequence to the yeast *ATG8* (Figure 18), *TcATG8.1* and *TcATG8.2* share the conserved glycine residue at the C-terminus. These *ATG8* homologues are 43 % identical to each other with strong similarity in sequences immediately upstream from the conserved Gly residue, whereas they have variable sequences in the downstream region. *TcATG8.1* is the orthologue with the highest sequence identity (53%) to yeast *ATG8* protein and also has two homologous genes (Tb07.10C21.40 and Tb07.10C21.50) in *T. brucei* (68 and 60% identity) and one (LmjF19.1630) in *L. major* (52% identity). *TcATG8.2* has one closer homolog (Tb07.28B13.800) in *T. brucei* (48% identity) (Table 3). Interestingly, *Leishmania major* presents several more distantly related *ATG8*-like sequences, whose direct orthologues don't seem to be present in *T. cruzi* and *T. brucei*.

```

TcATG8.1      MAPKKLESKYKNHTHTLEHRIAEEAAKVRERHPDRLPIICEKVDDSDIG----- 47
TcATG8.2      -MARKYR--YQRTHTFAERQKEVATIRGRFPQHVPPVCEP---ASIDTVLSAGPISDRCR 54
ScATG8        --MKST---FKSEYPFEKRKAESERADRFPKNRIPVICEKAEKSDIP----- 42
Tb07.10C21.40 --MSKKDSKYKMSHTFESRQSDAAKVRERHPDRLPIICEKVYNSDIG----- 45
Tb07.10C21.50 --MKYN---FKDHSLSVKRLNESAKVRKSHPNHFPVICEKVYNSDIG----- 42
Tb07.28B13.800 -MPSHYR--YQYTRSFAERAKETESARLRYPKHIPILCEPTSAASASTPRDVRFLFSTRQQ 57
LmjF19.1630   -MSSRVAGSYKKAHTLEARLRDAEKVRERAPDRILVICEKAENSPVP----- 46
HsmapLC3B     -MPSEKT--FKQRRTFEQRVEDVRLIREQHPTKIPVIERYKGEKQLP----- 45
              ::  .:  *  :  .:  .:  *

TcATG8.1      ---DLDKGKFLVPSDLTVGQFVLVLRKRVRVDADEAIFLFDV-N-GAVPPTTAQMSDLYAHH 103
TcATG8.2      LLRDLDCKSKFLVPGDASMQQLMVLRLSRLLVLDAEQAIFFLFD-DAVLPNSACVGDLYAQR 113
ScATG8        ---EIDKRKYLVPADLTVGQFVYVIRKRIMLPPEKAIFFVFN-DTLPPTAALMSAIYQEH 98
Tb07.10C21.40 ---ELDRCKFLVPSDLTVGQFVSVLKRVRVQLEAESALFVYTN-DTVLPSSAQMADIYSKY 101
Tb07.10C21.50 ---ELDRCKFLVPSDLTVGQFVSVLKRVRVQLEAESALFVYTN-DTVLPSSAQMADIYSKY 98
Tb07.28B13.800 VQRELDCKFLVPEATVMEFMMALRQLLLEEGQAVFVFIG-NELPPNSACLGDYARA 116
LmjF19.1630   ---DLDKSKFLVPPDATVGGFLVSIIRRRITMEAEKALFLFVG-DSVPANSTLMSDLFNRY 102
HsmapLC3B     ---VLDKTKFLVDPDHVNMSELIKIIRRRQLNANQAFLLVNGHSMVSVSTPISEVYESE 102
              :*  *:*:*  .:  .:  :*  *  :  .:*:*  .  .  .:  .:  .:

TcATG8.1      KDEDGFLYIKYSGEATFGSW----- 123
TcATG8.2      KDADGFLYMTYSIESAFGGAARRNS 139
ScATG8        KDKDGLYVVTYSGENTFGR----- 117
Tb07.10C21.40 KDEDGFLYMKYSGEATFGC----- 120
Tb07.10C21.50 KDEDGFLYMKYSGEAAFGE----- 116
Tb07.28B13.800 KDPDGFLYVSYGVENTFG----- 134
LmjF19.1630   KDEDGFLYVVTYSGENTYGGQLH--- 125
HsmapLC3B     KDEDGFLYMVYASQETFGMKLSV--- 125
              **  *****:  *.  .:  .:  *

```

Figure 18 Alignment of *ATG8*-like protein amino acid sequences from trypanosomatid organisms, yeast and humans. (Tc = *Trypanosoma cruzi*, Tb = *Trypanosoma brucei*, Lm = *Leishmania major*, Sc = *Saccharomyces cerevisiae*, Hs = *Homo sapiens*). Conserved region upstream of the P1 Gly residue (marked in red) is marked in yellow. Upstream conserved basic region is marked in cyan.

	<i>TcATG</i> 8.1	<i>TcATG</i> 8.2	<i>Sc</i> <i>ATG8</i>	<i>Tb07.10C2</i> 1.40	<i>Tb07.10C2</i> 1.50	<i>Tb07.28B1</i> 3.800	<i>LmjF19.</i> 1630	<i>HsmapL</i> <i>C3B</i>
<i>TcATG8.1</i>		43	53	68	60	36	52	35
<i>TcATG8.2</i>	43		37	42	44	48	41	35
<i>ScATG8</i>	53	37		50	52	37	50	34
<i>Tb07.10C21.40</i>	68	42	50		81	38	52	36
<i>Tb07.10C21.50</i>	60	44	52	81		38	47	33
<i>Tb07.28B13.800</i>	36	48	37	38	38		36	32
<i>LmjF19.1630</i>	52	41	50	52	47	36		38
<i>HsmapLC3B</i>	35	35	34	36	33	32	38	

Table 3. Percentage of identity among *ATG8*-like genes from amino terminal Met residue till Gly residue at the P1 site of autophagin cleavage.

## 4.6 Expression and purification of recombinant autophagins and recombinant *Atg8.1* and *Atg8.2*

We amplified the *ATG4.1*, *ATG4.2*, *ATG8.1* and *ATG8.2* genes by PCR and cloned them into the pET-28 expression vector taking advantage of the vector's feature to add (His)<sub>6</sub> tag to the C-terminal end of recombinant proteins. We performed the expression in the cytosol of *E. coli* BL21 (DE3) pLysS cells at 28 °C for 4-5 h in case

of Atg8 proteins and at 18 °C for 8 h in case of the Atg4 peptidases. The yield of expression was in the order of several mg per liter for the smaller Atg8.1 and Atg8.2 and in the order of 100 µg per liter for the autophagin-1 and -2. All recombinant proteins were readily purified using Ni-NTA or affinity chromatography (Figure 19; Figure 20). Co-NTA resin was also tried for purification of the peptidases, however, no change in yield or activity was observed as compared to Ni-NTA.

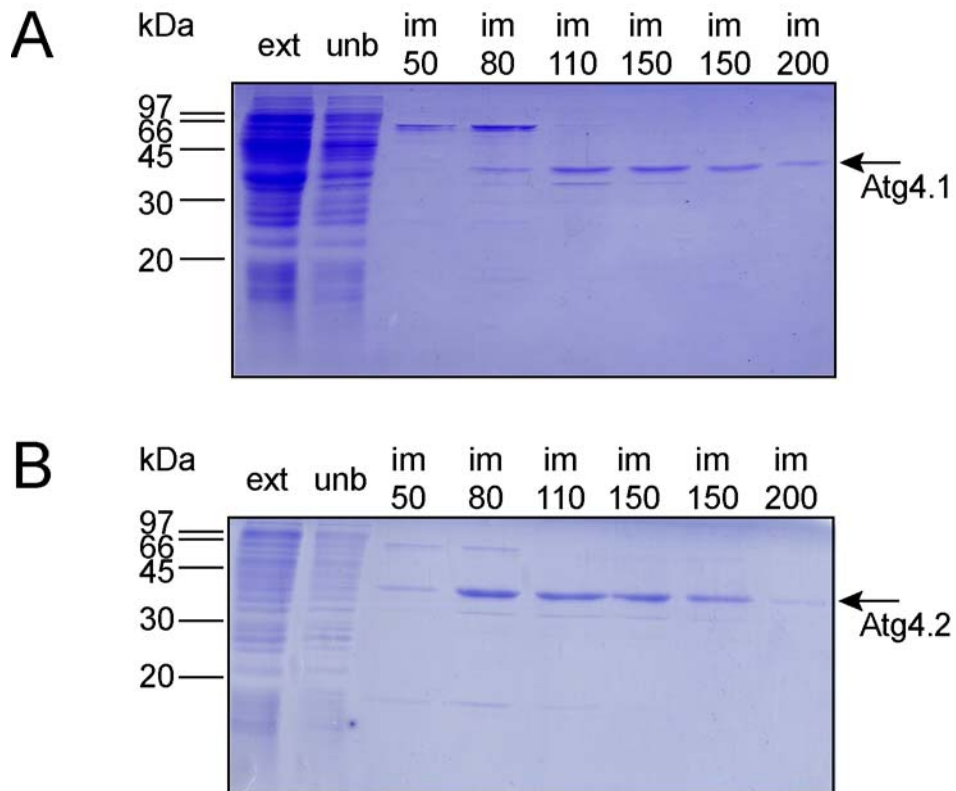


Figure 19 Purification of Atg4.1 (panel A) and Atg4.2 (panel B) with Ni-NTA affinity chromatography. The results were analyzed by SDS PAGE with Coomassie Brilliant Blue staining. In the first lane induced bacterial protein extract is shown; in the second lane the unbound fraction is presented; in the next lanes, washing/elution steps with 50, 80, 110, 150 and 200 mM imidazole are analyzed showing a band of approx. 40 kDa, which is in good agreement with the predicted molecular mass.

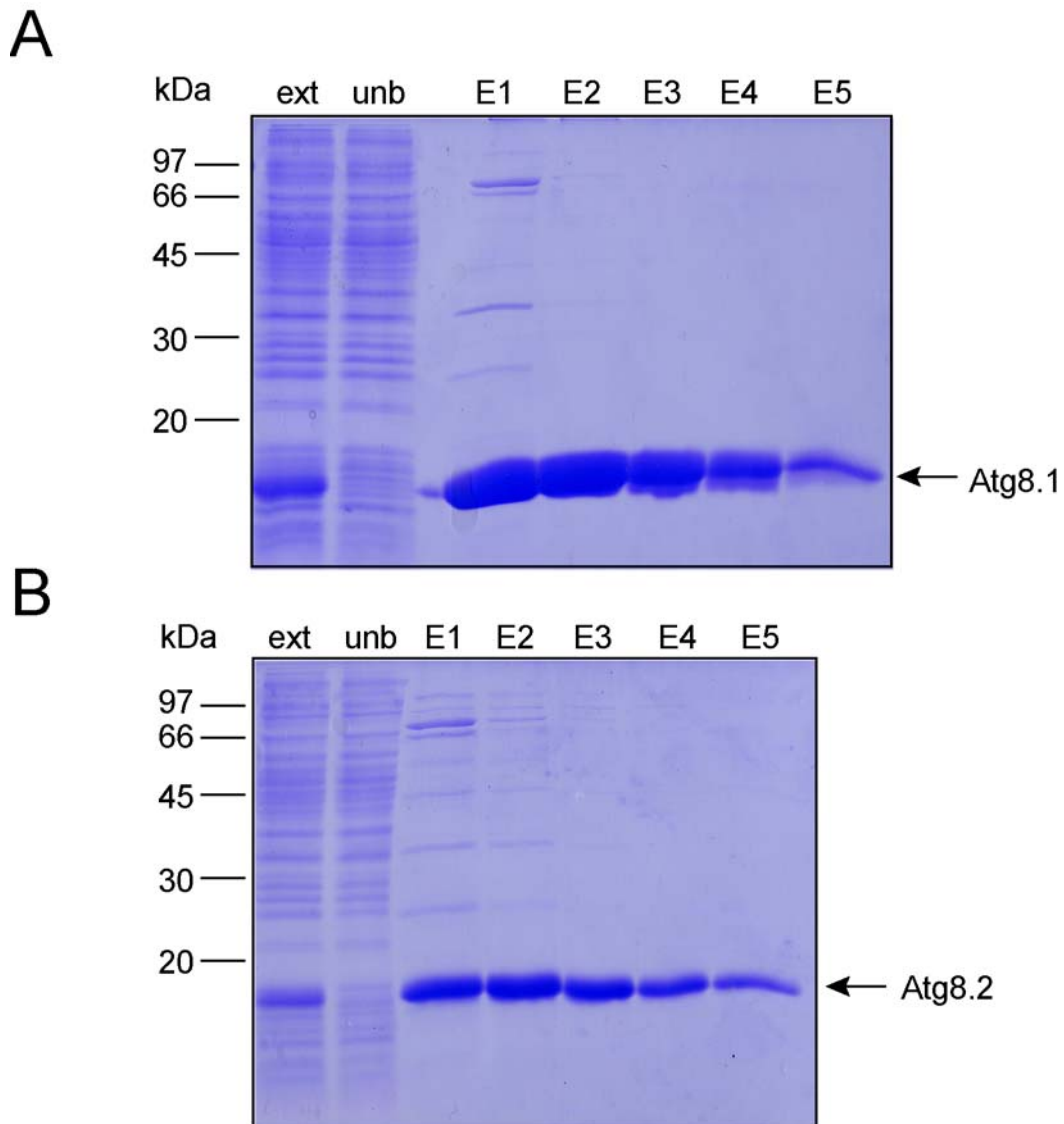


Figure 20 Purification of Atg8.1 (panel A) and Atg8.2 (panel B) with Ni-NTA affinity chromatography. The results were analyzed by SDS PAGE with Coomassie Brilliant Blue staining. In the first lane induced bacterial protein extract is shown; in the second lane the unbound fraction is presented; in the next lanes eluates with 150 mM imidazole are analyzed showing a band of approx. 15 kDa, which is in good agreement with the predicted molecular mass.

#### 4.7 Proteolytic activity of recombinant autophagins on recombinant Atg8.1 and Atg8.2

We expressed and purified recombinant autophagins and Atg8.1 and Atg8.2 proteins. Then we evaluated whether Atg8.1 and Atg8.2 are substrates for autophagin-1 and -2. Figure 21 shows that autophagin-1 cleaves the two *T. cruzi* Atg8 proteins at similar rates and the reaction is inhibited by iodoacetamide. The reaction was also inhibited by N-ethylmaleimide but not by E-64, cystatin C, EDTA, *o*-phenantroline, PMSF and pepstatin (not shown).

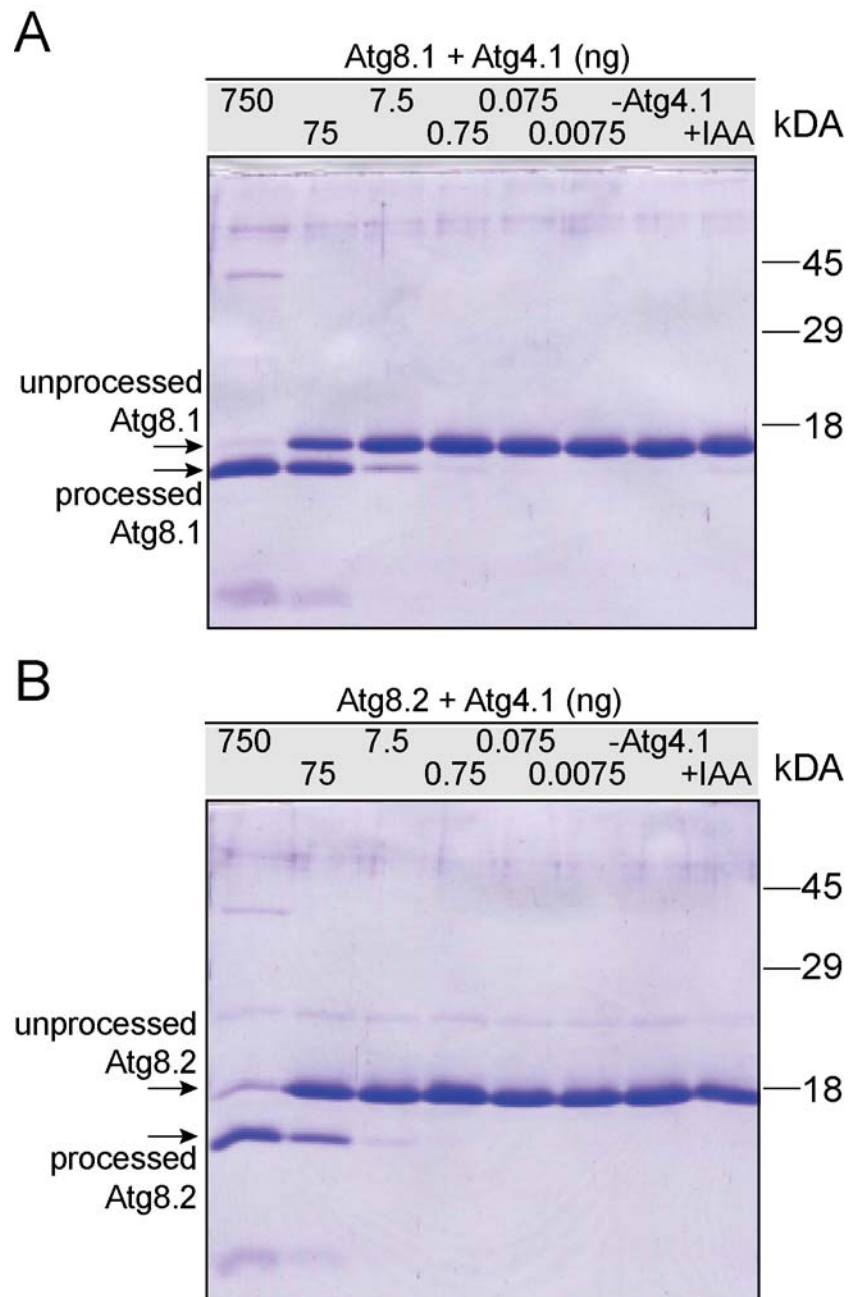


Figure 21 *In Vitro* cleavage assay. Constant amounts (17,2  $\mu$ g) of Atg8.1 (Panel A) or Atg8.2 (Panel B) were incubated with different amounts of recombinant autophagin-1 for 35 min and one fifth of the reaction mixtures was analyzed by SDS-PAGE using Coomassie Brilliant Blue staining. In the first lane Atg8.1 was completely processed after the addition of 750 ng of autophagin-1. In next 5 lanes: subsequent 10 fold dilutions of autophagin-2 were added to the substrate resulting in less cleavage product. Second lane from the right represents control without autophagin-1 addition and the last lane processing with 75 ng autophagin-1, however, inhibited with iodoacetamide.

In contrast, autophagin-2 seems to process Atg8.1 and Atg8.2 very poorly. The reaction seems to proceed about four orders of magnitude slower than processing with autophagin-1 (Figure 22).

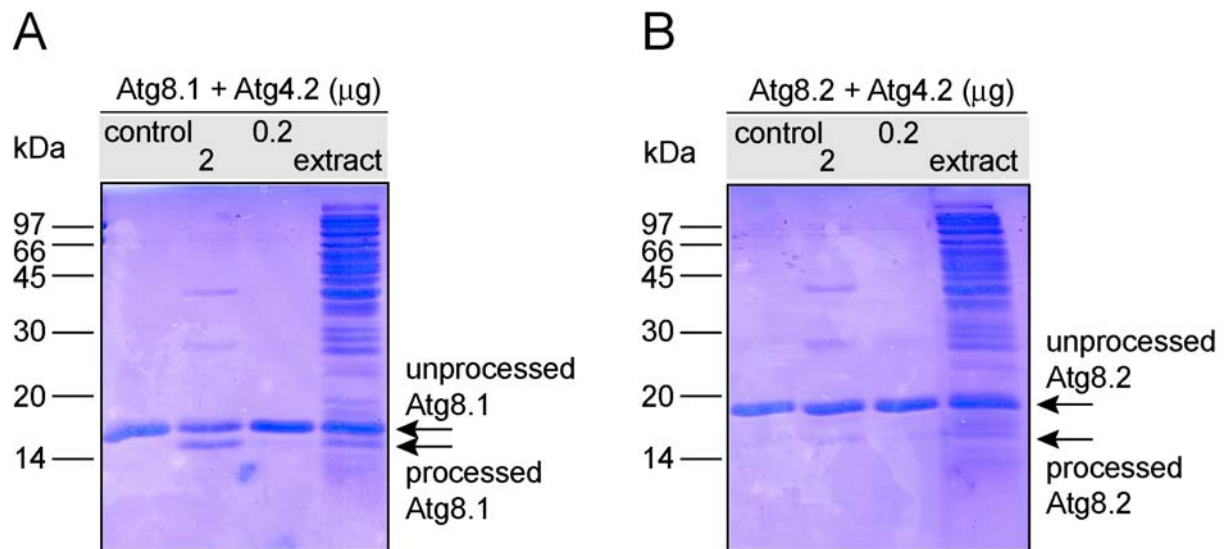


Figure 22 *In Vitro* cleavage assay. Constant amounts (17,2 µg) of Atg8.1 (Panel A) or Atg8.2 (Panel B) were incubated with different amounts of recombinant autophagin-2 for 18 h and one fifth of the reaction mixtures was analyzed by SDS-PAGE using Coomassie Brilliant Blue staining. The first lane represents control sample with no autophagin-2 added; in the second lane 2 µg of autophagin were added resulting in a weak band of processed Atg8.1 and barely detectable band of processed Atg8.2. In the third lane, 0,2 µg of autophagin-2 were added and almost no processing product can be observed in case of either substrate. In the last lane cell free protein extract of autophagin-2 expressing bacteria was added, corresponding to about 150 µL of induced cell culture. Very weak bands corresponding to the processed form of products indicate, that autophagin-2 is poorly active even before Ni-NTA purification step.

Reaction products of Atg8.1 and Atg8.2 proteolytic processing with autophagin-1 were separated by reverse phase HPLC C8 column and the cleaved C-terminal was isolated (Figure 23). Edman N-terminal sequencing was performed (kind acknowledgement to Adrijana Leonardi) to identify the exact cleavage site. In the case of Atg8.1 the sequence was "SWWDP" and in the case of Atg8.2 "GAAVR" both corresponding to sequences downstream of the conserved Gly residue. Reaction products of the equivalent reaction with autophagin-2 were similarly applied to the same HPLC system and their retention times were the same as for autophagin-1 cleavage. We conclude that both autophagins cleave Atg8.1 and Atg8.2 at the same site, although autophagin-2 much less efficiently.

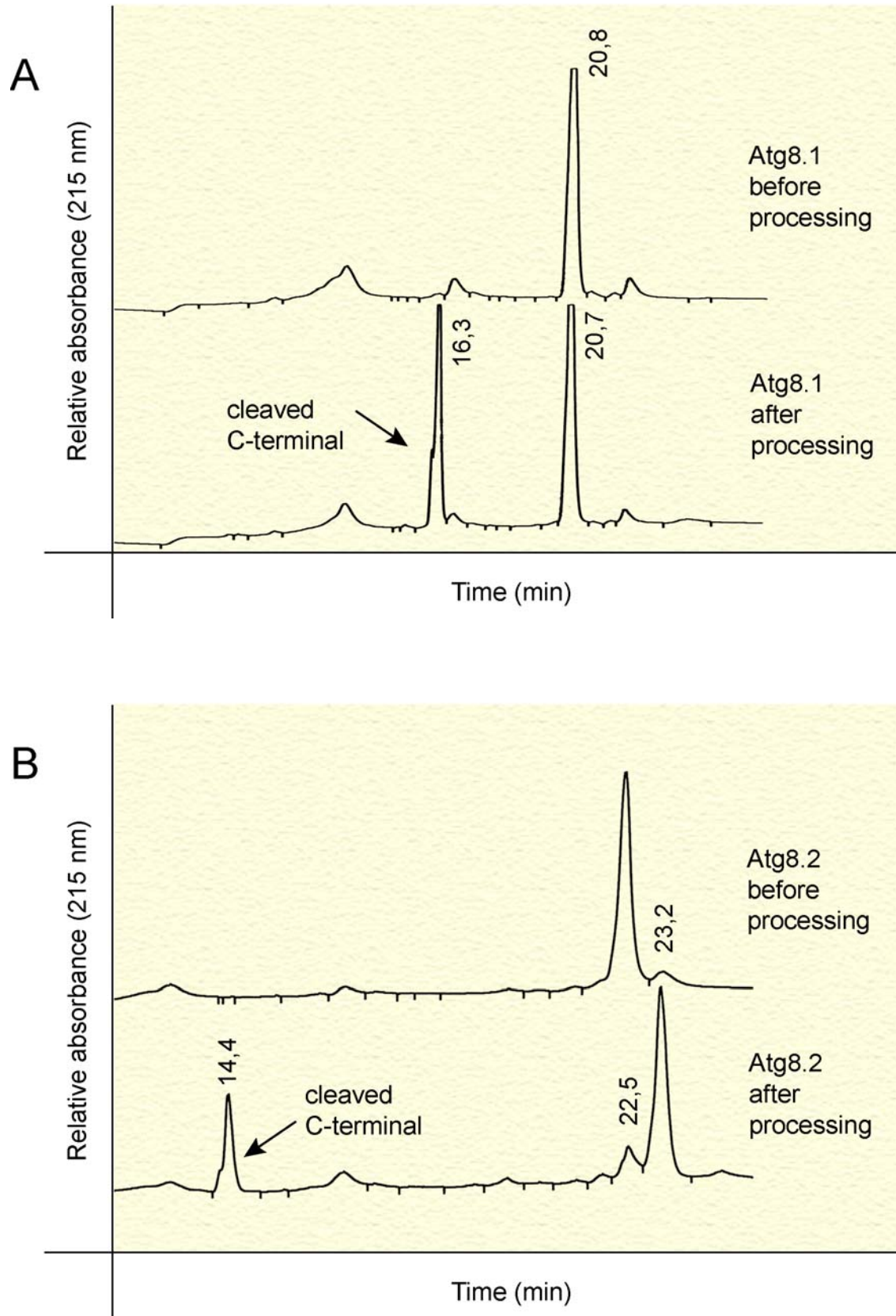


Figure 23 Reverse phase HPLC chromatograms of Atg8.1 untreated sample and autophagin processed sample (panel A) and Atg8.2 untreated sample and autophagin processed sample (panel B). Cleaved C-terminal peaks are clearly recognizable (at 16,3 and 14,4 min) in both cases and the retention of the processed Atg8.2 is moderately augmented after cleavage with respect to the unprocessed protein. The images were obtained with analog recorder and digitalized respecting the relative sizes of the peaks.

## 4.8 Autophagin activity is expressed in all four *T. cruzi* developmental stages

As a preliminary step to study the physiological role of autophagins in *T. cruzi*, we evaluated the autophagin activity in all four developmental stages of the parasite. For this purpose, cell-free extracts of epimastigotes, metacyclic trypomastigotes, amastigotes and cell-derived trypomastigotes were mixed with the recombinant substrate proteins, Atg8.1 or Atg8.2. Following incubation at room temperature during 18 hours, we determined the cleavage activity by immunoblotting using anti-Atg8.1 or anti-Atg8.2 antibodies. Figure 24 shows that proteolytic processing of the substrates takes place in all life cycle stages. It is noteworthy that, although the band seems to be more intense after treatment with amastigote extract, greater number of amastigotes is needed to obtain the same amount of protein (Figure 24). Therefore, it appears that autophagins are expressed roughly constitutively all around the parasitic cycle.

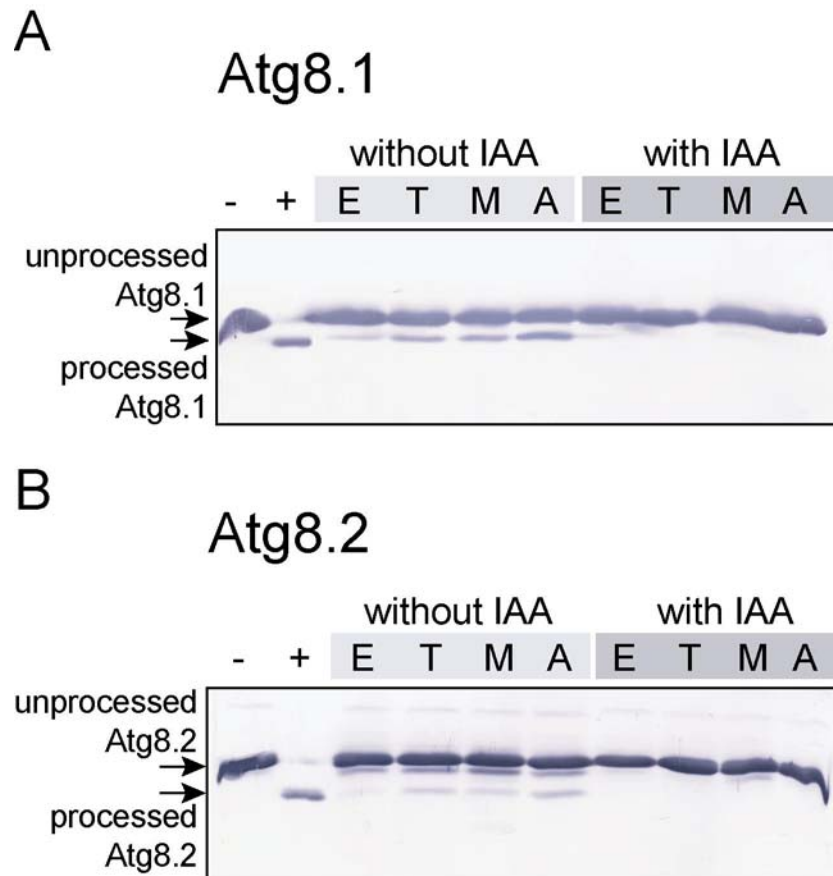


Figure 24 Autophagin activity in cell-free extracts of *T. cruzi* different life cycle stages. Constant amounts (17,2 µg) of Atg8.1 (Panel A) or Atg8.2 (Panel B) were incubated with 100 µg of cell-free extracts of different *T. cruzi* life cycle stages. One third of the reaction mixture was analyzed by Western blot using specific polyclonal antibodies (Panel A: anti-Atg8.1 and Panel B: anti-Atg8.2). In the first lane of each blot, control of the corresponding untreated Atg8 is shown; while in the second lane of each blot the corresponding Atg8 cleaved by *T. cruzi* recombinant autophagin-1 is displayed. In the next four lanes of each blot the corresponding Atg8 was incubated with cell-free extracts of: epimastigotes (E), cell-derived trypomastigotes (T), metacyclic trypomastigotes (M) and amastigotes. In the last four lanes of every blot equivalent reactions were inhibited with iodoacetamide.

## 4.9 *ATG4.1*, *ATG4.2* and *ATG8.1* reconstitute autophagy in autophagy deficient yeast knock-outs

We were interested to know whether *T. cruzi* *ATG4.x* and *ATG8.x* can play a functional role in autophagic processes. It is known that *S. cerevisiae atg4Δ* and *atg8Δ* strains are deficient in autophagy and cvt-pathway and therefore cannot deliver proaminopeptidase I from the cytosol to the vacuole where it is processed to mature enzyme. *atg4Δ* strain was transformed with *TcATG4.1* and *TcATG4.2* and *atg8Δ* strain with *TcATG8.1* and *TcATG8.2*. Transformants were evaluated for their ability to process proaminopeptidase I in normal growth

conditions and under nitrogen starvation. Figure 25 shows that *TcATG4.1* and *TcATG4.2* reconstitute cvt- and autophagic pathways producing a mature aminopeptidase I band in nutrient rich and starvation conditions. Neither of the *TcATG8.x* proteins reconstitutes the cvt-pathway in nutrient rich conditions, however, under nitrogen starvation conditions a weak mature aminopeptidase band is observed in *TcATG8.1* transformant suggesting that autophagy is at least partially reconstituted.

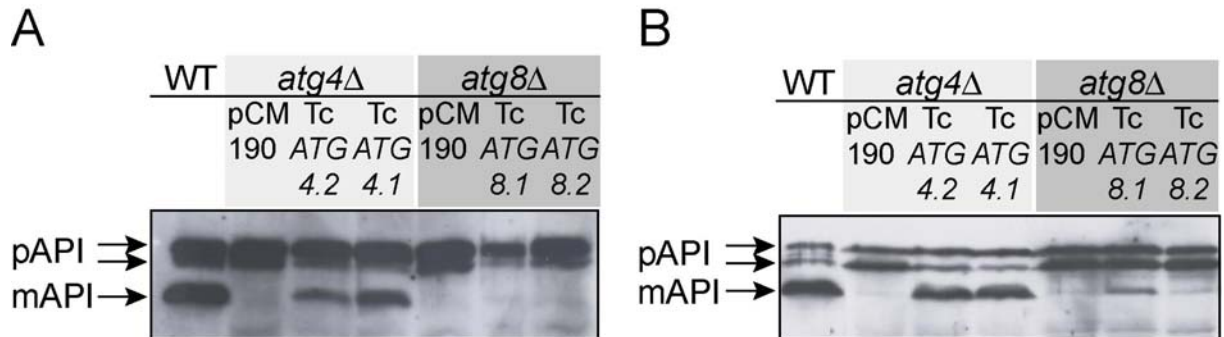


Figure 25 Complementation of *atg4Δ* and *atg8Δ* yeast strains with *T. cruzi* homologues. Transport of proaminopeptidase I (pAPI) to the vacuole, where it matures, only takes place when a functional autophagy/cvt pathway is present. The two bands with the higher molecular mass represent pAPI while the band with the lower molecular mass corresponds to mature aminopeptidase (mAPI). *S. cerevisiae atg4* and *atg8* knockout strains were transformed with: empty pCM190 plasmid or the same plasmid containing *TcATG4.2* or *TcATG4.1* in the case of *atg4Δ* and *TcATG8.1* or *TcATG8.2* for *atg8Δ*. **A)** Western blot analysis of transformants under normal growth conditions using anti-pAPI antibodies. *atg4* knock-out shows no mAPI band when transformed with pCM190 plasmid alone whereas *TcATG4.1* and *TcATG4.2* expression clearly restores the cvt-pathway. The defect of *atg8* deficient yeasts could not be overcome by expression of *TcATG8.1* or *TcATG8.2* under these conditions. **B)** Western blot analysis of the same transformants in starvation conditions. The result is similar in case of *ATG4* complementation; however, a mAPI band can also be observed in case of *atg8* knock-out expressing *TcATG8.1*. In case of *TcATG8.2* expression no mature aminopeptidase band can be observed, similarly to the nutrient rich conditions.

#### 4.10 Assessment of binding of Atg8.1 and Atg8.2 to microtubules *in vitro*

In order to further characterize biological role of the Atg8.1 and Atg8.2 in cellular processes we performed an *in vitro* experiment to see whether these proteins bind to microtubules, similar to human *ATG8* homolog, which was first identified as a microtubule binding subunit of MAP1A and MAP1B (MAP-LC3) (Mann and Hammarback 1994). In addition plant *ATG8*-homologs also bind to microtubules (Ketelaar et al. 2004), however, in yeast this does not seem to be the case (Kirisako et al. 1999). Purified bovine tubulin was polymerized to form microtubules which were later incubated with Atg8.1 or Atg8.2. Proteins were cross-linked and immunofluorescence microscopy study was performed to detect colocalization. Figure 26 shows that no similarity can be found between microtubule pattern (panels a and d) and TcAtg8.1 or TcAtg8.2 distribution (panels b and e) and it is therefore improbable that Atg8.1 or Atg8.2 bind to *T. cruzi* microtubules.

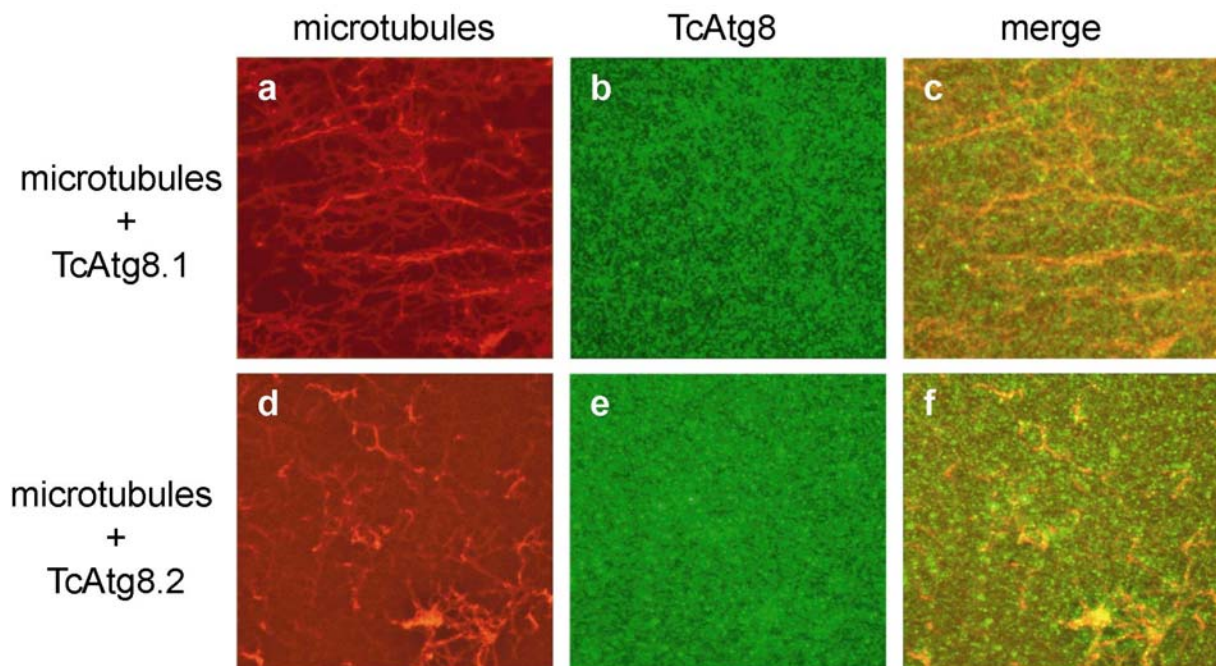


Figure 26 Colocalization of microtubules and TcAtg8.1 and TcAtg8.2 proteins *in vitro*. Microtubules were incubated with Atg8.1 protein (panels a – c) or Atg8.2 protein (panels d – f). Microtubule pattern was detected in red with monoclonal anti-tubulin antibody (panels a and d) and Atg8.1 and Atg8.2 distribution in green with polyclonal antibodies raised in rabbits (panels b and e). Merge images without probable colocalization are shown in panels c and f.

#### 4.11 Atg8.1 and Atg8.2 are localized in small punctate pattern in *T. cruzi* epimastigotes and reveal larger structures in starvation conditions

Sub-cellular localization of Atg8.1 and Atg8.2 was determined in epimastigotes using antisera raised against recombinant proteins for immunofluorescence studies. Both proteins show a small punctate pattern in normal growth conditions with few larger spots for ATG8.1 (Figure 27, panels a and c). After prolonged starvation for 20 h in PBS, when the parasites stopped moving, an equivalent immunofluorescence experiment was performed. Anti-Atg8.1 antibody revealed the concentration of this protein in several bright spots per cell, a distribution compatible with autophagosome formation. Anti-Atg8.2 antibody reveals severe vacuolization of the cell, moreover, several vacuoles show “rings” around their circumference suggesting membrane localized Atg8.2 (panel d). Apart from that, in some parasites Atg8.2 revealed a pattern of bright spots, very similar to the Atg8.1. Based on these observations we believe that *TcATG8.1* is a functional homolog of yeast *ATG8* mediating autophagosome formation in *T. cruzi*. *TcATG8.2* also seems to be involved in autophagy, however, it is still not possible to envision its exact role in the process.

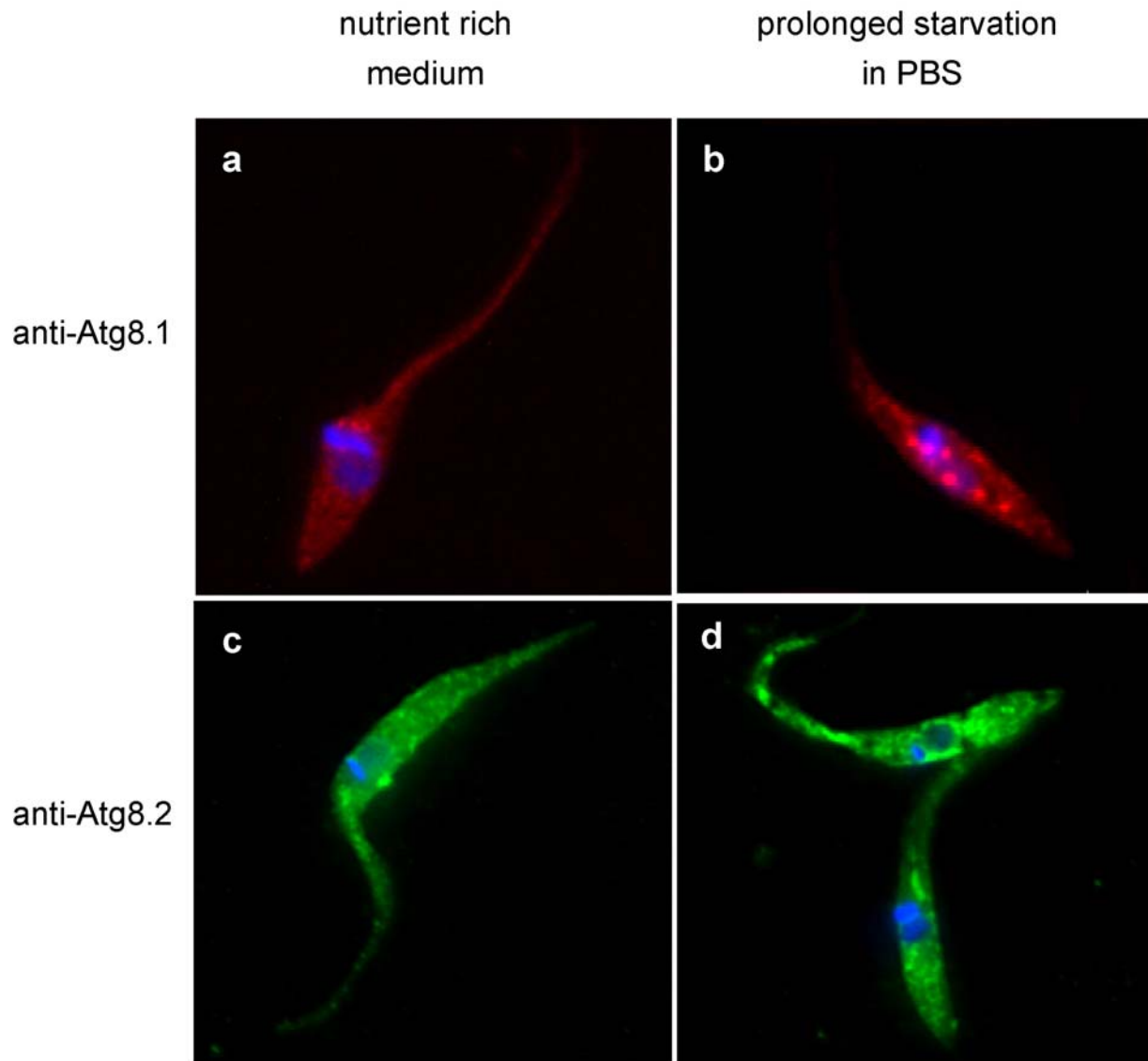


Figure 27 Sub-cellular localization of Atg8.1 (in red) and Atg8.2 (in green) proteins in nutrient rich BHT medium + 10 % FCS and after prolonged starvation in PBS for 20 h as seen in indirect immunofluorescence experiments. Pictures in panels a and b were obtained with anti-Atg8.1 antibody and panels c and d with anti-Atg8.2 antibody. Blue color reveals DAPI stained nuclear (bigger and more faint) and kinetoplast (smaller, brighter and elongated) DNA. Several bright spots can be observed in panel B corresponding to Atg8.1 localized to the autophagosomes.

## 5 Discussion

### 5.1 The metacaspase family

In this work two families of cysteine peptidases were characterized in the unicellular protozoan parasite *T. cruzi*, the metacaspases and the autophagins, and their physiological role was partially elucidated. Continuing our previous work on *TcMCA3* gene (metacaspase-3) copies we determined that metacaspases might be involved in the fresh human serum induced programmed cell death of epimastigotes, although the mechanism of their action seems to be clearly different from that of the metazoan caspases. *T. cruzi* metacaspases seem to translocate from the cytosol to the nucleus upon FHS exposure. More detailed genetic analyses showed that two clusters of tandemly repeated genes are present per haploid genome of *T. cruzi*. We also observed metacaspase-3 to be expressed in all four developmental stages of *T. cruzi* suggesting that possible new roles of this family of enzymes should be sought for, especially in developmental stages present in the mammalian host.

In order to completely characterize the metacaspase family in *T. cruzi*, the second metacaspase gene present, *TcMCA5*, was also investigated as part of our collaboration project (V. Alvarez, personal communication, (Kosec et al. 2006)). In contrast to *TcMCA3* gene, which is present in tandemly arrayed multiple copies of genes, *TcMCA5* seems to be present as a single copy per haploid genome. Performing a similar PFGE experiment as described above for *TcMCA3*, where we found two tandems localized on two different chromosomes (Figure 14 A), we determined that *TcMCA5* is located on a chromosome of apparent size of 1,88 Mbp. Apart from the p-20-like and p-10-like subunits present in *TcMCA3*, the *TcMCA5* also contains a signal peptide for translocation to the ER and secretory pathway and an unusual C-terminal domain rich in Pro, Gln and Tyr. Two overlapping repeats are present, similar to those of wheat gliadins: QPYYPQPQQPY. *TcMCA5* was found to be transcribed in epimastigote stage of *T. cruzi* forming a mRNA of 2,5 kb. In contrast to the metacaspase-3 which was found to be expressed in all four main developmental stages of the parasite (Figure 14 B), metacaspase-5 only seems to be present in the cell free protein extract obtained from the epimastigote stage, present in the insect vector. The apparent molecular mass of the band seen on western blot is 75 kDa suggesting N-glycosylation at several sites. Moreover, chronic Chagasic patients do not possess antibodies reactive against metacaspase-5 confirming that this metacaspase is not expressed in developmental stages present in the mammalian host. Such antibodies are present in a vast majority of Chagasic patients against metacaspase-3 (Kosec 2004; Kosec et al. 2006).

In parallel with our work, the expression and role of *T. brucei* metacaspases have been partially elucidated. Five metacaspase genes are present in this parasite and three of them, *TbMCA2*, *TbMCA3* and *TbMCA5*, predict active peptidases with intact catalytic residues. Metacaspases-2 and -3 are expressed only in the mammalian bloodstream form (BSF) of the parasite whereas metacaspase-5 is also expressed in the insect procyclic form (Helms et al. 2006). Interestingly, in another closely related organism *Leishmania major*, only one *MCA5* homolog seems to be present (www.genedb.org), however, it has not been studied so far.

A reconstruction of the phylogenetic relationships between the trypanosomatid metacaspases and those of other representative organisms has been performed. This was done using a multiple sequence alignment of the p20-like subunit of the selected proteins. The reconstructed trees show that the metacaspases from trypanosomatids cluster together well separated from the type I and type II plant metacaspase clusters (Figure 28). Moreover, the two *T. brucei* sequences (*TbMCA1* and *TbMCA4*) that exhibit mutations in the putative catalytic dyad are clearly separated from the active ones (*TbMCA2-3*). This, together with the relative position of these branches in the tree, suggest that these two groups of genes have been evolving independently and that the branch that leads to the currently inactive genes departed from the ancestral *MCA* gene before the split that gave rise to the current *MCA5* and *MCA3* genes. The p20-like subunits of *T. cruzi* and *T. brucei* *MCA5* proteins are close to each other and to the single protein found in *L. major* (LmjF35.158). Nevertheless, they show substantial differences in their C-terminal extensions (which were not included in the phylogenetic analysis), which share only their aminoacid composition (they are rich in Pro, Gln and Tyr) and repetitive motives (Kosec et al. 2006).

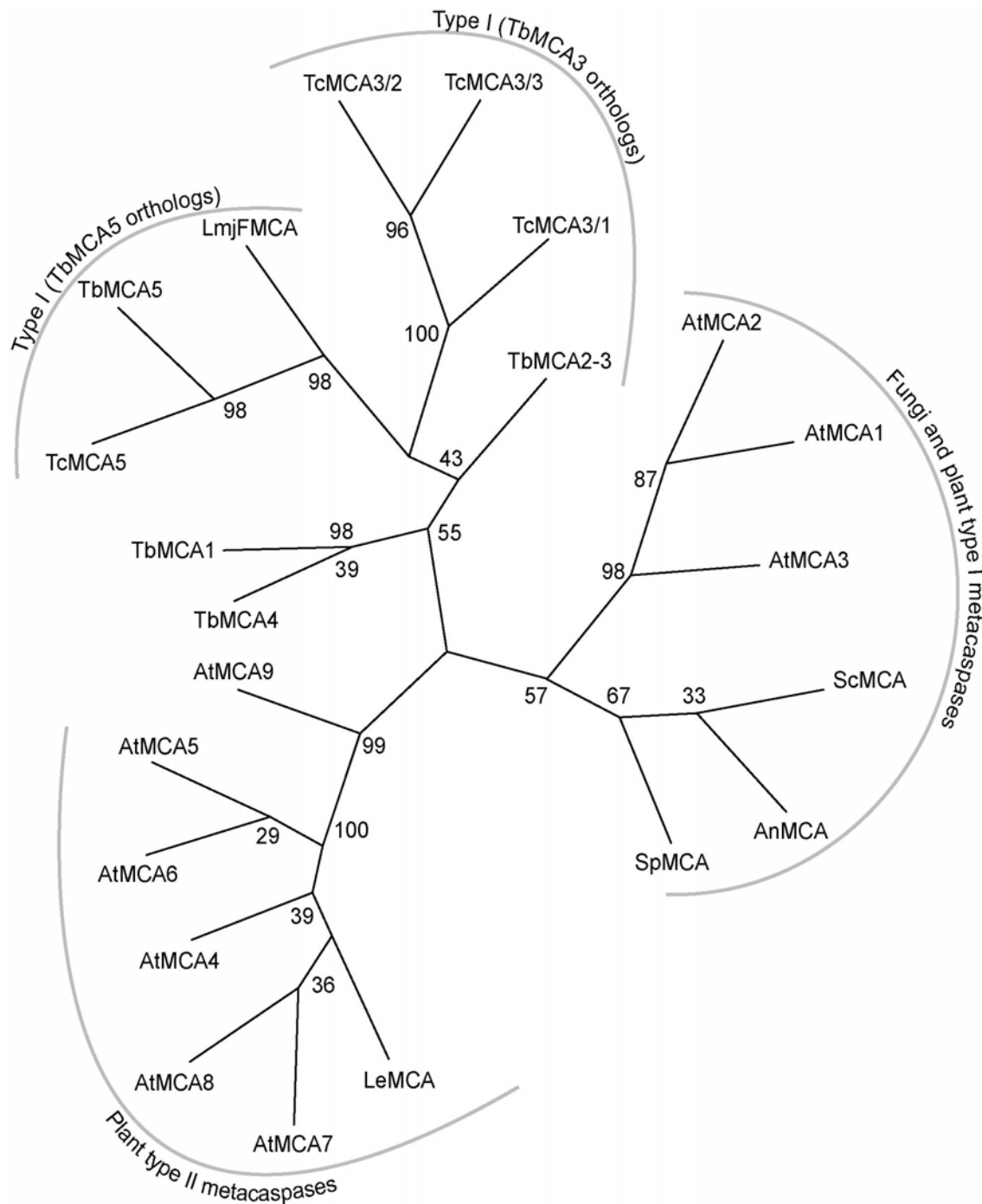


Figure 28 Phylogenetic reconstruction of selected metacaspases. Bootstrap values are shown on the nodes. Metacaspases in the tree are from *Arabidopsis thaliana* (At), *Lycopersicon esculentum* (Le), *Aspergillus nidulans* (An), *Leishmania major* (Lm), *Saccharomyces cerevisiae* (Sc), *Schizosaccharomyces pombe* (Sp), *Trypanosoma brucei* (Tb) and *Trypanosoma cruzi* (Tc) (Kosec et al. 2006).

Type II plant metacaspases have been expressed in *E. coli* expression system and readily showed autoproteolytic processing to p20-like and p10-like subunits by a cleavage after an Arg residue (Vercammen et al. 2004). In the same study, however, type I metacaspases failed to undergo such processing and also to exhibit proteolytic activity towards synthetic substrates. It seems that the metacaspases from *T. cruzi* resemble type I plant homologs, since we could not detect any autoproteolytic processing of recombinant metacaspase-3 or -5 nor measure proteolytic activity of purified recombinant proteins using fluorescence quenched combinatorial peptide libraries. Moreover, in western blot experiments only bands corresponding to the full length, unprocessed metacaspase-3 and -5 were observed in *T. cruzi* cell free proteic extracts. The same was true for *T. brucei* metacaspases that similarly appeared only as full length proteins (Helms et al. 2006). The authors were also unsuccessful in measuring proteolytic activity of the recombinant *T. brucei* metacaspases (J. Mottram, personal communication). Therefore, whether metacaspases from trypanosomatids must undergo proteolytic processing in

order to be active and which conditions or cofactors are necessary for the activation remains obscure at this moment. Moreover, the inability to measure proteolytic activity of metacaspases in trypanosomatids greatly impairs further characterization of their biological role, which can only be deduced by indirect means.

Approaching the issue of the possible implication of *T. cruzi* metacaspases in PCD of epimastigotes, three questions have to be addressed independently. Are metacaspases involved in regulation and/or execution of PCD? Are metacaspases directly or indirectly responsible for the augmented caspase-like (cleavage of synthetic substrates with Asp residue at P1) proteolytic activity during the process? Is caspase-like activity causing morphological changes characteristic of metazoan apoptosis?

During the FHS-induced PCD of epimastigotes metacaspases-3 and -5 changed their subcellular localization and co-localized with DAPI staining, corresponding to the degrading nucleus. A similar finding has been reported for the elongation factor subunit TcEF-1 $\alpha$ , which has been suggested to be involved in PCD (Ouaisi 2003). Moreover, Szallies *et al* (Szallies *et al.* 2002) suggested that overexpression of *T. brucei* metacaspase caused clonal cell death of *S. cerevisiae* by acting in the nucleus. Finally, overexpression of metacaspase-5 in epimastigotes rendered them more susceptible to FHS-induced PCD and overexpression of metacaspase-3 seemed to have a lethal effect. All this suggests that metacaspases are likely to be involved in PCD of *T. cruzi*.

Metacaspases have been implicated in PCD of many other organisms. For example, RNA interference studies showed that the type II plant metacaspase from *Picea abies* was responsible for PCD during embryogenesis (Suarez *et al.* 2004). Further more it was recently shown that in this organism the Arg-specific proteolytic activity of this metacaspase is responsible for the cell death function. Similarly to our results, the metacaspase translocates from the cytosol to the nucleus of the cells destined to die, where it colocalizes with nuclear pore assembly and causes nuclear envelope disassembly (Bozhkov *et al.* 2005). In addition, the *S. cerevisiae* metacaspase (YOR197w) was claimed to be a functional homologue of metazoan caspases including processing and substrate specificity (Madeo *et al.* 2002) although these results have been, in part, questioned recently (Wysocki and Kron 2004). Similarly, both types of *A. thaliana* metacaspases were shown to participate in cell death when overexpressed in *S. cerevisiae* (Watanabe and Lam 2005). In summary, metacaspases seem to be involved in cell death although the mechanism may differ from that of classical caspases. Our results show that overexpression of *TcMCA3* in human immortalized cell line Hek 293 did not induce death or morphological changes typical of apoptosis (Kosec 2004).

Another possible role for metacaspases in trypanosomatids has been recently proposed in *T. brucei*. Triple RNAi studies showed that *TbMCA2*, *TbMCA3* and *TbMCA5* are essential for proliferation of BSF. Mitosis and DNA replication still occurred but cell division invariably failed. In addition it was shown, that the metacaspases can individually compensate for the loss of each other. In contrast to our findings in *T. cruzi*, the same study also revealed the sub-cellular localization of the three *T. brucei* metacaspases to be related to RAB-11 containing recycling endosomes. Nevertheless, recycling of the variant surface glycoprotein (VSG) was not impaired in metacaspase triple RNAi parasites. The study found no indication of the involvement of *T. brucei* metacaspases in cell death or stress response (Helms *et al.* 2006).

Although no direct caspase homologs are present in plants and unicellular organisms, caspase-like proteolytic activity (cleavage after Asp-residue) was shown to be increased in several PCD models of these organisms (Das *et al.* 2001; Madeo *et al.* 2002; Bozhkov *et al.* 2004). Analogously, YVAD-ase activity was analyzed during FHS-induced PCD of *T. cruzi* in more detail and it was determined that it is considerably increased (up to 300% after 4 h of apoptosis induction). Taking into account that purified native cruzipain, the major cysteine peptidase of *T. cruzi*, is able to act on caspase substrates at low rates (Stoka *et al.* 2001) these measurements were performed in the presence of 100  $\mu$ M E-64, a potent cruzipain inhibitor (Kosec *et al.* 2006).

Using the SR-VAD-FMK *in vivo* staining specific activation of a protein capable to bind this probe could be detected in the degrading nucleus of epimastigotes undergoing apoptosis-like cell death (Kosec *et al.* 2006). However, as mentioned above, various factors were considered to exclude the possibility that cruzipain might be responsible for this labeling. First, control epimastigotes (untreated parasites) that contain high amounts of cruzipain were not stained with SR-VAD-FMK. Second, immunolocalization studies carried out on FHS-treated parasites with anti-cruzipain specific antibodies revealed that this peptidase remained lysosomal/reservosomal during the whole process and therefore does not co-localize with the SR-VAD-FMK signal. All this strongly suggests that there is another peptidase or several peptidases with caspase-like activity, likely to be involved in the process. This was already suggested (Piacenza *et al.* 2001) when pretreatment of epimastigotes with 100  $\mu$ M DEVD-CHO caspase inhibitor prevented FHS-induced cell death. We proved that caspase-like activity is cell death specific and is not caused by cruzipain; furthermore, *in vitro* assays with purified native cruzipain showed that this protease is not inhibited by DEVD-CHO up to 200  $\mu$ M. Although metacaspases-3 and -5 showed partial co-localization with SR-VAD-FMK staining in the dying epimastigotes we could not obtain any evidence that metacaspases were binding this inhibitor. Indeed, comparing YVAD-ase activities of the metacaspase-5 overexpressing and pRibotex control epimastigotes during the death process we could not detect any significant difference (Kosec *et al.* 2006).

Interestingly, it was recently described that in *Avena sativa* (oat) programmed cell death signaling cascade is mediated by two subtilisin-like serine peptidases that exhibit caspase specificity (Coffeen and Wolpert 2004). Nevertheless, performing a search for subtilisin like peptidase homologs in trypanosomatid genomes we couldn't find any close homologs. Therefore, the origin of the measured YVAD-ase activity in dying *T. cruzi* epimastigotes remains unknown. The available genome sequence data should be taken advantage of and new thus far uncharacterized families of peptidases should be investigated biochemically and functionally. In this way, the involvement of proteolytic signaling cascades in programmed cell death will become easier to elucidate possibly giving insight into evolutionary beginnings of nowadays complex process in mammalian cells and opening possibilities for new strategies of fighting the parasite and benefiting the patient.

## 5.2 Autophagy and autophagins in *T. cruzi*

As the mechanism of programmed cell death in *T. cruzi* was found to be most probably different from metazoan caspase-mediated proteolytic cascades we decided to search for the presence of other pathways that could take part in the death process of this organism. Caspase independent pathways were suggested to operate in mammals and autophagic cell death, also termed "Type II programmed cell death" was proposed to be an important route. Interestingly, during fresh human serum induced cell death of *T. cruzi* severe vacuolization was observed further strengthening this possibility. However, autophagy had not been described in trypanosomatids, therefore a strategy was developed and implemented for a basic description of this process. Despite the lack of a recognizable *ATG12* homologue Atg8-conjugation system is functional in the parasite with Atg8.1 protein being primarily involved in autophagosome formation during prolonged starvation of epimastigotes. Two *ATG4* homologues encoded in the genome represent functional autophagins with *ATG4.1* most probably playing a prominent role in Atg8 processing. Based on our results, further studies have already been undertaken that identified autophagy in trypanosomatid species as a crucial mechanism in cell remodeling during differentiation between different developmental stages.

Our analyses and also studies from other groups (Rigden et al. 2005) brought to light that essential core genes for viable autophagy are present in trypanosomatid genomes. Interestingly however, one of the ubiquitin-like conjugation system involved in autophagosome formation, the *ATG12-ATG5* system, seems to be incomplete. Interestingly, the homolog of *ATG12* ubiquitin-like gene is missing from the *T. cruzi* genome, although homologs involved in its conjugation and function in yeast, *ATG5*, *ATG10*, *ATG16* seem to be present. On the other hand, the remaining *ATG8* conjugation system, also involved in autophagosome growth and closure, seems complete and may be the only one to modulate this process. We decided to take a closer look at the genes homologous to the mediators of this conjugation system and their involvement in autophagy. Two homologs of *ATG8* are present in *T. cruzi* and *T. brucei* and one direct homolog seems to be present in the *Leishmania*. Interestingly, more than 20 more distant *ATG8* homologs can be identified in *Leishmania* genome. Whether these genes take part in autophagy or they are ubiquitin-like proteins involved in other processes, has not been elucidated so far. Comparatively, only one *ATG8* gene is found in yeast genome and four homologs can be identified in mammalian genomes. Autophagins or *ATG4* cysteine peptidases are essential for processing and deconjugation of Atg8 proteins and therefore also essential for autophagy (Kirisako et al. 2000). In *T. cruzi*, *T. brucei* and *Leishmania* two *ATG4* homologs are found in each genome all of them coding for the Cys-Asp-His catalytic triad and, in addition, conserving the Tyr residue essential for the oxyanion hole formation (Figure 17). Another protein, essential for Atg8 conjugation to PE is Atg7, an E1-ubiquitin-activating-enzyme-like protein. A homolog has been clearly identified in the *T. cruzi* genome (Tc00.1047053509641.30) ([www.genedb.org](http://www.genedb.org)). The conjugation of activated Atg8 to PE is carried out by the E2-ubiquitin-conjugating-enzyme-like Atg3 protein, which also has a clear homolog in *T. cruzi* genome (Tc00.1047053509213.130).

Our next goal was to assess the biochemical and functional characteristics of the two Atg4 proteins, autophagin-1 and -2 and two Atg8 proteins Atg8.1 and Atg8.2. We chose the *E. coli* expression system as both autophagins and both Atg8 proteins are predicted to be cytosolic proteins without ER-transportation signal peptides or N-glycosylation sites. We were able to obtain sufficient amounts of reasonably pure proteins after a single metal-affinity chromatographic purification step. In order to measure proteolytic activity of the recombinantly expressed *T. cruzi* autophagin-1 and -2 we employed the recombinant purified Atg8 proteins as substrates. We observed the reaction with SDS PAGE analysis of the cleaved Atg8.1 and Atg8.2 observing a change in the molecular mass. In the case of Atg8.1 only two aminoacid residues are predicted to be cleaved off from the native protein when processed by autophagins and in case of Atg8.2 the number of cleaved residues is 8. Therefore, when designing our expression products we added a (His)<sub>6</sub> tag to the C-terminal in order to assure a sufficient difference in molecular mass for the processing to be observed in SDS-PAGE gel. The enzymes showed a typical cysteine peptidase behaviour being activated by DTT and  $\beta$ -mercapto ethanol and inhibited by general inhibitors of this class of peptidases, N-ethylmaleimide and iodoacetamide/iodoacetate. Inhibitors of C1 family peptidases, like E-64 and cystatin C, showed no inhibition towards autophagins exposing the specific nature of

C54 family inside the clan CA. Expectedly, inhibitors of other classes of peptidases also showed no inhibition towards the enzymes. Autophagin-1 was readily active at neutral pH (7.5), which is in accordance with its cytosolic localization. The cleavage site in Atg8.1 and Atg8.2 was confirmed to be after the Gly residue close to the C-terminus, as predicted by bioinformatic analyses of Atg8 proteins from other species. We made sure that the observed proteolysis was not a consequence of a bacterial peptidase by incubating recombinant Atg8.1 and Atg8.2 in the same conditions with a bacterial protein extract lacking Atg4.1 or Atg4.2. In this case the faster migrating band was not observed, moreover, during expression of Atg8.1 and Atg8.2 in the bacterial cytosol no band resulting from degradation of full-length protein was observed.

Autophagin-1 cleaved *T. cruzi* Atg8.1 and Atg8.2 substrates at similar rates *in vitro*, which means that no specificity of this autophagin towards one particular Atg8 substrate can be predicted for this peptidase. Autophagin-2 exhibited poor cleavage of both Atg8.1 and Atg8.2 that was about 4 orders of magnitude slower than with autophagin-1. This suggests that TcAtg4.1 is the functional homolog of yeast ATG4 peptidase and that TcAtg4.2 may have a different role in the parasite. Interestingly, in *Leishmania* an *in vivo* study revealed that *LmATG4.2* null mutant exhibits a higher number of autophagosomes per cell than observed for wild type cells in a similar stage of growth. The same mutant was also less able to withstand starvation suggesting that the accumulated autophagosomes are not able to proceed along the autophagy pathway (Besteiro et al. 2006). The prominent role of *LmATG4.1* was still emphasized however, as the null mutant for this gene was not viable (J. Mottram, personal communication). It would seem that the *T. cruzi* ATG8 conjugation system depends mainly on Atg4.1, although similarly to *Leishmania* Atg4.2 may have an important role in Atg8 deconjugation. If this is confirmed by *atg4.1* and *atg4.2* gene knockout experiment in *T. cruzi*, these proteins could be considered a new cysteine peptidase virulence factors and drug targets of *T. cruzi* and other trypanosomatids. In this case, inhibitors of this peptidase should be sought for and tested as potential therapeutic agents for Chagas disease and potentially sleeping sickness and leishmaniasis. Interestingly, in autophagy reconstitution experiments in yeast the *TcATG4.2* gene was almost as successful as *TcATG4.1* in replacing yeast autophagin in cleaving and deconjugating yeast Atg8. The explanation could be that only very little autophagin activity is enough to yield substantial proaminopeptidase processing, or that the *T. cruzi* Atg8 proteins evolved in a way that permits a better interaction with Atg4.1 peptidase and not with Atg4.2. The question that arises is the role of Atg4.2. In contrast with *Leishmania* genome, where many more distant ATG8-like genes were detected, the *T. cruzi* genome seems to lack any additional ATG8-like sequences that could potentially be substrates of Atg4.2. A similar dilemma is present in human cells, where four autophagin genes are present in the genome, however, it seems that only one of them (HsAtg4B) efficiently cleaves all four substrates that belong to the ATG8 family.

In order to measure kinetic parameters of autophagin proteolytic activity we designed a fluorescence quenched synthetic substrate Abz-TFGQ-EDDnp (kindly provided by Dr. Luiz Juliano, Sao Paulo, Brazil) based on the sequence around the cleavage site of TcAtg8.1. However, no significant proteolytic activity could be observed when incubating autophagins with this substrate (not shown). This means that similarly to human HsAtg4B (Sugawara et al. 2005)(human autophagin-1) short peptides cannot enter the active site of *T. cruzi* autophagins due to a short loop occluding the active site. Although another study on human autophagins suggested that human autophagin-3 (HsAtg4C) presented very small activity on Mca-TFGM-Dpa-NH<sub>2</sub> (Marino et al. 2003) suitable, fast and reliable, preferentially colorimetric or fluorimetric proteolytic activity assay for *T. cruzi* autophagins and possibly for autophagins in general, should be developed. Such assay would enable faster screening of potential inhibitors and routine measurement of autophagin activity in different cell processes.

In order to elucidate the role of Atg4.1, Atg4.2, Atg8.1 and Atg8.2 in ATG8 conjugation system and autophagy we performed experiments on *S. cerevisiae* yeasts, null mutants for *ScATG4* and *ScATG8* genes (kindly provided by Dr. Michael Thumm, Göttingen, Germany). We cloned the *T. cruzi* genes into the pCM190 vector used for expression of proteins in *S. cerevisiae*. *TcATG4.1* and *TcATG4.2* were expressed in *atg4Δ* yeast and *TcATG8.1* and *TcATG8.2* in *atg8Δ* yeast strain. Both mutated yeast strains are defective in the biosynthetic cvt-pathway as no cvt-vesicles are formed. Autophagosomes are formed in starvation conditions, however, they are aberrantly small and hence unable to deliver cargo to the vacuole (Klionsky 2005).

Functionality of cvt and autophagy pathways is routinely assessed by observing the processing of proaminopeptidase I to the mature form, slightly faster migrating in SDS PAGE. Using antibodies against aminopeptidase I (kind gift from Dr. I. Sandoval and Dr. M. J. Mazon, Madrid, Spain) we could observe trafficking of this protein to the vacuole in nutrient rich and starvation conditions. Our observations show that both *T. cruzi* autophagins, *TcATG4.1* and *TcATG4.2*, reconstitute the cvt-pathway in nutrient rich conditions as well as autophagy in starvation conditions. Interestingly, in case of the *TcATG8* genes, the expression of neither reconstitutes the cvt-pathway in yeast, however, *TcATG8.1* partially reconstitutes autophagy in starvation conditions. In a similar experiment *Arabidopsis thaliana AtATG8* genes were expressed in yeast and only one of them showed partial reconstitution of autophagy (Ketelaar et al. 2004). One of the reasons for this is the fact that Atg8 protein specifically interacts with more host proteins than Atg4 and each one of these interactions can be impaired by inter-species differences.

An interesting and still somehow controversial topic is the binding of Atg8 proteins to microtubules. The mammalian homolog was first identified as MAPI LC3, light chain of microtubule binding protein (Mann and Hammarback 1994) and its role in autophagy was discovered later (Kabeya et al. 2000). Plant Atg8 proteins also readily bound to microtubules suggesting a role of microtubules for trafficking of autophagosomes (Ketelaar et al. 2004). In contrast, yeast ScAtg8 was shown not to bind microtubules and microtubule dynamics is not necessary for autophagy in yeast (Kirisako et al. 1999). Our results do not show any specific binding of TcAtg8.1 and TcAtg8.2 to bovine microtubules. This observation possibly suggests that microtubules are involved in autophagy of bigger animal and plant cells and not in the smaller yeast and protozoan cells. Nevertheless, the absence of binding might also be due to the bovine origin of the microtubules. In order to elucidate the role of microtubules in autophagy of *T. cruzi* an *in vivo* disruption of microtubules should be performed and their effect on autophagy should be observed.

In several studies vacuolization of *T. cruzi* was reported upon adverse conditions. Recently, ultra structural analysis of the epimastigote stage treated with lysophospholipid analogues and ketoconazole revealed the presence of autophagy related structures including double membrane vesicles (Santa-Rita et al. 2005). We intended to observe autophagy during starvation, the most general stimulus leading to degradation of cytoplasmic proteins. Indeed, when performing immunofluorescence studies with anti-TcAtg8.1 antibodies we observed several bright dots after prolonged starvation whereas in normal growth conditions the signal was weaker and distributed all over the parasite in the form of small spots.

To confirm this finding we expressed *TcATG8.1* with N-terminal HA-tag in *T. cruzi* epimastigotes and performed an immunofluorescence study of equivalently treated parasites with commercial anti-HA antibodies. The observed pattern was compatible with the one obtained using our anti-TcAtg8.1 antibodies (G. Kosec, V. Alvarez, unpublished results) (Figure 27; Figure 29). The images were also similar to mammalian LC3 localization (Kabeya et al. 2000), yeast Atg8 distribution (Kirisako et al. 1999) and also recently published result for LmAtg8 in *Leishmania* (Besteiro et al. 2006). This autophagosome-compatible distribution was not observed when epimastigotes were transfected with an HA-tagged *TcATG8.1* mutant, which lacked the Gly residue involved in cleavage by autophagins and conjugation to PE. Therefore, we can conclude that *TcATG8.1* is the functional *ATG8* homolog of *T. cruzi* and can be used for future routine assessments of the role of autophagy upon diverse stimuli.

We performed equivalent experiments for TcAtg8.2 that similarly to TcAtg8.1 reveals cytosolic localization in untreated epimastigotes. However, after prolonged starvation the localization of this protein, apart from slightly bigger and brighter spots, from reveals a beehive pattern, where TcAtg8.2 seems to be excluded from the interior of the vacuoles (Figure 27). This was confirmed also by immunofluorescence microscopy of epimastigotes expressing an HA-tagged *TcATG8.2*. Nevertheless, this kind of pattern was also observed in epimastigotes transfected with the *TcATG8.2* mutant, which lacked the Gly residue involved in conjugation. This suggests that conjugation to the lipid is not necessary for the observed localization. We have not observed a similar pattern in the literature; therefore more studies will have to be carried out in order to elucidate the function of this protein in *T. cruzi*. Based on immunoprecipitation and western blotting results of HA-tagged wild type Atg8.2 and HA-tagged Gly 131 Ala mutant, TcAtg8.2 seems to be entirely conjugated to PE. The wild type protein runs as a much faster migrating band in SDS PAGE, characteristic of PE conjugated forms of *ATG8* homologs (V. Alvarez, G. Kosec, unpublished results).

Using anti-TcAtg8.1 antibodies we performed immunofluorescence studies of the epimastigotes differentiation to metacyclic trypomastigotes. The process is induced by exposing epimastigotes, grown in nutrient rich BHT medium, to very poor growth conditions resembling the passage from insect gut to the rectum. Sometimes the process is also triggered spontaneously in BHT medium. In both cases the differentiating parasites exhibited many autophagosome related bright spots when stained with anti-TcAtg8.1 antibody (V. Alvarez, G. Kosec unpublished results). A similar finding was observed in *Leishmania major*, where it was also seen, that *atg4.2* knockout is unable to differentiate (Besteiro et al. 2006). Autophagy seems to be a general mechanism of differentiation between different developmental stages in trypanosomatids, however, proteasome mediated proteolysis also seems to take place in *T. cruzi* (Gonzalez et al. 1996; de Diego et al. 2001).

In order to inhibit autophagy 3-methyladenine, the phosphatidylinositol (PI) 3' kinase inhibitor, was added to parasite cultures during starvation. Surprisingly, in contrast to other organisms where this compound acted as strong inhibitor of autophagy (Marino and Lopez-Otin 2004) and prevented the appearance of autophagosomes, in *T. cruzi* TcAtg8.1 was still localized to large puncta. Moreover, when 3-methyladenine was added to nutrient rich medium it seemed to induce the appearance of autophagosomes without any other stimulus. In accordance with these observations, wortmannin, another strong PI 3' kinase inhibitor, was found toxic to epimastigotes in very low concentrations causing large structural damage (Braga and de Souza 2006). This means that autophagy might not be regulated by the same proteins in *T. cruzi* as in other eukaryotes and/or that 3-methyladenine and wortmannin also act on other targets in *T. cruzi* cells.

All this suggests that autophagy is mechanistically conserved in early divergent eukaryotic lineages like the

trypanosomatids, however, several distinct characteristics and peculiarities deserve a more detailed study in the future. The absence of *ATG12* homologue and possibly a different role of PI3 kinase signaling in *T. cruzi* are examples, whose elucidation could give suggestions related to the general mechanism of autophagy in humans and yeast. In fact, vesicle nucleation is one of the least understood steps in autophagy (Klionsky 2005). On the other hand, the role of autophagy in cellular remodeling of trypanosomatid parasites, vitally dependent on differentiation between several developmental stages, is important in the light of searching for new strategies for treatment of Chagas disease, sleeping sickness and various forms of leishmaniasis.



## 6 Conclusions

- Metacaspases are expressed in *T. cruzi* and change their sub-cellular localization concentrating in the nucleus during fresh human serum induced programmed cell death of epimastigotes.
- Metacaspases might mediate the programmed cell death process of *T. cruzi*; however, the mechanism of their action seems clearly unrelated to metazoan caspases.
- We were unable to provide evidence for proteolytic activity of metacaspases from *T. cruzi*.
- *T. cruzi* *ATG4.1* (autophagin-1) gene codes for an active cysteine peptidase that processes both predicted substrates, TcAtg8.1 and TcAtg8.2, cleaving after the conserved Gly residue.
- *T. cruzi* *ATG4.2* (autophagin-2) gene also codes for an active cysteine peptidase, however, it does not seem to be important for TcAtg8.1 or TcAtg8.2 processing. Its function remains unknown so far.
- Neither of the autophagins cleaves a synthetic substrate designed upon the sequence of cleavage in their protein substrates suggesting that the induced fit mechanism dependent upon the 3D structure of the substrate (Atg8) is taking place in this proteolytic reaction.
- *TcATG8.1* was revealed to be the functional homolog of yeast *ATG8* being localized to the autophagosomes during starvation induced autophagy of *T. cruzi* epimastigotes.
- Autophagin activity is expressed constitutively in all major developmental stages of *T. cruzi* suggesting that a basal level of autophagy is always taking place in this parasite.
- Autophagy in *T. cruzi* is viable although the gene encoding the Atg12 ubiquitin like protein is absent from its genome, opening the possibility that this conjugation system might not be essential for the general mechanism of autophagy.



## 7 Acknowledgements

I am thankful to my mentors prof. Vito Turk, PhD., and prof. Juan José Cazzulo, PhD., for giving me the opportunity to work in the very interesting field of cysteine peptidases from parasitic organisms. I'm grateful to Vanina Alvarez for being a great teacher and companion and the rest of my colleagues from Jožef Stefan Institute and Instituto de investigaciones biotecnológicas for all the help, good working environment and the Buenos Aires lab for incomparable hospitality. I would also like to thank prof. Boris Turk, PhD., PhD., for advice and support.

Special thanks goes to everybody who helped us with their advice, technical knowledge or their valuable materials: Adrijana Leonardi, Luiz Juliano, Michael Thumm, Maria Jesus Meson, Ignacio Sandoval, Jeremy Mottram, Berta Franke de Cazzulo and many others.

I am thankful to the members of the evaluating commission for careful reading of the manuscript and thoughtful remarks.

I would like to thank my family and friends for continuing love and support.



## 8 References

- Al-Olayan, E. M., G. T. Williams, et al. (2002). "Apoptosis in the malaria protozoan, *Plasmodium berghei*: a possible mechanism for limiting intensity of infection in the mosquito." *Int J Parasitol* **32**(9): 1133-43.
- Ameisen, J. C. (2002). "On the origin, evolution, and nature of programmed cell death: a timeline of four billion years." *Cell Death Differ* **9**(4): 367-93.
- Ameisen, J. C., Izidorek, T., Billaut-Mulot, O., et al. (1995). "Apoptosis in a unicellular eukaryote (*Trypanosoma cruzi*): implications for the evolutionary origin and role of programmed cell death in the control of cell proliferation, differentiation and survival." *Cell Death Differ* **2**: 285-300.
- Aravind, L., V. M. Dixit, et al. (1999). "The domains of death: evolution of the apoptosis machinery." *Trends Biochem Sci* **24**(2): 47-53.
- Aravind, L., V. M. Dixit, et al. (2001). "Apoptotic molecular machinery: vastly increased complexity in vertebrates revealed by genome comparisons." *Science* **291**(5507): 1279-84.
- Aravind, L. and E. V. Koonin (2002). "Classification of the caspase-hemoglobinase fold: detection of new families and implications for the origin of the eukaryotic separins." *Proteins* **46**(4): 355-67.
- Arnoult, D., K. Akarid, et al. (2002). "On the evolution of programmed cell death: apoptosis of the unicellular eukaryote *Leishmania major* involves cysteine proteinase activation and mitochondrion permeabilization." *Cell Death Differ* **9**(1): 65-81.
- Asgian, J. L., K. E. James, et al. (2002). "Aza-peptide epoxides: a new class of inhibitors selective for clan CD cysteine proteases." *J Med Chem* **45**(23): 4958-60.
- Ashkenazi, A. and V. M. Dixit (1998). "Death receptors: signaling and modulation." *Science* **281**(5381): 1305-8.
- Ausubel, F. (1998). *Current protocols in molecular biology*, John Wiley & Sons, Inc.
- Barrett, A. J. and N. D. Rawlings (2001). "Evolutionary lines of cysteine peptidases." *Biol Chem* **382**(5): 727-33.
- Barrett, A. J., Rawlings, Woessner, J. F. (2004). *Handbook of proteolytic enzymes*, Academic Press.
- Barrett, M. P., R. J. Burchmore, et al. (2003). "The trypanosomiasis." *Lancet* **362**(9394): 1469-80.
- Besteiro, S., R. A. Williams, et al. (2006). "Endosome Sorting and Autophagy Are Essential for Differentiation and Virulence of *Leishmania major*." *J Biol Chem* **281**(16): 11384-96.
- Bozhkov, P. V., L. H. Filonova, et al. (2004). "VEIDase is a principal caspase-like activity involved in plant programmed cell death and essential for embryonic pattern formation." *Cell Death Differ* **11**(2): 175-82.
- Bozhkov, P. V., M. F. Suarez, et al. (2005). "Cysteine protease mcII-Pa executes programmed cell death during plant embryogenesis." *Proc Natl Acad Sci U S A* **102**(40): 14463-8.
- Braga, M. V. and W. de Souza (2006). "Effects of protein kinase and phosphatidylinositol-3 kinase inhibitors on growth and ultrastructure of *Trypanosoma cruzi*." *FEMS Microbiol Lett* **256**(2): 209-16.
- Brisse, S., C. Barnabe, et al. (2000). "Identification of six *Trypanosoma cruzi* phylogenetic lineages by random amplified polymorphic DNA and multilocus enzyme electrophoresis." *Int J Parasitol* **30**(1): 35-44.
- Burleigh, B. A., E. V. Caler, et al. (1997). "A cytosolic serine endopeptidase from *Trypanosoma cruzi* is required for the generation of Ca<sup>2+</sup> signaling in mammalian cells." *J Cell Biol* **136**(3): 609-20.
- Burleigh, B. A. and A. M. Woolsey (2002). "Cell signalling and *Trypanosoma cruzi* invasion." *Cell Microbiol* **4**(11): 701-11.
- Camargo, E. P. (1964). "Growth and Differentiation in *Trypanosoma Cruzi*. I. Origin of Metacyclic Trypanosomes in Liquid Media." *Rev Inst Med Trop Sao Paulo* **12**: 93-100.
- Cazzulo, J. J. (1994). "Intermediate metabolism in *Trypanosoma cruzi*." *J Bioenerg Biomembr* **26**(2): 157-65.
- Cazzulo, J. J. (2002). "Proteinases of *Trypanosoma cruzi*: potential targets for the chemotherapy of Chagas disease." *Curr Top Med Chem* **2**(11): 1261-71.
- Cazzulo, J. J., V. Stoka, et al. (1997). "Cruzipain, the major cysteine proteinase from the protozoan parasite *Trypanosoma cruzi*." *Biol Chem* **378**(1): 1-10.
- Chapman, H. A., R. J. Riese, et al. (1997). "Emerging roles for cysteine proteases in human biology." *Annu Rev Physiol* **59**: 63-88.
- Chen, J. M., N. D. Rawlings, et al. (1998). "Identification of the active site of legumain links it to caspases, clostripain and gingipains in a new clan of cysteine endopeptidases." *FEBS Lett* **441**(3): 361-5.
- Cirman, T., K. Oresic, et al. (2004). "Selective disruption of lysosomes in HeLa cells triggers apoptosis mediated by cleavage of Bid by multiple papain-like lysosomal cathepsins." *J Biol Chem* **279**(5): 3578-87.

- Coffeen, W. C. and T. J. Wolpert (2004). "Purification and characterization of serine proteases that exhibit caspase-like activity and are associated with programmed cell death in *Avena sativa*." Plant Cell **16**(4): 857-73.
- Das, M., S. B. Mukherjee, et al. (2001). "Hydrogen peroxide induces apoptosis-like death in *Leishmania donovani* promastigotes." J Cell Sci **114**(Pt 13): 2461-9.
- de Diego, J. L., J. M. Katz, et al. (2001). "The ubiquitin-proteasome pathway plays an essential role in proteolysis during *Trypanosoma cruzi* remodeling." Biochemistry **40**(4): 1053-62.
- De Souza, W. (2002). "Basic cell biology of *Trypanosoma cruzi*." Curr Pharm Des **8**(4): 269-85.
- del Pozo, O. and E. Lam (1998). "Caspases and programmed cell death in the hypersensitive response of plants to pathogens." Curr Biol **8**(24): R896.
- Dorn, B. R., W. A. Dunn, Jr., et al. (2002). "Bacterial interactions with the autophagic pathway." Cell Microbiol **4**(1): 1-10.
- DosReis, G. A. and M. A. Barcinski (2001). "Apoptosis and parasitism: from the parasite to the host immune response." Adv Parasitol **49**: 133-61.
- El-Sayed, N. M., P. J. Myler, et al. (2005). "The genome sequence of *Trypanosoma cruzi*, etiologic agent of Chagas disease." Science **309**(5733): 409-15.
- Engel, J. C., P. S. Doyle, et al. (1998). "Cysteine protease inhibitors cure an experimental *Trypanosoma cruzi* infection." J Exp Med **188**(4): 725-34.
- Figarella, K., M. Rawer, et al. (2005). "Prostaglandin D2 induces programmed cell death in *Trypanosoma brucei* bloodstream form." Cell Death Differ **12**(4): 335-46.
- Franke de Cazzulo, B. M., J. Martinez, et al. (1994). "Effects of proteinase inhibitors on the growth and differentiation of *Trypanosoma cruzi*." FEMS Microbiol Lett **124**(1): 81-6.
- Freire-de-Lima, C. G., D. O. Nascimento, et al. (2000). "Uptake of apoptotic cells drives the growth of a pathogenic trypanosome in macrophages." Nature **403**(6766): 199-203.
- Gari, E., L. Piedrafita, et al. (1997). "A set of vectors with a tetracycline-regulatable promoter system for modulated gene expression in *Saccharomyces cerevisiae*." Yeast **13**(9): 837-48.
- Gerdes, K., P. B. Rasmussen, et al. (1986). "Unique type of plasmid maintenance function: postsegregational killing of plasmid-free cells." Proc Natl Acad Sci U S A **83**(10): 3116-20.
- Glickman, M. H. and A. Ciechanover (2002). "The ubiquitin-proteasome proteolytic pathway: destruction for the sake of construction." Physiol Rev **82**(2): 373-428.
- Gonzalez, J., F. J. Ramalho-Pinto, et al. (1996). "Proteasome activity is required for the stage-specific transformation of a protozoan parasite." J Exp Med **184**(5): 1909-18.
- Goulet, B., A. Baruch, et al. (2004). "A cathepsin L isoform that is devoid of a signal peptide localizes to the nucleus in S phase and processes the CDP/Cux transcription factor." Mol Cell **14**(2): 207-19.
- Green, D. R. (1998). "Apoptotic pathways: the roads to ruin." Cell **94**(6): 695-8.
- Green, D. R. and J. C. Reed (1998). "Mitochondria and apoptosis." Science **281**(5381): 1309-12.
- Grutter, M. G. (2000). "Caspases: key players in programmed cell death." Curr Opin Struct Biol **10**(6): 649-55.
- Harth, G., N. Andrews, et al. (1993). "Peptide-fluoromethyl ketones arrest intracellular replication and intercellular transmission of *Trypanosoma cruzi*." Mol Biochem Parasitol **58**(1): 17-24.
- Hedges, S. B. (2002). "The origin and evolution of model organisms." Nat Rev Genet **3**(11): 838-49.
- Helms, M. J., A. Ambit, et al. (2006). "Bloodstream form *Trypanosoma brucei* depend upon multiple metacaspases associated with RAB11-positive endosomes." J Cell Sci **119**(Pt 6): 1105-17.
- Henriksson, J., L. Aslund, et al. (1990). "Chromosomal localization of seven cloned antigen genes provides evidence of diploidy and further demonstration of karyotype variability in *Trypanosoma cruzi*." Mol Biochem Parasitol **42**(2): 213-23.
- Janowski, R., M. Kozak, et al. (2004). "Two polymorphs of a covalent complex between papain and a diazomethylketone inhibitor." J Pept Res **64**(4): 141-50.
- Kabeya, Y., N. Mizushima, et al. (2000). "LC3, a mammalian homologue of yeast Apg8p, is localized in autophagosomal membranes after processing." Embo J **19**(21): 5720-8.
- Kabeya, Y., N. Mizushima, et al. (2004). "LC3, GABARAP and GATE16 localize to autophagosomal membrane depending on form-II formation." J Cell Sci **117**(Pt 13): 2805-12.
- Kametaka, S., A. Matsuura, et al. (1996). "Structural and functional analyses of APG5, a gene involved in autophagy in yeast." Gene **178**(1-2): 139-43.
- Kametaka, S., T. Okano, et al. (1998). "Apg14p and Apg6/Vps30p form a protein complex essential for autophagy in the yeast, *Saccharomyces cerevisiae*." J Biol Chem **273**(35): 22284-91.
- Ketelaar, T., C. Voss, et al. (2004). "Arabidopsis homologues of the autophagy protein Atg8 are a novel family of microtubule binding proteins." FEBS Lett **567**(2-3): 302-6.
- Kim, J. and D. J. Klionsky (2000). "Autophagy, cytoplasm-to-vacuole targeting pathway, and pexophagy in yeast and mammalian cells." Annu Rev Biochem **69**: 303-42.
- Kirisako, T., M. Baba, et al. (1999). "Formation process of autophagosome is traced with Apg8/Aut7p in yeast." J

- Cell Biol **147**(2): 435-46.
- Kirisako, T., Y. Ichimura, et al. (2000). "The reversible modification regulates the membrane-binding state of Apg8/Aut7 essential for autophagy and the cytoplasm to vacuole targeting pathway." J Cell Biol **151**(2): 263-76.
- Kirkegaard, K., M. P. Taylor, et al. (2004). "Cellular autophagy: surrender, avoidance and subversion by microorganisms." Nat Rev Microbiol **2**(4): 301-14.
- Klionsky, D. J. (2005). "The molecular machinery of autophagy: unanswered questions." J Cell Sci **118**(Pt 1): 7-18.
- Klionsky, D. J., J. M. Cregg, et al. (2003). "A unified nomenclature for yeast autophagy-related genes." Dev Cell **5**(4): 539-45.
- Kneussel, M. (2002). "Dynamic regulation of GABA(A) receptors at synaptic sites." Brain Res Brain Res Rev **39**(1): 74-83.
- Kosec, G. (2004). Metacaspase from *Trypanosoma cruzi*: cloning and expression in heterologous systems. Faculty of chemistry and chemical technology. Ljubljana, University of Ljubljana. **Masters**: 66.
- Kosec, G., V. E. Alvarez, et al. (2006). "Metacaspases of *Trypanosoma cruzi*: possible candidates for programmed cell death mediators." Mol Biochem Parasitol **145**(1): 18-28.
- Kumanomidou, T., T. Mizushima, et al. (2006). "The crystal structure of human Atg4b, a processing and de-conjugating enzyme for autophagosome-forming modifiers." J Mol Biol **355**(4): 612-8.
- Lang, T., E. Schaeffeler, et al. (1998). "Aut2p and Aut7p, two novel microtubule-associated proteins are essential for delivery of autophagic vesicles to the vacuole." Embo J **17**(13): 3597-607.
- Latterich, M., K. U. Frohlich, et al. (1995). "Membrane fusion and the cell cycle: Cdc48p participates in the fusion of ER membranes." Cell **82**(6): 885-93.
- Leist, M. and M. Jaattela (2001). "Four deaths and a funeral: from caspases to alternative mechanisms." Nat Rev Mol Cell Biol **2**(8): 589-98.
- Levine, A., R. I. Pennell, et al. (1996). "Calcium-mediated apoptosis in a plant hypersensitive disease resistance response." Curr Biol **6**(4): 427-37.
- Levine, B. and D. J. Klionsky (2004). "Development by self-digestion: molecular mechanisms and biological functions of autophagy." Dev Cell **6**(4): 463-77.
- Li, S. J. and M. Hochstrasser (1999). "A new protease required for cell-cycle progression in yeast." Nature **398**(6724): 246-51.
- Ligr, M., F. Madeo, et al. (1998). "Mammalian Bax triggers apoptotic changes in yeast." FEBS Lett **438**(1-2): 61-5.
- Macedo, A. M., Oliveira, R.P., Pena, S.D.J. . (2002, 5 March). "Chagas disease: role of parasite genetic variation in pathogenesis." Expert Reviews in Molecular Medicine, from <http://www.expertreviews.org/02004118h.htm>.
- Madeo, F., E. Herker, et al. (2002). "A caspase-related protease regulates apoptosis in yeast." Mol Cell **9**(4): 911-7.
- Mann, S. S. and J. A. Hammarback (1994). "Molecular characterization of light chain 3. A microtubule binding subunit of MAP1A and MAP1B." J Biol Chem **269**(15): 11492-7.
- Marino, G. and C. Lopez-Otin (2004). "Autophagy: molecular mechanisms, physiological functions and relevance in human pathology." Cell Mol Life Sci **61**(12): 1439-54.
- Marino, G., J. A. Uria, et al. (2003). "Human autophagins, a family of cysteine proteinases potentially implicated in cell degradation by autophagy." J Biol Chem **278**(6): 3671-8.
- Martinez, J., O. Campetella, et al. (1991). "The major cysteine proteinase (cruzipain) from *Trypanosoma cruzi* is antigenic in human infections." Infect Immun **59**(11): 4275-7.
- Meirelles, M. N., L. Juliano, et al. (1992). "Inhibitors of the major cysteinyl proteinase (GP57/51) impair host cell invasion and arrest the intracellular development of *Trypanosoma cruzi* in vitro." Mol Biochem Parasitol **52**(2): 175-84.
- Melo, R. L., L. C. Alves, et al. (2001). "Synthesis and hydrolysis by cysteine and serine proteases of short internally quenched fluorogenic peptides." Anal Biochem **293**(1): 71-7.
- Middelberg, A. P. (2002). "Preparative protein refolding." Trends Biotechnol **20**(10): 437-43.
- Mizushima, N., T. Noda, et al. (1999). "Apg16p is required for the function of the Apg12p-Apg5p conjugate in the yeast autophagy pathway." Embo J **18**(14): 3888-96.
- Mottram, J. C., M. J. Helms, et al. (2003). "Clan CD cysteine peptidases of parasitic protozoa." Trends Parasitol **19**(4): 182-7.
- Nakagawa, I., A. Amano, et al. (2004). "Autophagy defends cells against invading group A *Streptococcus*." Science **306**(5698): 1037-40.
- Noda, T. and Y. Ohsumi (1998). "Tor, a phosphatidylinositol kinase homologue, controls autophagy in yeast." J Biol Chem **273**(7): 3963-6.
- Ohsumi, Y. (2001). "Molecular dissection of autophagy: two ubiquitin-like systems." Nat Rev Mol Cell Biol **2**(3):

- 211-6.
- Ouaissi, A. (2003). "Apoptosis-like death in trypanosomatids: search for putative pathways and genes involved." *Kinetoplastid Biol Dis* **2**(1): 5.
- Pedroso, A., E. Cupolillo, et al. (2003). "Evaluation of *Trypanosoma cruzi* hybrid stocks based on chromosomal size variation." *Mol Biochem Parasitol* **129**(1): 79-90.
- Piacenza, L., G. Peluffo, et al. (2001). "L-arginine-dependent suppression of apoptosis in *Trypanosoma cruzi*: contribution of the nitric oxide and polyamine pathways." *Proc Natl Acad Sci U S A* **98**(13): 7301-6.
- Rawlings, N. D., F. R. Morton, et al. (2006). "MEROPS: the peptidase database." *Nucleic Acids Res* **34**(Database issue): D270-2.
- Reggiori, F. and D. J. Klionsky (2002). "Autophagy in the eukaryotic cell." *Eukaryot Cell* **1**(1): 11-21.
- Reggiori, F., C. W. Wang, et al. (2004). "Early stages of the secretory pathway, but not endosomes, are required for Cvt vesicle and autophagosome assembly in *Saccharomyces cerevisiae*." *Mol Biol Cell* **15**(5): 2189-204.
- Rigden, D. J., M. Herman, et al. (2005). "Implications of a genomic search for autophagy-related genes in trypanosomatids." *Biochem Soc Trans* **33**(Pt 5): 972-4.
- Roisin-Bouffay, C., M. F. Luciani, et al. (2004). "Developmental cell death in dictyostelium does not require paracaspase." *J Biol Chem* **279**(12): 11489-94.
- Ruefli-Brasse, A. A., D. M. French, et al. (2003). "Regulation of NF-kappaB-dependent lymphocyte activation and development by paracaspase." *Science* **302**(5650): 1581-4.
- Sagiv, Y., A. Legesse-Miller, et al. (2000). "GATE-16, a membrane transport modulator, interacts with NSF and the Golgi v-SNARE GOS-28." *Embo J* **19**(7): 1494-504.
- Sambrook, J., Fritsch, E.F., Maniatis, T (1989). *Molecular cloning: a laboratory manual*. Cold Spring Harbor, Cold Spring Harbor Laboratory Press.
- Santa-Rita, R. M., R. Lira, et al. (2005). "Anti-proliferative synergy of lysophospholipid analogues and ketoconazole against *Trypanosoma cruzi* (Kinetoplastida: Trypanosomatidae): cellular and ultrastructural analysis." *J Antimicrob Chemother* **55**(5): 780-4.
- Santana, J. M., P. Grellier, et al. (1997). "A *Trypanosoma cruzi*-secreted 80 kDa proteinase with specificity for human collagen types I and IV." *Biochem J* **325** ( Pt 1): 129-37.
- Scharfstein, J., V. Schmitz, et al. (2000). "Host cell invasion by *Trypanosoma cruzi* is potentiated by activation of bradykinin B(2) receptors." *J Exp Med* **192**(9): 1289-300.
- Scott, S. V., A. Hefner-Gravink, et al. (1996). "Cytoplasm-to-vacuole targeting and autophagy employ the same machinery to deliver proteins to the yeast vacuole." *Proc Natl Acad Sci U S A* **93**(22): 12304-8.
- Snipas, S. J., E. Wildfang, et al. (2004). "Characteristics of the caspase-like catalytic domain of human paracaspase." *Biol Chem* **385**(11): 1093-8.
- Solomon, M., B. Belenghi, et al. (1999). "The involvement of cysteine proteases and protease inhibitor genes in the regulation of programmed cell death in plants." *Plant Cell* **11**(3): 431-44.
- Stoka, V., B. Turk, et al. (2001). "Lysosomal protease pathways to apoptosis. Cleavage of bid, not pro-caspases, is the most likely route." *J Biol Chem* **276**(5): 3149-57.
- Sturm, N. R., N. S. Vargas, et al. (2003). "Evidence for multiple hybrid groups in *Trypanosoma cruzi*." *Int J Parasitol* **33**(3): 269-79.
- Suarez, M. F., L. H. Filonova, et al. (2004). "Metacaspase-dependent programmed cell death is essential for plant embryogenesis." *Curr Biol* **14**(9): R339-40.
- Sugawara, K., N. N. Suzuki, et al. (2005). "Structural basis for the specificity and catalysis of human Atg4B responsible for mammalian autophagy." *J Biol Chem* **280**(48): 40058-65.
- Sun, L., L. Deng, et al. (2004). "The TRAF6 ubiquitin ligase and TAK1 kinase mediate IKK activation by BCL10 and MALT1 in T lymphocytes." *Mol Cell* **14**(3): 289-301.
- Szallies, A., B. K. Kubata, et al. (2002). "A metacaspase of *Trypanosoma brucei* causes loss of respiration competence and clonal death in the yeast *Saccharomyces cerevisiae*." *FEBS Lett* **517**(1-3): 144-50.
- Turk, D. and G. Guncar (2003). "Lysosomal cysteine proteases (cathepsins): promising drug targets." *Acta Crystallogr D Biol Crystallogr* **59**(Pt 2): 203-13.
- Turk, V., B. Turk, et al. (2001). "Lysosomal cysteine proteases: facts and opportunities." *Embo J* **20**(17): 4629-33.
- Uhlmann, F., D. Wernic, et al. (2000). "Cleavage of cohesin by the CD clan protease separin triggers anaphase in yeast." *Cell* **103**(3): 375-86.
- Uren, A. G., K. O'Rourke, et al. (2000). "Identification of paracaspases and metacaspases: two ancient families of caspase-like proteins, one of which plays a key role in MALT lymphoma." *Mol Cell* **6**(4): 961-7.
- Vercammen, D., B. van de Cotte, et al. (2004). "Type II metacaspases Atmc4 and Atmc9 of *Arabidopsis thaliana* cleave substrates after arginine and lysine." *J Biol Chem* **279**(44): 45329-36.
- Walker, N. P., R. V. Talanian, et al. (1994). "Crystal structure of the cysteine protease interleukin-1 beta-converting enzyme: a (p20/p10)<sub>2</sub> homodimer." *Cell* **78**(2): 343-52.
- Watanabe, N. and E. Lam (2005). "Two *Arabidopsis* metacaspases AtMCP1b and AtMCP2b are arginine/lysine-

- specific cysteine proteases and activate apoptosis-like cell death in yeast." *J Biol Chem* **280**(15): 14691-9.
- Welburn, S. C. and I. Maudlin (1999). "Tsetse-trypanosome interactions: rites of passage." *Parasitol Today* **15**(10): 399-403.
- WHO. (1997). "Vector Control - Methods for Use by Individuals and Communities." from [http://www.who.int/docstore/water\\_sanitation\\_health/vectcontrol/begin.htm#Contents](http://www.who.int/docstore/water_sanitation_health/vectcontrol/begin.htm#Contents).
- Wilkinson, K. D. (1997). "Regulation of ubiquitin-dependent processes by deubiquitinating enzymes." *Faseb J* **11**(14): 1245-56.
- Wilson, K. P., J. A. Black, et al. (1994). "Structure and mechanism of interleukin-1 beta converting enzyme." *Nature* **370**(6487): 270-5.
- Wysocki, R. and S. J. Kron (2004). "Yeast cell death during DNA damage arrest is independent of caspase or reactive oxygen species." *J Cell Biol* **166**(3): 311-6.
- Yamin, T. T., J. M. Ayala, et al. (1996). "Activation of the native 45-kDa precursor form of interleukin-1-converting enzyme." *J Biol Chem* **271**(22): 13273-82.
- Yuan, J., M. Lipinski, et al. (2003). "Diversity in the mechanisms of neuronal cell death." *Neuron* **40**(2): 401-13.
- Yue, Z., S. Jin, et al. (2003). "Beclin 1, an autophagy gene essential for early embryonic development, is a haploinsufficient tumor suppressor." *Proc Natl Acad Sci U S A* **100**(25): 15077-82.
- Zangger, H., J. C. Mottram, et al. (2002). "Cell death in Leishmania induced by stress and differentiation: programmed cell death or necrosis?" *Cell Death Differ* **9**(10): 1126-39.
- Zeledon, R., R. Bolanos, et al. (1984). "Scanning electron microscopy of the final phase of the life cycle of *Trypanosoma cruzi* in the insect vector." *Acta Trop* **41**(1): 39-43.
- Zingales, B., M. E. Pereira, et al. (1997). "Biological parameters and molecular markers of clone CL Brener--the reference organism of the *Trypanosoma cruzi* genome project." *Mem Inst Oswaldo Cruz* **92**(6): 811-4.



## Index of Figures

- Figure 1 Typical morphology of *Trypanosoma cruzi* developmental stages. **A)** Trypomastigote, non-replicative form found in the bloodstream that is able to infect mammalian cells and measures about 12  $\mu\text{m}$  in length. Morphologically they are very similar to metacyclic trypomastigotes, but they have antigenic and metabolic differences. **B)** Amastigote, replicative and non-motile form present inside mammalian cells, that is only 5  $\mu\text{m}$  long. **C)** Epimastigote, the stage present in the insect vector gut, which is the form that can be readily grown in axenic culture, and is used for most biochemical studies for this reason. Drawings obtained from [www.uta.edu/chagas/html/biolTcru.html](http://www.uta.edu/chagas/html/biolTcru.html). ..... 2
- Figure 2 Schematic representation of the life cycle of the flagellate protozoan *Trypanosoma cruzi* (Macedo 2002). ..... 2
- Figure 3 Crystal structure of papain in complex with zLFG-DAM. The image was prepared from the Protein Data Bank entry (1KHQ) (Janowski et al. 2004) with the PYMOL program. Chemical bonds of the catalytic residues are shown as sticks: Cys25 in yellow, His159 in blue and Asn175 in orange (numbering as in PDB entry). z-LFG-DAM is shown in gray. .... 5
- Figure 4 Crystal structure of HsAtg4B. The image was prepared from the Protein Data Bank entry (2CY7) (Sugawara et al. 2005) with the PYMOL program. Chemical bonds of the catalytic residues are shown as sticks: Cys74 in yellow, His280 in blue and Asp278 in orange (numbering as in PDB entry). The loop covering the active cleft (residues 259 – 262) is shown in pink and the  $\alpha/\beta$ -fold domain, specific for C54 family is surrounded with a cyan dashed line. .... 6
- Figure 5 Crystal Scheme of macroautophagic pathway. A portion of cytoplasm is enclosed by the preautophagosomal structure to form an autophagosome. The outer membrane then fuses with lysosome to degrade inside materials. This pathway can also degrade organelles such as mitochondria and peroxisomes (Marino and Lopez-Otin 2004). ..... 7
- Figure 6 The role of two ubiquitin like proteins Atg8 and Atg12 in vesicle expansion and completion. Atg8 is cleaved at the C-terminal by Atg4 (autophagin) to expose a Gly residue, which is then conjugated to phosphatidylethanolamine (PE). Atg8-PE is inserted into both faces of the preautophagosomal structure and remains inserted in inner and outer autophagosome membrane. Atg8 from the outer membrane is released back to the cytosol in a deconjugation reaction mediated by Atg4 (autophagin) peptidase. Atg12 is conjugated to Atg5 and together with Atg16 the complex is believed to form a transient coat during vesicle expansion. .... 9
- Figure 7 Crystal structure of caspase-1 representing the conserved structural core of the clan CD cysteine peptidases. The image was prepared from the Protein Data Bank entry (1ICE) (Wilson et al. 1994) with the PYMOL program. Chemical bonds of the catalytic residues are shown as sticks: Cys285 in yellow and His237 in blue (numbering as in PDB entry). ..... 10
- Figure 8 Schematic representation of the proteolytic activation of caspases. Caspases are synthesized as single-chain precursors. Activation proceeds by cleavage of the N-terminal peptide at Asp119 and at the conserved sites Asp296 and Asp316 (all caspase-1 numbering convention), leading to the formation of a large p20 subunit and a small p10 subunit. The activity- and specificity-determining residues Arg179, His237, Cys285 and Arg341 are brought into the characteristic structural arrangement for catalysis. Cys285 is the catalytic nucleophile and His237 represents the general base (Grutter 2000). ..... 11

- Figure 9 Domain structure of caspases, paracaspases and metacaspases. Traditional caspases contain a C-terminal caspase domain (empty box) and in some cases a prodomain with CARD or DED oligomerization motifs. Paracaspases, metacaspases, and a number of bacterial cysteine proteases also contain a predicted caspase-like proteolytic domain. Metazoan paracaspase prodomains encode a death domain (“DD”) and either one or two Ig domains. Metacaspases fall into two classes, type I and type II, based on overall structure and the level of sequence similarity. Type I metacaspases from fungi and plants have prodomains with a proline-rich repeat motif (“Pro”). Plant type I metacaspases also have a zinc finger motif (“Zn”) similar to those of the plant hypersensitive response protein lsd-1. Type II metacaspases (in plants) have no prodomain but an insertion of approximately 200 amino acids directly C-terminal to their p20-like subunit. pk3, a protein from *Streptomyces coelicolor*, contains a caspase-like domain and a protein kinase domain. *Rhizobium* sp. plasmid also encodes a caspase-like protein. Gingipain R has a caspase-like catalytic domain (empty box) followed by an Ig-like domain. All sequences are represented as their unprocessed zymogen forms (Uren et al. 2000). ..... 12
- Figure 10. Alignment of the p20 subunits of caspases, paracaspases, and metacaspases. From top to bottom the sequences are grouped as caspases, paracaspases, type I metacaspases, type II metacaspases, gingipains, miscellaneous eukaryotic cysteine peptidases, and miscellaneous bacterial cysteine peptidases. The 80% consensus is compiled from the caspase, paracaspase, and metacaspase sequences. Residues matching the 80% consensus are shaded as follows: hydrophobic (h, yellow); polar (p, blue); charged (c, red); tiny (t, dark green); small (s, light green); big (b, gray). The Cys-His catalytic diad is shaded black (Uren et al. 2000). ..... 13
- Figure 11 Schematic representation of the known apoptotic pathways in which caspases are involved. The cytokine pathway leading to inflammation is activated by caspase-1 (Grutter 2000). ..... 14
- Figure 12B Genomic organization of *TcMCA3* copies. Genome sequence data deduced for one *TcMCA3* tandem (Kosec et al. 2006). ..... 18
- Figure 13 In order to express a soluble metacaspase-3 two N-terminal truncated sequences were obtained starting from the proteins second and third Met residue (marked in yellow). In both cases the putative p20-like subunit (marked in cyan) remains intact together with the His and Cys residues of the catalytic site (marked in red). ..... 24
- Figure 14 **A**) PFGE – Southern blot of *T. cruzi* chromosomes developed with radioactively labeled *TcMCA3* probe. Two strong bands are visible at 0,98 and 0,54 Mbp. *S. cerevisiae* chromosomes were run as molecular weight markers. **B**) Differential expression of metacaspase-3 in *T. cruzi* developmental stages. Western blots of soluble extracts of epimastigotes (E), amastigotes (A), cell derived trypomastigotes (T) and metacyclic trypomastigotes (M) probed with anti-metacaspase-3 antibody. .... 29
- Figure 15 Expression of recombinant metacaspase-3 in *E. coli* BL21 (DE3) cells observed in a western blot with anti-metacaspase-3 antibodies and developed with diaminobenzidine method. **A**) Two N-terminal truncated forms of metacaspase-3 were expressed. When translations started at the second Met residue, a vast majority of the protein was found in the insoluble fraction of bacterial cells (first lane), showing several degradation bands. Only very little was present in the soluble fraction (second lane). However, when 3<sup>rd</sup> Met construct was expressed a greater proportion of metacaspase-3 was expressed as a soluble protein (third & fourth lanes). **B**) Cell free protein extract of bacteria expressing metacaspase-3<sup>3Met</sup> was applied to Ni-NTA chromatograph column. The first lane shows an extract of bacteria transformed with empty pET28 vector as negative control and in the second lane (extract of metacaspase-3 producing bacteria) a strong band corresponding to soluble metacaspase-3 can be observed. This band diminishes in intensity in the third lane (Ni-NTA unbound fraction) and is intensified in next lanes corresponding to subsequent eluates of Ni-NTA column (Ni E1 to Ni E5). ..... 30
- Figure 16 **A**) Light microscopy analysis of FHS treated epimastigotes. Normal epimastigotes (E), metacyclic trypomastigotes (M) and spheroid shaped epimastigotes (SSE) are depicted in the figure. **B**) Parasites were exposed to 10 % FHS and at different times after the treatment the numbers of dead (spheroid shaped, non-motile) epimastigotes were assessed under the light microscope. **C**) Localization of DAPI staining (a and d) and anti-metacaspase-3 antibody signal (b and e) during FHS-induced PCD of *T. cruzi* epimastigotes (d – f) and control epimastigotes (a – c). (c and f) Merge images of a + b and d + e respectively. .... 31

- Figure 17 Alignment of C54 family peptidase domain aminoacid sequences of *ATG4*-like genes from trypanosomatid organisms, yeast and humans. (Tc = *Trypanosoma cruzi*, Tb = *Trypanosoma brucei*, Lm = *Leishmania major*, Sc = *Saccharomyces cerevisiae*, Hs = *Homo sapiens*). Active site C, D and H residues are marked in red and, additionally, Y residue that participates in the oxyanion hole formation (Sugawara et al. 2005) is marked in yellow. .... 33
- Figure 18 Alignment of *ATG8*-like protein amino acid sequences from trypanosomatid organisms, yeast and humans. (Tc = *Trypanosoma cruzi*, Tb = *Trypanosoma brucei*, Lm = *Leishmania major*, Sc = *Saccharomyces cerevisiae*, Hs = *Homo sapiens*). Conserved region upstream of the P1 Gly residue (marked in red) is marked in yellow. Upstream conserved basic region is marked in cyan. .... 35
- Figure 19 Purification of Atg4.1 (panel A) and Atg4.2 (panel B) with Ni-NTA affinity chromatography. The results were analyzed by SDS PAGE with Coomassie Brilliant Blue staining. In the first lane induced bacterial protein extract is shown; in the second lane the unbound fraction is presented; in the next lanes, washing/elution steps with 50, 80, 110, 150 and 200 mM imidazole are analyzed showing a band of approx. 40 kDA, which is in good agreement with the predicted molecular mass. .... 36
- Figure 20 Purification of Atg8.1 (panel A) and Atg8.2 (panel B) with Ni-NTA affinity chromatography. The results were analyzed by SDS PAGE with Coomassie Brilliant Blue staining. In the first lane induced bacterial protein extract is shown; in the second lane the unbound fraction is presented; in the next lanes eluates with 150 mM imidazole are analyzed showing a band of approx. 15 kDA, which is in good agreement with the predicted molecular mass. .... 37
- Figure 21 *In Vitro* cleavage assay. Constant amounts (17,2 µg) of Atg8.1 (Panel A) or Atg8.2 (Panel B) were incubated with different amounts of recombinant autophagin-1 for 35 min and one fifth of the reaction mixtures was analyzed by SDS-PAGE using Coomassie Brilliant Blue staining. In the first lane Atg8.1 was completely processed after the addition of 750 ng of autophagin-1. In next 5 lanes: subsequent 10 fold dilutions of autophagin-2 were added to the substrate resulting in less cleavage product. Second lane from the right represents control without autophagin-1 addition and the last lane processing with 75 ng autophagin-1, however, inhibited with iodoacetamide. .... 38
- Figure 22 *In Vitro* cleavage assay. Constant amounts (17,2 µg) of Atg8.1 (Panel A) or Atg8.2 (Panel B) were incubated with different amounts of recombinant autophagin-2 for 18 h and one fifth of the reaction mixtures was analyzed by SDS-PAGE using Coomassie Brilliant Blue staining. The first lane represents control sample with no autophagin-2 added; in the second lane 2 µg of autophagin were added resulting in a weak band of processed Atg8.1 and barely detectable band of processed Atg8.2. In the third lane, 0,2 µg of autophagin-2 were added and almost no processing product can be observed in case of either substrate. In the last lane cell free protein extract of autophagin-2 expressing bacteria was added, corresponding to about 150 µL of induced cell culture. Very weak bands corresponding to the processed form of products indicate, that autophagin-2 is poorly active even before Ni-NTA purification step. .... 39
- Figure 23 Reverse phase HPLC chromatograms of Atg8.1 untreated sample and autophagin processed sample (panel A) and Atg8.2 untreated sample and autophagin processed sample (panel B). Cleaved C-terminal peaks are clearly recognizable (at 16,3 and 14,4 min) in both cases and the retention of the processed Atg8.2 is moderately augmented after cleavage with respect to the unprocessed protein. The images were obtained with analog recorder and digitalized respecting the relative sizes of the peaks. .... 40
- Figure 24 Autophagin activity in cell-free extracts of *T. cruzi* different life cycle stages. Constant amounts (17,2 µg) of Atg8.1 (Panel A) or Atg8.2 (Panel B) were incubated with 100 µg of cell-free extracts of different *T. cruzi* life cycle stages. One third of the reaction mixture was analyzed by Western blot using specific polyclonal antibodies (Panel A: anti-Atg8.1 and Panel B: anti-Atg8.2). In the first lane of each blot, control of the corresponding untreated Atg8 is shown; while in the second lane of each blot the corresponding Atg8 cleaved by *T. cruzi* recombinant autophagin-1 is displayed. In the next four lanes of each blot the corresponding Atg8 was incubated with cell-free extracts of: epimastigotes (E), cell-derived trypomastigotes (T), metacyclic trypomastigotes (M) and amastigotes. In the last four lanes of every blot equivalent reactions were inhibited with iodoacetamide. .... 41

- Figure 25 Complementation of *atg4Δ* and *atg8Δ* yeast strains with *T. cruzi* homologues. Transport of proaminopeptidase I (pAPI) to the vacuole, where it matures, only takes place when a functional autophagy/cvt pathway is present. The two bands with the higher molecular mass represent pAPI while the band with the lower molecular mass corresponds to mature aminopeptidase (mAPI). *S. cerevisiae atg4* and *atg8* knockout strains were transformed with: empty pCM190 plasmid or the same plasmid containing *TcATG4.2* or *TcATG4.1* in the case of *atg4Δ* and *TcATG8.1* or *TcATG8.2* for *atg8Δ*. **A)** Western blot analysis of transformants under normal growth conditions using anti-pAPI antibodies. *atg4* knock-out shows no mAPI band when transformed with pCM190 plasmid alone whereas *TcATG4.1* and *TcATG4.2* expression clearly restores the cvt-pathway. The defect of *atg8* deficient yeasts could not be overcome by expression of *TcATG8.1* or *TcATG8.2* under these conditions. **B)** Western blot analysis of the same transformants in starvation conditions. The result is similar in case of *ATG4* complementation; however, a mAPI band can also be observed in case of *atg8* knock-out expressing *TcATG8.1*. In case of *TcATG8.2* expression no mature aminopeptidase band can be observed, similarly to the nutrient rich conditions..... 42
- Figure 26 Colocalization of microtubules and TcAtg8.1 and TcAtg8.2 proteins *in vitro*. Microtubules were incubated with Atg8.1 protein (panels a – c) or Atg8.2 protein (panels d – f). Microtubule pattern was detected in red with monoclonal anti-tubulin antibody (panels a and d) and Atg8.1 and Atg8.2 distribution in green with polyclonal antibodies raised in rabbits (panels b and e). Merge images without probable colocalization are shown in panels c and f..... 43
- Figure 27 Sub-cellular localization of Atg8.1 (in red) and Atg8.2 (in green) proteins in nutrient rich BHT medium + 10 % FCS and after prolonged starvation in PBS for 20 h as seen in indirect immunofluorescence experiments. Pictures in panels a and b were obtained with anti-Atg8.1 antibody and panels c and d with anti-Atg8.2 antibody. Blue color reveals DAPI stained nuclear (bigger and more faint) and kinetoplast (smaller, brighter and elongated) DNA. Several bright spots can be observed in panel B corresponding to Atg8.1 localized to the autophagosomes..... 44
- Figure 28 Phylogenetic reconstruction of selected metacaspases. Bootstrap values are shown on the nodes. Metacaspases in the tree are from *Arabidopsis thaliana* (At), *Lycopersicon esculentum* (Le), *Aspergillus nidulans* (An), *Leishmania major* (Lm), *Saccharomyces cerevisiae* (Sc), *Schizosaccharomyces pombe* (Sp), *Trypanosoma brucei* (Tb) and *Trypanosoma cruzi* (Tc) (Kosec et al. 2006). ..... 46

## List of published articles

- Kosec, G., V. E. Alvarez, et al. (2006). "Metacaspases of Trypanosoma cruzi: possible candidates for programmed cell death mediators." Mol Biochem Parasitol **145**(1): 18-28.
- Kosec, G., Alvarez, V. E., Cazzulo, J. J. (2006) "Cysteine proteinases of Trypanosoma cruzi: from digestive enzymes to programmed cell death mediators" Biocell *in press*



**Razširjeni povzetek doktorske disertacije**

**Izražanje in karakterizacija cisteinskih  
peptidaz metakaspaz in avtofaginov iz  
parazita *Trypanosoma cruzi***

## Uvod

### ***Trypanosoma cruzi* in Chagasova bolezen**

*Trypanosoma cruzi* je enocelični parazit in eden prvih evkariontskih organizmov, ki vsebujejo mitohondrij. Ta je prisoten v eni kopiji in ima poseben predel, ki vsebuje vso mitohondrijsko DNA in se imenuje kinetoplast. Sestavlja ga preplet različno velikih krožnih molekul DNA in daje ime redu Kinetoplastida, v katerega spada tudi družina Trypanosomatidae. *Trypanosoma cruzi* se v infekcijskem ciklu diferencira v štiri morfološko popolnoma različne stadije. Parazit vstopi v človeškega gostitelja, ko insektni vektor izloči infektivne metaciklične tripomastigote v neposredno bližino vboda. Vbod povzroči srbenje, gostitelj pa s praskanjem prenese metaciklične tripomastigote v rano. Po vdoru metaciklični tripomastigoti infecirajo sosednje celice, kjer se transformirajo v amastigote. Le-ti se namnožijo, uničijo gostiteljske celice in se transformirajo v tripomastigote, ki po krvi migrirajo po celem telesu in okužijo nove celice (De Souza 2002).

Chagasova bolezen, infekcija s *T. cruzi* pri človeku, se začne z akutno fazo, ki jo označujejo vročina, mrzlica in slabost. Tej sledi asimptomatska faza, ki lahko traja do 20 let. Pri 20 – 30% bolnikov se nato pojavi kronična faza z miokarditisom in povečanim črevesjem, kar mnogokrat povzroči nenadno smrt. Zaenkrat za Chagasovo bolezen ni učinkovitih zdravil (Barrett, Burchmore et al. 2003).

Genom hibridnega klona *T. cruzi* CL Brenner so sekvenirali z metodo naključnega iskanja zaporedij (random sequence survey ali WGS – whole genome shotgun). Zaradi velikega deleža ponovitev in hibridne narave genoma ni mogoče dognati celotnih zaporedij posameznih kromosomov. V genomu se nahaja 20 zaporedij za različne cisteinske peptidaze, poleg teh pa so zastopani tudi drugi katalitični tipi (serinske, metalo, aspartatne, treoninske). Mnoge peptidaze različnih katalitičnih tipov iz *T. cruzi* so že znane kot virulenčni dejavniki (kruzipain, oligopeptidaza B, prolil oligopeptidaza, metaloproteaze družine gp63) (Cazzulo 2002; El-Sayed, Myler et al. 2005).

### **Cisteinske peptidaze**

Proteolizni encimi, ki za svojo aktivnost potrebujejo cistein (in histidin), imajo vsaj sedem med seboj neodvisnih evolucijskih začetkov. Iz vsakega od teh je nastala svoja skupina z značilno strukturo in lastnostmi. Nastanek mnogih cisteinskih peptidaz sega v čas skupnega prednika bakterij in arhej in verjetno to velja za vse peptidaze. Cisteinske peptidaze se torej spreminjajo že tri milijarde let. V tako dolgem času je iz posamezne peptidazne enote najprej nastala družina enot s podobnimi aminokislinskimi zaporedji, kasneje pa še bolj raznolik grozd (cluster) družin. Aminokislinska zaporedja znotraj grozda se med seboj tako razlikujejo, da jih nimamo več za homologna po klasičnih kriterijih. Kljub velikim razlikam so družine v takem grozdu evolucijsko povezane, kar se kaže z ohranitvijo sekundarne in terciarne strukture, oziroma zvitja (fold), proteinov. Skupino tako povezanih družin imenujemo klan (Barrett and Rawlings 2001).

### **Klan CA**

Klan CA je največji klan cisteinskih peptidaz z okoli polovico vseh družin. Karakteristična za ta klan je struktura družine papaina, C1. Strukturo lahko poenostavljeno opišemo tako, da gre za dve domeni, ki se nahajata na vsaki strani reže z aktivnim mestom. N-terminalna domena je sestavljena v glavnem iz  $\alpha$ -vijačnic, dolga vijačnica pa teče tudi skozi sredino molekule. C-terminalni del, ki vsebuje katalitični histidin, ima strukturo  $\beta$ -sodčka. Pred katalitičnim cisteinom je zavoje, za njim pa dolga vijačnica. Tudi pred katalitičnim histidinom je zavoje, sledi pa mu kratka  $\beta$ -struktura. Za katalizo je pomemben tudi asparagin oz. aspartat, ki skrbi za pravilno orientacijo histidina v aktivnem mestu (Barrett and Rawlings 2001). V klan CA spada tudi pred kratkim odkrita družina C54, v katero spadajo Atg4 proteaze oziroma avtofagini. Poleg papainu podobne domene ima še majhno domeno z  $\alpha/\beta$  zvitjem, ki verjetno sodeluje pri specifičnem prepoznavanju substratov, ubikvitinu podobnih proteinov Atg8. Dostop v aktivno mesto preprečuje zanka 4 aminokislinskih preostankov, ki se umakne šele, ko se na peptidazo veže Atg8, kar je temelj izredne specifičnosti teh citosolnih peptidaz (Sugawara, Suzuki et al. 2005).

## Avtofagija

Avtofagija je evolucijsko zelo ohranjen proces, pri katerem se sestavine citoplazme obdajo z dvojno membrano in tvorijo avtofagosome. Tako ujete proteine in organele razgradijo lizosomske hidrolaze, potem ko se avtofagosomi zlijejo z lizosomi. Pri nastajanju avtofagosomov sodelujeta dve modifikaciji, ki sta podobni ubikvitilaciji. Ena od teh je modifikacija ubikvitinu podobnega proteina Atg8; avtofagin (oziroma proteaza Atg4) cepi protein Atg8 za ohranjenem Gly preostankom, kar omogoči vezavo fosfatidiletanolamina na karboksiterminal Atg8 in s tem vključitev tega proteina v membrano preavtofagosomov (izolacijskih membran). Atg4 proteaza pred zlitjem avtofagosoma z lizosomom tudi dekonjugira Atg8 s fosfatidiletanolamina in s tem z zunanje membrane avtofagosoma in omogoči ponovno uporabo tega proteina pri tvorbi avtofagosomov (Klionsky 2005).

S sekveniranjem genoma *T. cruzi* so našli gene za proteine, ki sodelujejo pri avtofagiji, med drugim tudi *ATG4* in *ATG8*. Sicer ta proces pri tem in sorodnih organizmih še ni raziskan.

## Klan CD

Prve strukture kaspaz, pridobljene z rentgensko kristalografijo, so pokazale, da sta katalitična cistein in histidin razporejena na koncih  $\beta$ -strukture, ki sestavlja edinstveno  $\alpha/\beta$ -zvitje ( $\alpha/\beta$ -fold). To ni podobno strukturam drugih prej poznanih peptidaz klana CA (Wilson, Black et al. 1994). Kasnejše študije aktivnih mest vakuolnih endopeptidaz iz družine legumainov (oz. hemoglobinaz) so predvidele podobno postavitve katalitičnih preostankov in podobno zvitje, kot ga imajo kaspaze. Sorodno razporeditev aktivnega mesta so našli tudi pri klostripainih iz *Clostridium sp.* in gingipainih iz *Porphyromones gingivalis* (Chen, Rawlings et al. 1998). Pred kratkim so odkrili separin, peptidazo, ki omogoča ločitev sestrskih kromatid pri evkariontski mitozii in ima prav tako podobno aktivno mesto (Uhlmann, Wernic et al. 2000).

Metakaspaze so oddaljeni homologji kaspaz, ki so prisotni v rastlinah, glivah in praživalih. Celice mnogih organizmov iz teh skupin v določenih pogojih kažejo značilne morfološke znake apoptoze oziroma programirane celične smrti. Kaže, da pri teh procesih pomembno vlogo igrajo tudi metakaspaze, čeprav natančen mehanizem njihovega delovanja še ni poznan (Madeo, Herker et al. 2002; Suarez, Filonova et al. 2004). V *T. cruzi* sta prisotna dva gena za metakaspazi *TcMCA3* in *TcMCA5*. Prvi je prisoten v približno 16 kopijah na haploidni genom, nanizanih v tandemske zaporedju, slednji pa v eni kopiji na haploidni genom. Metakaspaza-3 se izraža v vsaj enem od stadijev *T. cruzi*, ki so prisotni v sesalskem gostitelju, saj serumu večine pacientov s Chagasovo boleznijo vsebujejo protetelesa proti temu proteinu (Kosec 2004).

## Programirana celična smrt pri *T. cruzi*

Če epimastigote *T. cruzi* gojimo v laboratoriju in jim prenehamo menjavati medij, se deloma diferencirajo v metaciklične tripomastigote, deloma pa umrejo in pri tem kažejo značilne morfološke znake apoptoze pri sesalcih. Mrtvi epimastigoti imajo obliko sferoida, membrana brbota (blebbing), citoplazma se vakuolizira, jedrni kromatin pa kondenzira. *In situ* z deoksitransferazo katalizirano končno označevanje zarez z dUTP (TUNEL) kaže na precejšnjo fragmentacijo DNA. Proces lahko sprožimo tudi z geneticinom ali spojino G418, medtem ko saponin sproži mnogo hitrejšo smrt, ki je podobna nekrozi (Ameisen 1995). Če epimastigote inkubiramo z 10% raztopino svežega človeškega seruma, je proces počasnejši in bolj kontroliran. Jedrna DNA se fragmentira do diskretnih fragmentov, ki na agarozni elektroforezi kažejo obliko lestve (ladder), opazimo inhibicijo procesa s 100  $\mu$ M DEVD-CHO ter spojinami, ki sprožijo proizvodnjo dušikovega oksida (NO) (Piacenza, Peluffo et al. 2001). Tudi *Trypanosoma brucei* in različne vrste rodu *Leishmania* kažejo podobne znake v različnih situacijah, kar kaže na to, da je proces ohranjen v družini kinetoplastid (Welburn and Maudlin 1999).

## Namen dela in hipoteza

Cisteinske peptidaze igrajo številne nepogrešljive vloge v biologiji parazitov. Poleg splošnih katabolnih funkcij in procesiranja proteinov so pomembne tudi pri izogibanju imunskemu sistemu in invaziji v celice in tkiva. Cisteinske peptidaze parazitov so tudi neobičajno imunogene in zato možni serodiagnostični markerji in cepiva. Čeprav so deloma podobne gostiteljskim homologom, se razlikujejo v biokemijskih značilnostih, na primer specifičnosti, kar odpira možnosti za kemoterapijo.

Izmed 20 genov, ki so jih identificirali v genomu *T. cruzi* in ki kodirajo za cisteinske peptidaze, smo se osredotočili na dve družini, metakaspaze in avtofagine. Homologi obeh družin sodelujejo pri signalizaciji pomembnih celičnih procesov v drugih organizmih, zato smo predvidevali, da bi boljše poznavanje biokemijskih in fizioloških lastnosti teh peptidaz pomembno prispevalo k razumevanju podobnih procesov v parazitih in odprlo možnosti za razvoj novih protiparazitских terapij.

Hipoteza našega dela je, da se geni za metakaspazo-3 in avtofagin-1 ter -2 izražajo v življenjskih stadijih *T. cruzi* in kodirajo aktivne cisteinske peptidaze. Poleg tega mislimo, da je metakaspaza-3 udeležena pri programirani celični smrti epimastigotov *T. cruzi*, ki jo sprožimo s svežim človeškim serumom. Predvidevamo, da avtofagin-1 in -2 procesirata predvidena substrata Atg8.1 in Atg8.2 iz *T. cruzi* in da ti proteini predstavljajo funkcionalen sistem konjugacije ubikvitinu podobnih proteinov Atg8 na fosfatidiletanolamin, ki je temelj funkcionalne avtofagije v *T. cruzi*.

## Metode

### Bioinformatika

S programom BLAST smo preiskali baze podatkov sekveniranega genoma *T. cruzi* (El-Sayed, Myler et al. 2005)([www.genedb.org](http://www.genedb.org)) za prisotnost homologov Atg4 proteaz (avtofaginov) in njihovih predvidenih substratov *ATG8*. Pridobljena zaporedja smo primerjali med seboj in s tistimi iz drugih organizmov s programom Clustal W za poravnavo zaporedij.

### Gelska elektroforeza v utripajočem polju

Za ločitev celotnih kromosomov *T. cruzi* smo uporabili gelsko elektroforezo v utripajočem polju (PFGE). Epimastigote *T. cruzi* smo imobilizirali v agaroznih kvadrnih, razgradili proteine in nato DNA iz njih elektroforezno ločili na agaroznem gelu, primernem za velike fragmente.

### Izražanje rekombinantnih proteinov

Izdelali smo novo strategijo za izražanje rekombinantne metakaspaze-3, pri kateri smo v bakteriji *E. coli* BL21 DE3 pLys S v vektor za citosolno izražanje pET-28 klonirali zaporedji za metakaspazo-3, ki sta se začeli z drugim ali tretjim metioninskim preostankom proteina divjega tipa. Tudi gena za avtofagina *TcATG4.1* in *TcATG4.2* ter njuna predvidena substrata *TcATG8.1* in *TcATG8.2* smo izrazili v istih bakterijskih celicah s kloniranjem v isti vektor. Temperaturo izražanja smo znižali na 18 °C za avtofagina in na 28 °C za *TcATG8.1* in *TcATG8.2*. Vse rekombinantne proteine smo iz bakterijskih ekstraktov izolirali z Ni-kelatno afinitetno kromatografijo s pomočjo dodanega heksahistidinskega repa.

### Merjenje aktivnosti cisteinskih peptidaz

Proteolitično aktivnost cisteinskih peptidaz smo merili s sintetičnimi in proteinskimi substrati. Aktivnost metakaspaze-3 smo skušali meriti s kombinatoričnimi knjižnicami fluorescentno označenih peptidov, ki so imeli isti aminokislinski preostanek na enem mestu, na drugih mestih pa so se preostanki razlikovali. Aktivnost smo merili v pufrih različnega pH, ionske moči, detergentov ipd (Melo, Alves et al. 2001).

Aktivnost avtofaginov smo merili z izraženimi proteinskimi substrati Atg8.1 in Atg8.2, tako da smo na karboksiterminal teh proteinov dodali dovolj dolga zaporedja, da smo lahko opazovali spremembo molekulske mase ob cepitvi z SDS PAGE. Tudi aktivnost avtofaginov v proteinskih celičnih ekstraktih smo opazovali s pomočjo istih rekombinantnih substratov na podoben način.

### Opazovanje vloge genov *TcATG4.1*, *TcATG4.2*, *TcATG8.1* in *TcATG8.2* pri avtofagiji v kvasovkah

Gene *TcATG4.1*, *TcATG4.2*, *TcATG8.1* in *TcATG8.2* smo klonirali v vektor pCM190 za izražanje v kvasovkah *Saccharomyces cerevisiae* (Gari, Piedrafita et al. 1997). S pridobljenimi konstrukti smo transformirali seva kvasovk, ki so jima predhodno izbili ustrezna lastna gena *ATG4* oziroma *ATG8*. Transformirane seve smo opazovali v gojiščih bogatih s hranili in po daljšem stradanju. Celične proteine smo ločili s SDS PAGE, jih z western prenosom prenesli na nitrocelulozno membrano, nato pa s protitelesi proti proaminopeptidazi opazovali procesiranje tega proteina v zrelo obliko ob prehodu iz citosola v vakuolo. Ta prehod je bil mogoč samo, če so geni iz *T. cruzi* uspeli vzpostaviti delovanje avtofagije v sevih, pri katerih ta proces zaradi izbitja ključnih genov *ATG4* ali *ATG8* ni deloval.

## **Opazovanje vezave TcAtg8.1 in TcAtg8.2 na mikrotubule**

Po opisanem postopku smo mikrotubule pridobili s polimerizacijo komercialno dostopnega tubulina v ustreznem pufri, nato pa smo jim dodali izolirani rekombinantni TcAtg8.1 oziroma TcAtg8.2 (Ketelaar, Voss et al. 2004). V nastalo raztopino smo dodali glutaraldehid, nato pa jo nanesli na krovna stekelca. Imunofluorescenco smo izvedli s primarnimi protitelesi proti tubulinu in TcAtg8.1 oziroma TcAtg8.2 ter sekundarnimi protitelesi, konjugiranimi z rdečim oziroma zelenim fluoroforom.

## **Delo s paraziti *Trypanosoma cruzi***

Parazite smo gojili po ustaljenih postopkih (Franke de Cazzulo, Martinez et al. 1994). Programirano celično smrt epimastigotov smo sprožili z dodatkom 10 % svežega človeškega seruma v gojišče, nato pa smo število in obliko parazitov spremljali 4 ure. Parazite smo nanesli na krovna stekelca in nato izvedli imunofluorescenčno detekcijo metakaspaze-3 z lastnimi poliklonskimi primarnimi protitelesi in sekundarnimi protitelesi, konjugiranimi z zelenim fluoroforom. Za določitev položaja jedra in kinetoplasta smo dodali tudi DAPI, modro fluorescenčno barvilo za DNA.

Stradanje smo inducirali z inkubacijo epimastigotov v PBS 20 ur. Podobno kot pri programirani celični smrti, smo parazite nanesli na krovna stekelca in izvedli imunofluorescenčno detekcijo z lastnimi poliklonski primarnimi protitelesi proti TcAtg8.1 in TcAtg8.2 in sekundarnimi protitelesi z rdečim oziroma zelenim fluoroforom.

## Rezultati

### Metakaspaza-3

Z gelsko elektroforezo v utripajočem polju, prenosom po Southernu in avtoradiografijo smo ugotovili, da sta v genomu klona CL Brenner *T. cruzi* prisotni dve tandemski ponovitvi genov za metakaspazo-3 na dveh različnih kromosomih. Z western prenosom celičnih ekstraktov smo pokazali, da se metakaspaza-3 izraža v vseh štirih življenjskih stadijih *T. cruzi*. Zaznali smo le protein molekulske mase približno 44 kDa, kar ustreza dolžini celotne polipeptidne verige, ne pa tudi morebitnih hitreje potujočih lis fragmentov, ki bi bili posledica kaspazam podobnega procesiranja.

Uspešno smo izrazili v topni obliki in delno izolirali metakaspazo-3 v *E. coli* s konstruktom, pri katerem se je izražanje začelo s tretjim metioninskim preostankom nativnega proteina. S tako pridobljenim proteinom smo merili proteolitično aktivnost s pomočjo kombinatoričnih knjižnic fluorescenčno označenih sintetičnih peptidnih substratov. Kljub testiranju velikega števila različnih pogojev aktivnosti nismo zaznali, morda zato, ker metakaspaza-3 potrebuje specifične pogoje za aktivacijo, kofaktorje, specifični proteinski substrat, ali pa se v bakterijskih celicah izraža v deaktivirani obliki. Podobne negativne rezultate so dobili tudi pri metakaspazah iz *T. brucei* (J. Mottram, osebna komunikacija) in metakaspazah tipa I iz rastlin (Vercammen, van de Cotte et al. 2004)

Imunofluorescenčna mikroskopija je pokazala, da se metakaspaza-3 v procesu programirane celične smrti prestavi iz citosola v jedro. Zaradi nezmožnosti merjenja proteolitične aktivnosti njene vloge v jedru nismo mogli določiti, vendar pride to takega premika metakaspaze tudi pri rastlinah, kjer metakaspaza sodeluje pri razgradnji jedrne ovojnice (Bozhkov, Suarez et al. 2005).

### Avtofagini in avtofagija

V genomu *T. cruzi* ([www.genedb.org](http://www.genedb.org)) smo našli dva gena za avtofagine: *TcATG4.1* in *TcATG4.2*. Oba vsebujeta katalitično triado Cys, Asp, His, poleg tega pa še Tyr preostanek, ki sodeluje pri tvorbi oksianionske votline. Identificirali smo tudi dva gena za predvidene substrate *TcATG8.1* in *TcATG8.2*. Oba gena vsebujeta Gly preostanek, ki je v družini ohranjen in predstavlja preostanek P1 za cepitve z avtofagini. Vse štiri gene smo izrazili v bakterijskem ekspresijskem sistemu in jih izolirali z Ni-kelatno afinitetno kromatografijo.

Ugotovili smo da avtofagin-1 (*TcAtg4.1*) procesira *TcAtg8.1* in *TcAtg8.2* s približno enako hitrostjo, medtem ko avtofagin-2 sicer cepi ta dva proteina, vendar zelo počasi. Odcepljene fragmente smo izolirali z reverzno fazno HPLC kromatografijo in določili njihov N-terminalni aminokislinski preostanek. Ugotovili smo, da do cepitve pride za ohranjenim Gly preostankom. Vse štiri gene smo izrazili tudi v kvasovkah *Saccharomyces cerevisiae*, ki niso imele lastnih homolognih genov (*ScATG4* in *ScATG8*) in zato tudi ne delujoče avtofagne poti. Ugotovili smo, da tako *TcATG4.1* kot *TcATG4.2* uspešno nadomestita *ScATG4* in vzpostavita delujočo avtofagijo. Od *ATG8* genov iz *T. cruzi* le *TcATG8.1* delno vzpostavi avtofagijo v *S. cerevisiae* z izbitim lastnim genom *ScATG8*.

Zanimalo nas je tudi, ali *TcATG4.1*, *TcATG4.2*, *TcATG8.1* in *TcATG8.2* omogočajo delujočo avtofagijo tudi v *T. cruzi*, kjer ta proces še ni bil opisan. Ugotovili smo, da je aktivnost avtofaginov prisotna v vseh štirih življenjskih stadijih *T. cruzi*. Poleg tega smo z imunofluorescenčnimi študijami tudi pokazali, da se *TcAtg8.1* ob podaljšanem stradanju iz citosola premakne v nekaj večjih veziklov, ki verjetno predstavljajo avtofagosome. Lahko rečemo, da se v *T. cruzi* pri stradanju sproži avtofagija, kjer *TcAtg8.1* deluje podobno kot homolog *ATG8* pri kvasovkah in ljudeh. Za procesiranje in dekonjugacijo omenjenega proteina zelo verjetno skrbi avtofagin-1 (*TcAtg4.1*), medtem ko vlogi *TcAtg4.2* in *TcAtg8.2* še nista trdno določeni.

Zanimivo je, da se niti *TcAtg8.1* niti *TcAtg8.2* ne vežeta na mikrotubule, kar nakazuje, da to za avtofagijo v *T. cruzi* ni potrebno. Podobno velja tudi za *S. cerevisiae* (Kirisako, Baba et al. 1999) pri večjih človeških in rastlinski celicah pa se *ATG8* homolog *močno* vežejo na mikrotubule, ki so tudi nepogrešljivi za učinkovito avtofagijo (Mann and Hammarback 1994; Ketelaar, Voss et al. 2004; Marino and Lopez-Otin 2004).

## Zaključki

- Metakaspaze se izražajo v *T. cruzi* in v procesu s svežim človeškim serumom inducirane programirane celične smrti epimastigotov spremenijo svojo lokalizacijo iz citosola v jedro.
- Metakaspaze morda sodelujejo pri procesu programirane celične smrti v *T. cruzi*, vendar je mehanizem njihovega delovanja verjetno drugačen kot pri metazojskih kaspazah.
- Ni nam uspelo izmeriti proteolitične aktivnosti metakaspaz iz *T. cruzi*.
- Gen *ATG4.1* (avtofagin-1) iz *T. cruzi* kodira aktivno cisteinsko peptidazo, ki procesira oba predvidena substrata TcAtg8.1 in TcAtg8.2, tako da ju cepi za evolucijsko ohranjenim Gly preostankom.
- Gen *ATG4.2* (avtofagin-2) iz *T. cruzi* prav tako kodira aktivno cisteinsko peptidazo, ki pa verjetno ne prispeva pomembno k procesiranju TcAtg8.1 ali TcAtg8.2. Njena funkcija za enkrat ostaja neznana.
- Nobeden od avtofaginov ne cepi sintetičnega fluorescenčnega substrata, ki smo ga načrtovali glede na zaporedje mesta cepitve enega od substratov. Verjetno je mehanizem proteolize odvisen od prepoznavanja tridimenzionalne strukture proteinskega substrata.
- *TcATG8.1* se je izkazal kot funkcijski homolog gena *ATG8* iz *S. cerevisiae* in je lokaliziran v avtofoagosomih med avtofagijo epimastigotov *T. cruzi*, ki jo izzovemo s stradanjem.
- Aktivnost avtofaginov se izraža konstitutivno v vseh pomembnih razvojnih stadijih *T. cruzi*, kar nakazuje, da je avtofagija na bazalnem nivoju pri tem parazitu vedno prisotna.
- Avtofagija v *T. cruzi* je možna, čeprav v genomu ni ubikvitinu podobnega gena *ATG12*. To pomeni, da morda drugi konjugacijski sistem ni nujen za splošni mehanizem avtofagije.